TYPE III-A CRISPR-CAS MEDIATED RNA DEGRADATION AND PLASMID INTERFERENCE

by

WALTER THOMAS WOODSIDE

(Under the Direction of Michael P. Terns)

ABSTRACT

Clustered regularly interspaced short palindromic repeats (CRISPR) and their associated proteins (Cas) have exploded into the world of biological research and development due to the rapid adoption of genome engineering tools already developed from a tiny fraction of these microbial adaptive heritable immune systems. Type III-A CRISPR-Cas effector complexes (Csm crRNP) are constructed of multiple Cas proteins formed around a CRISPR RNA (crRNA) containing an 8-nucleotide 5' tag, from a repeat sequence, together with a (~30-40-nucleotide) spacer sequence, taken from a previous invader. The crRNP is guided by the spacer sequence to bind and cleave complementary (protospacer) RNA via an integral RNase of the crRNP. The work presented here demonstrates that heterologously expressed type III-A systems of *Lactococcus lactis*, *Staphylococcus epidermidis*, and *Streptococcus thermophilus* can be modified and programmed to specifically target diverse endogenous RNAs, causing gene knockdown at the post-transcriptional level. In addition to the specific RNase activity, during crRNP-protospacer RNA binding, a non-specific DNase and cyclic oligoadenylate (cOA) generation become switched on. The cOA binds and activates a trans-acting RNase, Csm6, to degrade encountered RNAs. We found that a short protospacer flanking sequence (PFS) adjacent to the crRNA-protospacer RNA paired region,

regulates the crRNP activities. We used heterologous Csm expression systems in combination with target plasmid libraries containing degenerate PFSs, to interrogate a large set of distinct PFSs on crRNP-mediated anti-plasmid immunity. We found that PFSs with potential to base-pair with certain nucleotides of the crRNA 5' tag result in loss of immune activity. In contrast, PFSs that do not exhibit much or any 5' tag complementary result in different degrees of function depending upon the precise sequence of the target RNA PFS tested. The results obtained with the heterologous Csm expression systems, that not all PFS sequences function the same in Type III-mediated immunity, were validated in the native *Streptococcus thermophilus* host. Collectively, our findings reveal that the precise sequence of a target RNA PFS can regulate immune activity. We additionally demonstrate that plasmid interference in *S. thermophilus* is dependent on activation of the non-specific RNase activity of Csm6, and not the DNase activity of Csm1.

INDEX WORDS: CRISPR, Cas, Type III, Csm, RNA, crRNA, *Lactococcus lactis*, *Staphylococcus epidermidis*, *Streptococcus thermophilus*

TYPE III-A CRISPR-CAS MEDIATED RNA DEGRADATION AND PLASMID INTERFERENCE

by

WALTER THOMAS WOODSIDE

BA, Occidental College, 2011

A Dissertation Submitted to the Graduate Faculty of The University of Georgia in Partial Fulfillment of the Requirements for the Degree

DOCTOR OF PHILOSOPHY

ATHENS, GEORGIA

2020

TYPE III-A CRISPR-CAS MEDIATED RNA DEGRADATION AND PLASMID INTERFERENCE

by

WALTER THOMAS WOODSIDE

Major Professor:	Michael Terns
Committee:	Sidney Kushner
	Jorge Escalante-Semerena
	Vincent Starai

Electronic Version Approved:

Ron Walcott
Dean of the Graduate School
The University of Georgia
December 2020

DEDICATION

This thesis is dedicated to my friends in Sierra Madre and Athens.

Let us find ourselves together again.

ACKNOWLEDGEMENTS

I give my deepest thanks to Dr. Terns and all members of the Terns Lab past and present. You have been my home and family for almost a quarter of my life, and I will always be appreciative of the roles you have all played in my development as a scientist.

Thank you to my committee members Dr. Sidney Kushner, Dr. Jorge Escalante-Semerena, and Dr. Vincent Starai for your mentorship, sage advice, and technical help along the way.

TABLE OF CONTENTS

Page

CHAPTER 1

INTRODUCTION AND LITERATURE REVIEW

Introduction to CRISPR-Cas systems

CRISPR-Cas systems are a unique family of heritable immune systems found in about half of all fully-sequenced bacteria and most archaea (1). CRISPR (clustered regularly interspaced short palindromic repeats) loci consist of an array of repeating ~20-50 nucleotide sequences with intervening DNA "spacers" of similar length which are derived from previous invaders (phage, plasmid, etc) (2, 3). CRISPR-associated (Cas) genes are also typically found adjacent to the array but can be associated with distant arrays (4). Each array is preceded by an AT- rich 100-500 bp leader sequence with an intrinsic transcription promoter (5, 6). Upon transcription of the CRISPR array into a pre-CRISPR RNA (pre-crRNA), a Cas protein typically fragments the transcript into operational units (crRNAs), containing a single spacer and part of the repeat sequence, which catalyze the assembly of Cas protein(s) to form an effector complex with the crRNA. The crRNA ribonucleoprotein (crRNP) is then guided by the crRNA sequence to bind to the invader's nucleic acid upon subsequent exposure, activating nuclease activities (Figure 1.1) (7).

While microbial hosts have evolved these systems to protect against deadly and parasitic invaders, humans have quickly found ways to exploit the specific DNA and RNA recognition and cleavage activities of CRISPR-Cas systems to expand the toolbox of genome editing, gene regulation, nucleic acid detection and tracking tools. These have had a major impact on all areas of life science research, biotechnology, and medicine.

Classification of CRISPR-Cas systems

The continued discovery of new diverse CRISPR-Cas systems over the last decade has led to an expansion and refinement of the classification system to where it now stands. 6 types and 33 subtypes are separated into 2 classes (Figure 1.2) (8). Class 1 CRISPR-Cas systems are those with effector complexes composed of multiple assembled protein subunits (types I, III, IV) and class 2 are those with a single, multi-domain protein (types II, V, VI).

Class 1 types I, III, and IV share similarly intricate multi-subunit effector complexes but their prevalence, Cas protein makeup, and mechanisms of defense vary greatly. The type I systems are identified by a DNA nuclease/helicase, Cas3. The prototypical surveillance complex (Cascade) contains multiple Cas proteins only recruits Cas3 to form the effector complex upon binding to a target DNA sequence which it then degrades (9, 10).

Type III systems, identified by the presence of a large multidomain Cas10 protein, uniquely target both DNA and RNA substrates (11, 12). They are very diverse, complex, and deserving of further study. The type III complexes (Csm & Cmr) contain distinct RNA and DNA nuclease sites integral to the complex, but also activate a third nuclease (Csm6/Csx1) through a secondary messenger upon crRNP-target binding (12-18). I will discuss Type III systems in further detail below.

Type IV systems and their target substrates and defense mechanisms are much less well understood (19, 20). These systems are almost exclusively found on plasmids and other mobile genetic elements (21). Their effector complex is identified by the presence of Csf1 but lacks an integral nuclease and most known type IV systems lack an adaptation module. Instead of generating their own spacers, they also seem to co-opt the adaptation module of type I systems,

together with which they are most often found, and this is reflected in the context of their protospacers (20).

Class 2 types II, V, and VI each employ a single-protein effector complex, but their methods of crRNA processing, catalytic active sites, and nucleic acid binding and cleavage specificities are varied. Type II CRISPR-Cas systems are identified by the presence of *cas9*. These systems usually contain only two or three adaptation proteins in addition to Cas9, which comprises the effector complex (19). When the surveillance complex containing the mature crRNA binds and recognizes a guide complementary target DNA sequence, RuvC and HNH DNase catalytic sites on Cas9 are activated to cleave each strand of the DNA molecule, resulting in a double strand break. This DNA cleavage activity has been harnessed to direct cleavage of specific DNA sequences *in vivo* leading to one of the most widely used biotechnologies for genome editing.

Type V CRISPR-Cas systems, are identified by a Cas12 single protein effector complex (8, 22, 23). Most Cas12 variants, when guided by a crRNA to bind a target DNA sequence, activate specific dsDNA cleavage activity via a single RuvC domain, but one variant, Cas12g, has a RuvC domain additionally capable of RNase activity (8, 22). Cas12a, which activates non-specific DNase activity upon binding a guide complementary target DNA, has been harnessed as a programmable DNA endonuclease-targeted CRISPR trans reporter (DETECTR) (24).

Type VI is the most recently discovered and described class 2 system, comprising of a single Cas13 protein, and guided by its crRNA to bind and cleave a complementary ssRNA (25). This sequence specific recognition event triggers additional non-specific RNase activity (26-28). This RNA sequence dependent non-specific RNase activity has been harnessed for the programmable detection of RNA at single molecule sensitivity (26, 28, 29).

For each of these systems to form a crRNP effector complex, they require processing of the pre-crRNA into mature crRNAs. The different mechanics of this processing help classify types. Types I and III use a CRISPR repeat sequence specific ribonuclease, Cas6, maintained in the loci. The type IV systems typically borrow Cas6 from a type I system (20). Interestingly, type II, V, and VI systems don't use an additional RNase Cas protein for pre-crRNA processing. In type II a second RNA (tracrRNA), complementary to the repeat sequence, forms a duplex with each repeat sequence. This duplex is recognized and cleaved by the host's endogenous housekeeping RNase III (30). The type V and VI effector proteins typically catalyze maturation of their bound pre-crRNA (31, 32).

Type III CRISPR systems

Most known type III CRISPR-Cas systems are typically identified by the presence of a large multi-domain *cas10* (*cmr2*/*csm1*) gene. They are unique in that most are capable of targeting both RNA and DNA substrates using distinct RNA and DNA nuclease sites integral to the complex and can also activate a third nuclease (Csm6/Csx1) through a second messenger upon crRNP-target binding (12-18). Within the type III CRISPR-Cas arise 6 subtypes, A-F, characterized by presence/absence of specific *cas* genes (Figure 1.3) (8). Subtypes III-A and D have an effector complex (Csm) made of subunits of Csm1-5 (33). Type III-D typically have Cas10/Csm1 that lack an HD DNase domain. Types III-B and C have an effector complex (Cmr) made of Cmr1-6. Type III-C systems lack the Cas10/Cmr2 Palm domain (cyclic oligoadenylate synthetase active site) and therefore doesn't produce the second messenger, cOA. Subtype III-E is characterized by a class 2-like multidomain fusion protein containing multiple Cas7 subunits with a Csm2/Cas11. Subtype III-F uniquely contains only 1 *cas7* variant and like III-C, lacks a functional Cas10 Palm domain.

The effector complexes of subtypes III-A and -B are very similar in structure and defense activities and are also the most common type III systems found (11-14, 18, 34). While the sole focus of my work has been type III-A systems, due to the similarities of complex formation and defense activities with type III-B systems, I am including more background on these systems too (13).

Types III-A and -B

The pathway for CRISPR defense can be split into three phases: adaptation of new spacers into the array, transcription and processing of the array into mature crRNAs, and guided targeting and destruction of invader nucleic acids by the crRNP. New invader DNA sequences (spacers) are added to the arrays at the leader proximal end and with each new spacer insertion, a new repeat is added to the array. While invader DNA fragments available for adaptation can be generated in any number of ways, the precise trimming, orienting, and integration of new spacers into the CRISPR array is dependent on Cas1 and Cas2 and sometimes a third protein (35, 36). While the two Cas genes, *cas1* and *cas2*, comprise the adaptation module associated with most CRISPR loci, the subtype III-B lack these modules and CRISPR arrays while many III-A systems have adaptation modules and dedicted CRISPR arrays (37). Interestingly, type III systems are typically only found in strains that contain at least one additional CRISPR-Cas system type. In one such organism, *Pyrococcus furiosus*, the III-B (Cmr) complex is known to utilize crRNAs from type I associated CRISPR arrays, which explains how the system is still effective and why it has been maintained (6).

During crRNA biogenesis, the CRISPR array seems to be constitutively transcribed unidirectionally starting within the leader sequence. This long transcript (arrays can be hundreds of spacers long) is processed into shorter pre-crRNA by a sequence specific RNase included in the

loci, Cas6, which recognizes and cleaves within the repeat leaving an 8-nucleotide 5' tag upstream of the guide sequence (30, 38). *In vitro* studies have shown that this crRNA processing is a prerequisite for the assembly and formation of the Csm/Cmr crRNPs (6).

X-ray crystal and CryoEM structures of several type III subunits and sub- and complete complexes have shaped our understanding of the roles of each subunit. In the type III effector complexes, a large multidomain Cas10 protein (Csm1 in III-A and Cmr2 in III-B) recognizes the crRNA 5' tag (39, 40). The crRNA is anchored at the 3' end of this tag by a Cas5 (Csm4 or Cmr3) preceding recruitment of Cas7 paralogs (Csm3 or Cmr4) that bind to and stretch along the crRNA in filaments (13, 39, 41-43). A parallel minor filament is formed by small α-helical protein subunits, Cas11, (Csm2 or Cmr5) and the 3' end of the crRNA is capped by one or two more Cas7 paralogs (Csm5 or Cmr1 and Cmr6) (42-45). The size of native complexes is variable, with the repeating Cas7 and Cas11 subunits often found in an N : N-1 respective ratio where N is usually three to five (46-48). Larger structures are always found containing a longer crRNA, which vary by increments of 6-nucleotides.

The crRNAs of type III-A and -B crRNPs guide the surveillance complex to bind protospacer-derived complementary RNA. This binding event typically causes some allosteric conformational change opening a catalytic site for nucleic acid cleavage by the multimeric Cas7s (Csm3 and Cmr4) (49-53). The periodicity of Csm3/Cmr4 subunits and the frequency of RNA cleavage within each target RNA molecule indicates that the bound RNA is cleaved once at each subunit (53, 54). Thumb-like β-hairpins in each Csm3/Cmr4 subunit interrupt the RNA-RNA duplex at 6-nucleotide intervals, pushing each scissile bond near a conserved aspartic residue in each monomer (39, 47, 48). The resulting cleavages are limited to the target RNA region. This sequence-specific RNase activity is of potential biotechnological value as a post-transcriptional

expression regulator. Chapter 2 of my thesis is focused on utilizing the specific RNase activity mediated by Csm3. I demonstrate that the type III-A systems of *Streptococcus thermophilus*, *Staphylococcus epidermidis*, and *Lactococcus lactis* can be programmed with specific crRNAs and expressed heterologously in *E. coli* to target and reduce levels of targeted endogenous RNAs as observed via Northern blot analysis of total RNA.

The large subunit, Cas10, contains an HD domain that has single-stranded (ss)DNA-specific endo- and exonuclease activities that only become activated when the crRNP binds a target RNA (12, 15, 55). It is inactivated by cleavage and subsequent release of the target RNA (56). This suggests a transcription-dependent invader silencing mechanism wherein the crRNP is DNase active while tethered to the invader DNA through to an elongating RNA (12, 15, 57). A cyclic oligoadenylate (cOA) synthetase is also found in a Palm domain of Cas10 which converts ATP intro cyclic oligoadenylates of variable adenylate numbers. Like the DNase activity, this catalytic site is activated by crRNP binding to a target RNA (14, 17, 58, 59). cOA species produced by the Palm domain differ between systems with tetra (cOA_4) and penta (cOA_6) adenylate compounds being most common in the characterized systems.

The cOA molecules produced by Cas10 during target RNA binding activate sequence independent RNase activity by the higher eukaryotes and prokaryotes nucleotide-binding (HEPN) domains in Csm6 (type III-A) and Csx1 (type III-B), neither of which have been found to directly associate with the effector complex (60-63). Whether Csm6 or Csx1 have a specific affinity for target invader RNA or the crRNP upon target RNA binding, has not been established, but the activation of their HEPN RNase domain has been shown to be important or required for plasmid interference and phage clearance in some infection studies (14, 16, 34, 64, 65).

Self vs non-self recognition and defense activation

The specific RNA target cleavage activity by Csm3/Cmr4 seen in both Csm and Cmr systems only requires sufficient complementarity between the crRNA guide and matching target RNA sequence. In contrast, effector complexes of DNA targeting types I, II, and V CRISPR-Cas systems require a guide complementary target and additionally the presence of a specific short (1-5 nucleotide) protospacer adjacent motif (PAM) for nuclease activation (and nuclease recruitment) (19, 66). Type IV systems borrow the adaptation complex from type I systems and this is reflected in the observed consensus PAM (20). However, it is not known whether the PAM is required for the yet to be defined defense activities of type IV systems (67). Since PAMs limit the targeting ability of crRNPs, researchers wanting to remove this constraint on potential target sequences have done so through mutagenesis (32, 68, 69). Instead of a PAM, some type III complexes require a specific protospacer flanking sequence (PFS) on the crRNP-bound target RNA to activate the DNase and cOA synthetase in Cas10.

In both *P. furiosus* and *Thermotoga maritima* the Cmr complex DNase catalytic site is variably activated by target RNAs depending on the identities of the first three nucleotides adjacent to the 3' end of the guide-complementary region (12, 34, 70). In *T. maritima* only complementary nucleotides at all three positions deactivates DNase activity while in *P. furiosus*, complementary nucleotides at all three positions is one of the 28 combinations that inhibits interference activity. Interestingly, only a subset of DNase activating PFSs additionally activate cOA production in *P. furiosus* (34). *Thermus thermophilus* and *S. thermophilus* Csm DNase activity is switched on when the crRNP is bound to a target RNA with a non-complementary PFS *in vitro* (15, 71). A target RNA with a complementary PFS or without any PFS does not activate this activity (71). In vivo,

the type III-A system of *S. epidermidis* blocks target plasmid conjugation if the transcribed target has a PFS lacking complementarity at positions (-2)'-(-5)' (72).

Type III systems are thought to use complementarity between the repeat derived 5' tag and PFS to inactivate interference mechanisms if bound to a host CRISPR array-derived anti-sense RNA (11, 12, 54, 73). Crystal and cryo-EM structures of Cmr and Csm complexes in the absence and presence of cognate target RNAs have helped elucidate the mechanism of catalytic site activation in these systems (42, 46, 47, 49, 74, 75). A non-cognate target RNA (NTR) (not defense activating) is defined as a complementary protospacer sequence in which the 5' tag and PFS are complementary while a cognate target RNA (CTR) (defense activation) is defined as a complementary protospacer that lacks a 5' tag complementary PFS (Figure 1.4). Differences in the structure of the NTR or CTR bound Csm crRNP show shifting throughout the complex that correlate with DNase activation and cOA synthesis (47, 48). With the NTR bound, the 5' tag and PFS can form an RNA duplex from positions (-2)-(-5). A loop region near the HD DNase pocket that is locked in place when no target RNA is bound or with a bound NTR, shifts when bound to a CTR and when this linker is mutated, DNase and cOA synthesis activities are lost (47, 48).

What is still not well understood, is if all cognate target PFS sequences activate interference to the same extent. In Chapter 3, I examine PFS-dependent type III-A system activation utilizing Csm expression systems of *S. thermophilus*, *S. epidermidis*, and *L. lactis*. I show that plasmid interference with each system are activated by a majority of possible 8-nucleotide PFSs and in a range of activation levels. I further show this holds true in the native *S. thermophilus* host. In addition, I determined the components and catalytic sites of the *S. thermophilus* Csm system that are necessary for plasmid interference.

References

1. Burstein, D., C.L. Sun, C.T. Brown, I. Sharon, K. Anantharaman, A.J. Probst, B.C. Thomas, and J.F. Banfield, *Major bacterial lineages are essentially devoid of CRISPR-Cas viral defence systems.* Nat Commun, 2016. **7**: p. 10613.
2. Barrangou, R., C. Fremaux, H. Deveau, M. Richards, P. Boyaval, S. Moineau, D.A. Romero, and P. Horvath, *CRISPR provides acquired resistance against viruses in prokaryotes.* Science, 2007. **315**(5819): p. 1709-12.
3. Mojica, F.J., C. Diez-Villasenor, J. Garcia-Martinez, and E. Soria, *Intervening sequences of regularly spaced prokaryotic repeats derive from foreign genetic elements.* J Mol Evol, 2005. **60**(2): p. 174-82.
4. Makarova, K.S., D.H. Haft, R. Barrangou, S.J. Brouns, E. Charpentier, P. Horvath, S. Moineau, F.J. Mojica, Y.I. Wolf, A.F. Yakunin, J. van der Oost, and E.V. Koonin, *Evolution and classification of the CRISPR-Cas systems.* Nat Rev Microbiol, 2011. **9**(6): p. 467-77.
5. Carte, J., R.T. Christopher, J.T. Smith, S. Olson, R. Barrangou, S. Moineau, C.V. Glover, 3rd, B.R. Graveley, R.M. Terns, and M.P. Terns, *The three major types of CRISPR-Cas systems function independently in CRISPR RNA biogenesis in Streptococcus thermophilus.* Mol Microbiol, 2014. **93**(1): p. 98-112.
6. Hale, C.R., S. Majumdar, J. Elmore, N. Pfister, M. Compton, S. Olson, A.M. Resch, C.V. Glover, 3rd, B.R. Graveley, R.M. Terns, and M.P. Terns, *Essential features and rational design of CRISPR RNAs that function with the Cas RAMP module complex to cleave RNAs.* Mol Cell, 2012. **45**(3): p. 292-302.

7. Terns, R.M. and M.P. Terns, *CRISPR-based technologies: prokaryotic defense weapons repurposed.* Trends Genet, 2014. **30**(3): p. 111-8.

8. Makarova, K.S., Y.I. Wolf, J. Iranzo, S.A. Shmakov, O.S. Alkhnbashi, S.J.J. Brouns, E. Charpentier, D. Cheng, D.H. Haft, P. Horvath, S. Moineau, F.J.M. Mojica, D. Scott, S.A. Shah, V. Siksnys, M.P. Terns, C. Venclovas, M.F. White, A.F. Yakunin, W. Yan, F. Zhang, R.A. Garrett, R. Backofen, J. van der Oost, R. Barrangou, and E.V. Koonin, *Evolutionary classification of CRISPR-Cas systems: a burst of class 2 and derived variants.* Nat Rev Microbiol, 2020. **18**(2): p. 67-83.

9. Plagens, A., V. Tripp, M. Daume, K. Sharma, A. Klingl, A. Hrle, E. Conti, H. Urlaub, and L. Randau, *In vitro assembly and activity of an archaeal CRISPR-Cas type I-A Cascade interference complex.* Nucleic Acids Res, 2014. **42**(8): p. 5125-38.

10. Westra, E.R., P.B. van Erp, T. Kunne, S.P. Wong, R.H. Staals, C.L. Seegers, S. Bollen, M.M. Jore, E. Semenova, K. Severinov, W.M. de Vos, R.T. Dame, R. de Vries, S.J. Brouns, and J. van der Oost, *CRISPR immunity relies on the consecutive binding and degradation of negatively supercoiled invader DNA by Cascade and Cas3.* Mol Cell, 2012. **46**(5): p. 595-605.

11. Samai, P., N. Pyenson, W. Jiang, G.W. Goldberg, A. Hatoum-Aslan, and L.A. Marraffini, *Co-transcriptional DNA and RNA Cleavage during Type III CRISPR-Cas Immunity.* Cell, 2015. **161**(5): p. 1164-1174.

12. Elmore, J.R., N.F. Sheppard, N. Ramia, T. Deighan, H. Li, R.M. Terns, and M.P. Terns, *Bipartite recognition of target RNAs activates DNA cleavage by the Type III-B CRISPR-Cas system.* Genes Dev, 2016. **30**(4): p. 447-59.

13. Tamulaitis, G., C. Venclovas, and V. Siksnys, *Type III CRISPR-Cas Immunity: Major Differences Brushed Aside.* Trends Microbiol, 2017. **25**(1): p. 49-61.

14. Kazlauskiene, M., G. Kostiuk, C. Venclovas, G. Tamulaitis, and V. Siksnys, *A cyclic oligonucleotide signaling pathway in type III CRISPR-Cas systems.* Science, 2017. **357**(6351): p. 605-609.

15. Kazlauskiene, M., G. Tamulaitis, G. Kostiuk, C. Venclovas, and V. Siksnys, *Spatiotemporal Control of Type III-A CRISPR-Cas Immunity: Coupling DNA Degradation with the Target RNA Recognition.* Mol Cell, 2016. **62**(2): p. 295-306.

16. Jiang, W., P. Samai, and L.A. Marraffini, *Degradation of Phage Transcripts by CRISPR-Associated RNases Enables Type III CRISPR-Cas Immunity.* Cell, 2016. **164**(4): p. 710-21.

17. Estrella, M.A., F.T. Kuo, and S. Bailey, *RNA-activated DNA cleavage by the Type III-B CRISPR-Cas effector complex.* Genes Dev, 2016. **30**(4): p. 460-70.

18. Niewoehner, O., C. Garcia-Doval, J.T. Rostol, C. Berk, F. Schwede, L. Bigler, J. Hall, L.A. Marraffini, and M. Jinek, *Type III CRISPR-Cas systems produce cyclic oligoadenylate second messengers.* Nature, 2017. **548**(7669): p. 543-548.

19. Makarova, K.S., Y.I. Wolf, O.S. Alkhnbashi, F. Costa, S.A. Shah, S.J. Saunders, R. Barrangou, S.J. Brouns, E. Charpentier, D.H. Haft, P. Horvath, S. Moineau, F.J. Mojica, R.M. Terns, M.P. Terns, M.F. White, A.F. Yakunin, R.A. Garrett, J. van der Oost, R. Backofen, and E.V. Koonin, *An updated evolutionary classification of CRISPR-Cas systems.* Nat Rev Microbiol, 2015. **13**(11): p. 722-36.

20. Pinilla-Redondo, R., D. Mayo-Munoz, J. Russel, R.A. Garrett, L. Randau, S.J. Sorensen, and S.A. Shah, *Type IV CRISPR-Cas systems are highly diverse and involved in competition between plasmids.* Nucleic Acids Res, 2020. **48**(4): p. 2000-2012.

21. Koonin, E.V. and K.S. Makarova, *Mobile Genetic Elements and Evolution of CRISPR-Cas Systems: All the Way There and Back.* Genome Biol Evol, 2017. **9**(10): p. 2812-2825.

22. Yan, W.X., P. Hunnewell, L.E. Alfonse, J.M. Carte, E. Keston-Smith, S. Sothiselvam, A.J. Garrity, S. Chong, K.S. Makarova, E.V. Koonin, D.R. Cheng, and D.A. Scott, *Functionally diverse type V CRISPR-Cas systems.* Science, 2019. **363**(6422): p. 88-91.

23. Shmakov, S., O.O. Abudayyeh, K.S. Makarova, Y.I. Wolf, J.S. Gootenberg, E. Semenova, L. Minakhin, J. Joung, S. Konermann, K. Severinov, F. Zhang, and E.V. Koonin, *Discovery and Functional Characterization of Diverse Class 2 CRISPR-Cas Systems.* Mol Cell, 2015. **60**(3): p. 385-97.

24. Chen, J.S., E. Ma, L.B. Harrington, M. Da Costa, X. Tian, J.M. Palefsky, and J.A. Doudna, *CRISPR-Cas12a target binding unleashes indiscriminate single-stranded DNase activity.* Science, 2018. **360**(6387): p. 436-439.

25. Abudayyeh, O.O., J.S. Gootenberg, S. Konermann, J. Joung, I.M. Slaymaker, D.B. Cox, S. Shmakov, K.S. Makarova, E. Semenova, L. Minakhin, K. Severinov, A. Regev, E.S. Lander, E.V. Koonin, and F. Zhang, *C2c2 is a single-component programmable RNA-guided RNA-targeting CRISPR effector.* Science, 2016. **353**(6299): p. aaf5573.

26. Ackerman, C.M., C. Myhrvold, S.G. Thakku, C.A. Freije, H.C. Metsky, D.K. Yang, S.H. Ye, C.K. Boehm, T.F. Kosoko-Thoroddsen, J. Kehe, T.G. Nguyen, A. Carter, A. Kulesa, J.R. Barnes, V.G. Dugan, D.T. Hung, P.C. Blainey, and P.C. Sabeti, *Massively multiplexed nucleic acid detection with Cas13.* Nature, 2020. **582**(7811): p. 277-282.

27. Freije, C.A., C. Myhrvold, C.K. Boehm, A.E. Lin, N.L. Welch, A. Carter, H.C. Metsky, C.Y. Luo, O.O. Abudayyeh, J.S. Gootenberg, N.L. Yozwiak, F. Zhang, and P.C. Sabeti, *Programmable Inhibition and Detection of RNA Viruses Using Cas13.* Mol Cell, 2019. **76**(5): p. 826-837 e11.

28. Gootenberg, J.S., O.O. Abudayyeh, J.W. Lee, P. Essletzbichler, A.J. Dy, J. Joung, V. Verdine, N. Donghia, N.M. Daringer, C.A. Freije, C. Myhrvold, R.P. Bhattacharyya, J. Livny, A. Regev, E.V. Koonin, D.T. Hung, P.C. Sabeti, J.J. Collins, and F. Zhang, *Nucleic acid detection with CRISPR-Cas13a/C2c2.* Science, 2017. **356**(6336): p. 438-442.

29. Kellner, M.J., J.G. Koob, J.S. Gootenberg, O.O. Abudayyeh, and F. Zhang, *SHERLOCK: nucleic acid detection with CRISPR nucleases.* Nat Protoc, 2019. **14**(10): p. 2986-3012.

30. Deltcheva, E., K. Chylinski, C.M. Sharma, K. Gonzales, Y. Chao, Z.A. Pirzada, M.R. Eckert, J. Vogel, and E. Charpentier, *CRISPR RNA maturation by trans-encoded small RNA and host factor RNase III.* Nature, 2011. **471**(7340): p. 602-7.

31. Fonfara, I., H. Richter, M. Bratovic, A. Le Rhun, and E. Charpentier, *The CRISPR-associated DNA-cleaving enzyme Cpf1 also processes precursor CRISPR RNA.* Nature, 2016. **532**(7600): p. 517-21.

32. Slaymaker, I.M., P. Mesa, M.J. Kellner, S. Kannan, E. Brignole, J. Koob, P.R. Feliciano, S. Stella, O.O. Abudayyeh, J.S. Gootenberg, J. Strecker, G. Montoya, and F. Zhang, *High-Resolution Structure of Cas13b and Biochemical Characterization of RNA Targeting and Cleavage.* Cell Rep, 2019. **26**(13): p. 3741-3751 e5.

33. Chou-Zheng, L. and A. Hatoum-Aslan, *Expression and Purification of the Cas10-Csm Complex from Staphylococci.* Bio Protoc, 2017. **7**(11).

34. Foster, K., S. Gruschow, S. Bailey, M.F. White, and M.P. Terns, *Regulation of the RNA and DNA nuclease activities required for Pyrococcus furiosus Type III-B CRISPR-Cas immunity.* Nucleic Acids Res, 2020. **48**(8): p. 4418-4434.

35. Nunez, J.K., P.J. Kranzusch, J. Noeske, A.V. Wright, C.W. Davies, and J.A. Doudna, *Cas1-Cas2 complex formation mediates spacer acquisition during CRISPR-Cas adaptive immunity.* Nat Struct Mol Biol, 2014. **21**(6): p. 528-34.

36. Shiimori, M., S.C. Garrett, B.R. Graveley, and M.P. Terns, *Cas4 Nucleases Define the PAM, Length, and Orientation of DNA Fragments Integrated at CRISPR Loci.* Mol Cell, 2018. **70**(5): p. 814-824 e6.

37. Silas, S., G. Mohr, D.J. Sidote, L.M. Markham, A. Sanchez-Amat, D. Bhaya, A.M. Lambowitz, and A.Z. Fire, *Direct CRISPR spacer acquisition from RNA by a natural reverse transcriptase-Cas1 fusion protein.* Science, 2016. **351**(6276): p. aad4234.

38. Wakefield, N., R. Rajan, and E.J. Sontheimer, *Primary processing of CRISPR RNA by the endonuclease Cas6 in Staphylococcus epidermidis.* FEBS Lett, 2015. **589**(20 Pt B): p. 3197-204.

39. Osawa, T., H. Inanaga, C. Sato, and T. Numata, *Crystal structure of the CRISPR-Cas RNA silencing Cmr complex bound to a target analog.* Mol Cell, 2015. **58**(3): p. 418-30.

40. Mogila, I., M. Kazlauskiene, S. Valinskyte, G. Tamulaitiene, G. Tamulaitis, and V. Siksnys, *Genetic Dissection of the Type III-A CRISPR-Cas System Csm Complex Reveals Roles of Individual Subunits.* Cell Rep, 2019. **26**(10): p. 2753-2765 e4.

41. Osawa, T., H. Inanaga, and T. Numata, *Crystal structure of the Cmr2-Cmr3 subcomplex in the CRISPR-Cas RNA silencing effector complex.* J Mol Biol, 2013. **425**(20): p. 3811-23.

42. Spilman, M., A. Cocozaki, C. Hale, Y. Shao, N. Ramia, R. Terns, M. Terns, H. Li, and S. Stagg, *Structure of an RNA silencing complex of the CRISPR-Cas immune system.* Mol Cell, 2013. **52**(1): p. 146-52.

43. Staals, R.H., Y. Zhu, D.W. Taylor, J.E. Kornfeld, K. Sharma, A. Barendregt, J.J. Koehorst, M. Vlot, N. Neupane, K. Varossieau, K. Sakamoto, T. Suzuki, N. Dohmae, S. Yokoyama, P.J. Schaap, H. Urlaub, A.J. Heck, E. Nogales, J.A. Doudna, A. Shinkai, and J. van der Oost, *RNA targeting by the type III-A CRISPR-Cas Csm complex of Thermus thermophilus.* Mol Cell, 2014. **56**(4): p. 518-30.

44. Venclovas, C., *Structure of Csm2 elucidates the relationship between small subunits of CRISPR-Cas effector complexes.* FEBS Lett, 2016. **590**(10): p. 1521-9.

45. Sun, J., J.H. Jeon, M. Shin, H.C. Shin, B.H. Oh, and J.S. Kim, *Crystal structure and CRISPR RNA-binding site of the Cmr1 subunit of the Cmr interference complex.* Acta Crystallogr D Biol Crystallogr, 2014. **70**(Pt 2): p. 535-43.

46. Taylor, D.W., Y. Zhu, R.H. Staals, J.E. Kornfeld, A. Shinkai, J. van der Oost, E. Nogales, and J.A. Doudna, *Structural biology. Structures of the CRISPR-Cmr complex reveal mode of RNA target positioning.* Science, 2015. **348**(6234): p. 581-5.

47. Jia, N., C.Y. Mo, C. Wang, E.T. Eng, L.A. Marraffini, and D.J. Patel, *Type III-A CRISPR-Cas Csm Complexes: Assembly, Periodic RNA Cleavage, DNase Activity Regulation, and Autoimmunity.* Mol Cell, 2019. **73**(2): p. 264-277 e5.

48. You, L., J. Ma, J. Wang, D. Artamonova, M. Wang, L. Liu, H. Xiang, K. Severinov, X. Zhang, and Y. Wang, *Structure Studies of the CRISPR-Csm Complex Reveal Mechanism of Co-transcriptional Interference.* Cell, 2019. **176**(1-2): p. 239-253 e16.

49. Benda, C., J. Ebert, R.A. Scheltema, H.B. Schiller, M. Baumgartner, F. Bonneau, M. Mann, and E. Conti, *Structural model of a CRISPR RNA-silencing complex reveals the RNA-target cleavage activity in Cmr4.* Mol Cell, 2014. **56**(1): p. 43-54.

50. Hrle, A., A.A. Su, J. Ebert, C. Benda, L. Randau, and E. Conti, *Structure and RNA-binding properties of the type III-A CRISPR-associated protein Csm3.* RNA Biol, 2013. **10**(11): p. 1670-8.

51. Numata, T., H. Inanaga, C. Sato, and T. Osawa, *Crystal structure of the Csm3-Csm4 subcomplex in the type III-A CRISPR-Cas interference complex.* J Mol Biol, 2015. **427**(2): p. 259-73.

52. Zhu, X. and K. Ye, *Cmr4 is the slicer in the RNA-targeting Cmr CRISPR complex.* Nucleic Acids Res, 2015. **43**(2): p. 1257-67.

53. Hale, C.R., A. Cocozaki, H. Li, R.M. Terns, and M.P. Terns, *Target RNA capture and cleavage by the Cmr type III-B CRISPR-Cas effector complex.* Genes Dev, 2014. **28**(21): p. 2432-43.

54. Tamulaitis, G., M. Kazlauskiene, E. Manakova, C. Venclovas, A.O. Nwokeoji, M.J. Dickman, P. Horvath, and V. Siksnys, *Programmable RNA shredding by the type III-A CRISPR-Cas system of Streptococcus thermophilus.* Mol Cell, 2014. **56**(4): p. 506-17.

55. Jung, T.Y., Y. An, K.H. Park, M.H. Lee, B.H. Oh, and E. Woo, *Crystal structure of the Csm1 subunit of the Csm complex and its single-stranded DNA-specific nuclease activity.* Structure, 2015. **23**(4): p. 782-90.

56. Rouillon, C., J.S. Athukoralage, S. Graham, S. Gruschow, and M.F. White, *Control of cyclic oligoadenylate synthesis in a type III CRISPR system.* Elife, 2018. **7**.

57. Liu, T.Y., J.J. Liu, A.J. Aditham, E. Nogales, and J.A. Doudna, *Target preference of Type III-A CRISPR-Cas complexes at the transcription bubble.* Nat Commun, 2019. **10**(1): p. 3001.

58. Nasef, M., M.C. Muffly, A.B. Beckman, S.J. Rowe, F.C. Walker, A. Hatoum-Aslan, and J.A. Dunkle, *Regulation of cyclic oligoadenylate synthesis by the Staphylococcus epidermidis Cas10-Csm complex.* RNA, 2019. **25**(8): p. 948-962.

59. Athukoralage, J.S., C. Rouillon, S. Graham, S. Gruschow, and M.F. White, *Ring nucleases deactivate type III CRISPR ribonucleases by degrading cyclic oligoadenylate.* Nature, 2018. **562**(7726): p. 277-280.

60. Garcia-Doval, C., F. Schwede, C. Berk, J.T. Rostol, O. Niewoehner, O. Tejero, J. Hall, L.A. Marraffini, and M. Jinek, *Activation and self-inactivation mechanisms of the cyclic oligoadenylate-dependent CRISPR ribonuclease Csm6.* Nat Commun, 2020. **11**(1): p. 1596.

61. Jia, N., R. Jones, G. Yang, O. Ouerfelli, and D.J. Patel, *CRISPR-Cas III-A Csm6 CARF Domain Is a Ring Nuclease Triggering Stepwise cA4 Cleavage with ApA>p Formation Terminating RNase Activity.* Mol Cell, 2019. **75**(5): p. 944-956 e6.

62. Molina, R., S. Stella, M. Feng, N. Sofos, V. Jauniskis, I. Pozdnyakova, B. Lopez-Mendez, Q. She, and G. Montoya, *Structure of Csx1-cOA4 complex reveals the basis of RNA decay in Type III-B CRISPR-Cas.* Nat Commun, 2019. **10**(1): p. 4302.

63. Sheppard, N.F., C.V. Glover, 3rd, R.M. Terns, and M.P. Terns, *The CRISPR-associated Csx1 protein of Pyrococcus furiosus is an adenosine-specific endoribonuclease.* RNA, 2016. **22**(2): p. 216-24.

64. Gruschow, S., J.S. Athukoralage, S. Graham, T. Hoogeboom, and M.F. White, *Cyclic oligoadenylate signalling mediates Mycobacterium tuberculosis CRISPR defence.* Nucleic Acids Res, 2019. **47**(17): p. 9259-9270.

65. Rostol, J.T. and L.A. Marraffini, *Non-specific degradation of transcripts promotes plasmid clearance during type III-A CRISPR-Cas immunity.* Nat Microbiol, 2019. **4**(4): p. 656-662.

66. Jore, M.M., M. Lundgren, E. van Duijn, J.B. Bultema, E.R. Westra, S.P. Waghmare, B. Wiedenheft, U. Pul, R. Wurm, R. Wagner, M.R. Beijer, A. Barendregt, K. Zhou, A.P. Snijders, M.J. Dickman, J.A. Doudna, E.J. Boekema, A.J. Heck, J. van der Oost, and S.J. Brouns, *Structural basis for CRISPR RNA-guided DNA recognition by Cascade.* Nat Struct Mol Biol, 2011. **18**(5): p. 529-36.

67. Newire, E., A. Aydin, S. Juma, V.I. Enne, and A.P. Roberts, *Identification of a Type IV-A CRISPR-Cas System Located Exclusively on IncHI1B/IncFIB Plasmids in Enterobacteriaceae.* Front Microbiol, 2020. **11**: p. 1937.

68. Gao, L., D.B.T. Cox, W.X. Yan, J.C. Manteiga, M.W. Schneider, T. Yamano, H. Nishimasu, O. Nureki, N. Crosetto, and F. Zhang, *Engineered Cpf1 variants with altered PAM specificities.* Nat Biotechnol, 2017. **35**(8): p. 789-792.

69. Kleinstiver, B.P., M.S. Prew, S.Q. Tsai, V.V. Topkar, N.T. Nguyen, Z. Zheng, A.P. Gonzales, Z. Li, R.T. Peterson, J.R. Yeh, M.J. Aryee, and J.K. Joung, *Engineered CRISPR-Cas9 nucleases with altered PAM specificities.* Nature, 2015. **523**(7561): p. 481-5.

70. Johnson, K., B.A. Learn, M.A. Estrella, and S. Bailey, *Target sequence requirements of a type III-B CRISPR-Cas immune system.* J Biol Chem, 2019. **294**(26): p. 10290-10299.

71. Liu, T.Y., A.T. Iavarone, and J.A. Doudna, *RNA and DNA Targeting by a Reconstituted Thermus thermophilus Type III-A CRISPR-Cas System.* PLoS One, 2017. **12**(1): p. e0170552.

72. Marraffini, L.A. and E.J. Sontheimer, *Self versus non-self discrimination during CRISPR RNA-directed immunity.* Nature, 2010. **463**(7280): p. 568-71.

73. Pyenson, N.C., K. Gayvert, A. Varble, O. Elemento, and L.A. Marraffini, *Broad Targeting Specificity during Bacterial Type III CRISPR-Cas Immunity Constrains Viral Escape.* Cell Host Microbe, 2017. **22**(3): p. 343-353 e3.

74. Dorsey, B.W., L. Huang, and A. Mondragon, *Structural organization of a Type III-A CRISPR effector subcomplex determined by X-ray crystallography and cryo-EM.* Nucleic Acids Res, 2019. **47**(7): p. 3765-3783.

75. Guo, M., K. Zhang, Y. Zhu, G.D. Pintilie, X. Guan, S. Li, M.F. Schmid, Z. Ma, W. Chiu, and Z. Huang, *Coupling of ssRNA cleavage with DNase activity in type III-A CRISPR-Csm revealed by cryo-EM and biochemistry.* Cell Res, 2019. **29**(4): p. 305-312.

Figure 1.1 CRISPR-Cas defense. During host infection, adaptation occurs when a fragment of invader DNA called a protospacer is integrated into the host genome within the CRISPR locus generating a new spacer adjacent to the leader sequence. Recognition and selection of new spacers is often dependent on an adjacent sequence (protospacer adjacent motif (PAM) or protospacer flanking sequence (PFS)) specific to each CRISPR system. The CRISPR array is transcribed into a pre-crRNA and processed during crRNA biogenesis. Once formed together with a Cas protein complex (crRNA-ribonucleoprotein (crRNP), the crRNA guides the crRNP to bind and cleave the invader nucleic acid during invader silencing. Adapted from Terns and Terns 2014 (7).

-

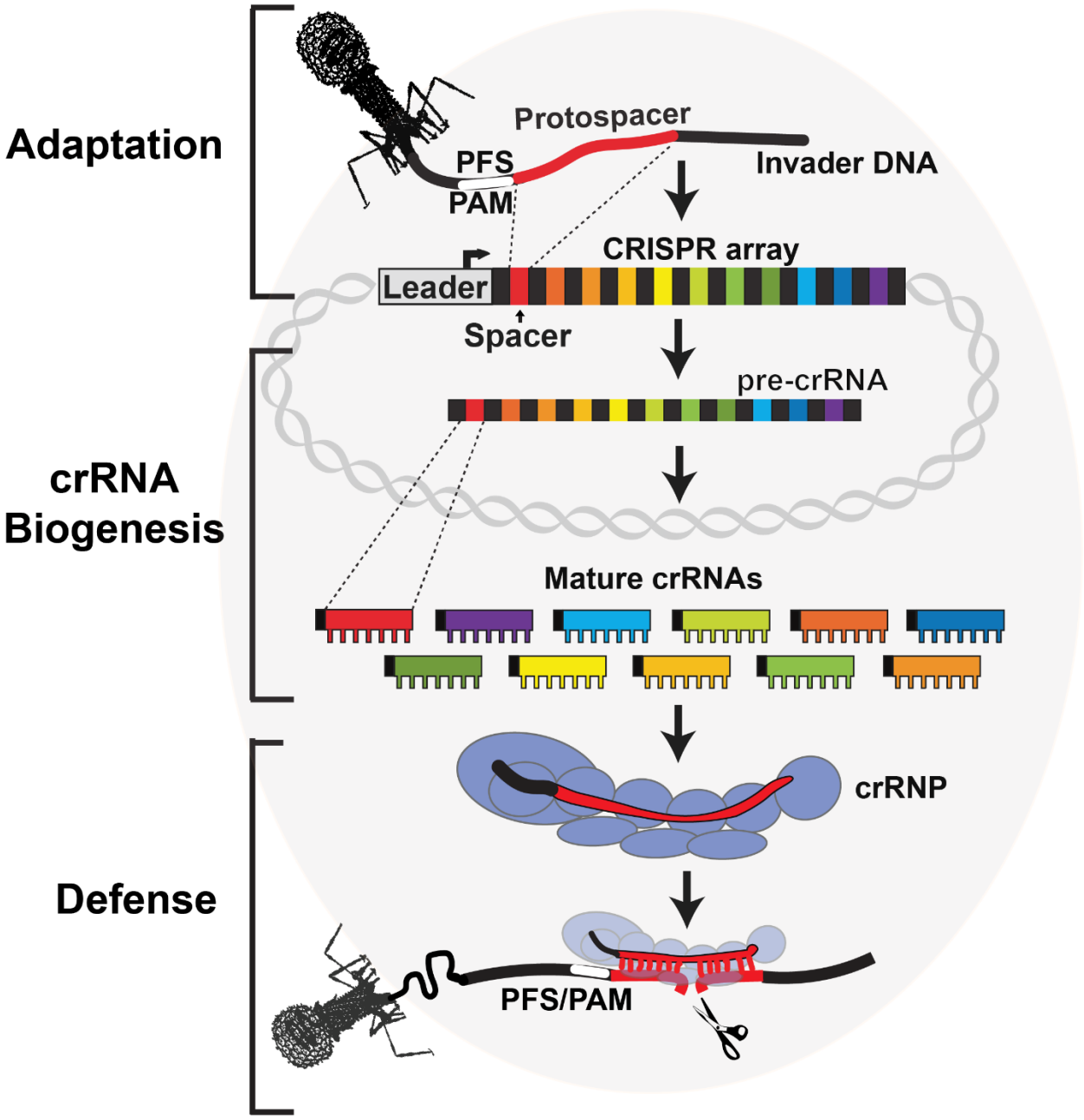
Adaptation
Protospacer
PFS
PAM
Invader DNA
CRISPR array
Leader
Spacer
pre-crRNA
crRNA
Biogenesis
Mature crRNAs
crRNP
Defense
PFS/PAM

Figure 1.2 Classification of CRISPR-Cas systems. (A) Representative arrangements of class 1 and class 2 CRISPR-Cas loci. Dashed outlines indicate variable members of loci. (B) Representative functional modules for each CRISPR-Cas type with description of roles each element plays in adaptation and defense. Adapted from Makarova et al. 2020 (8).

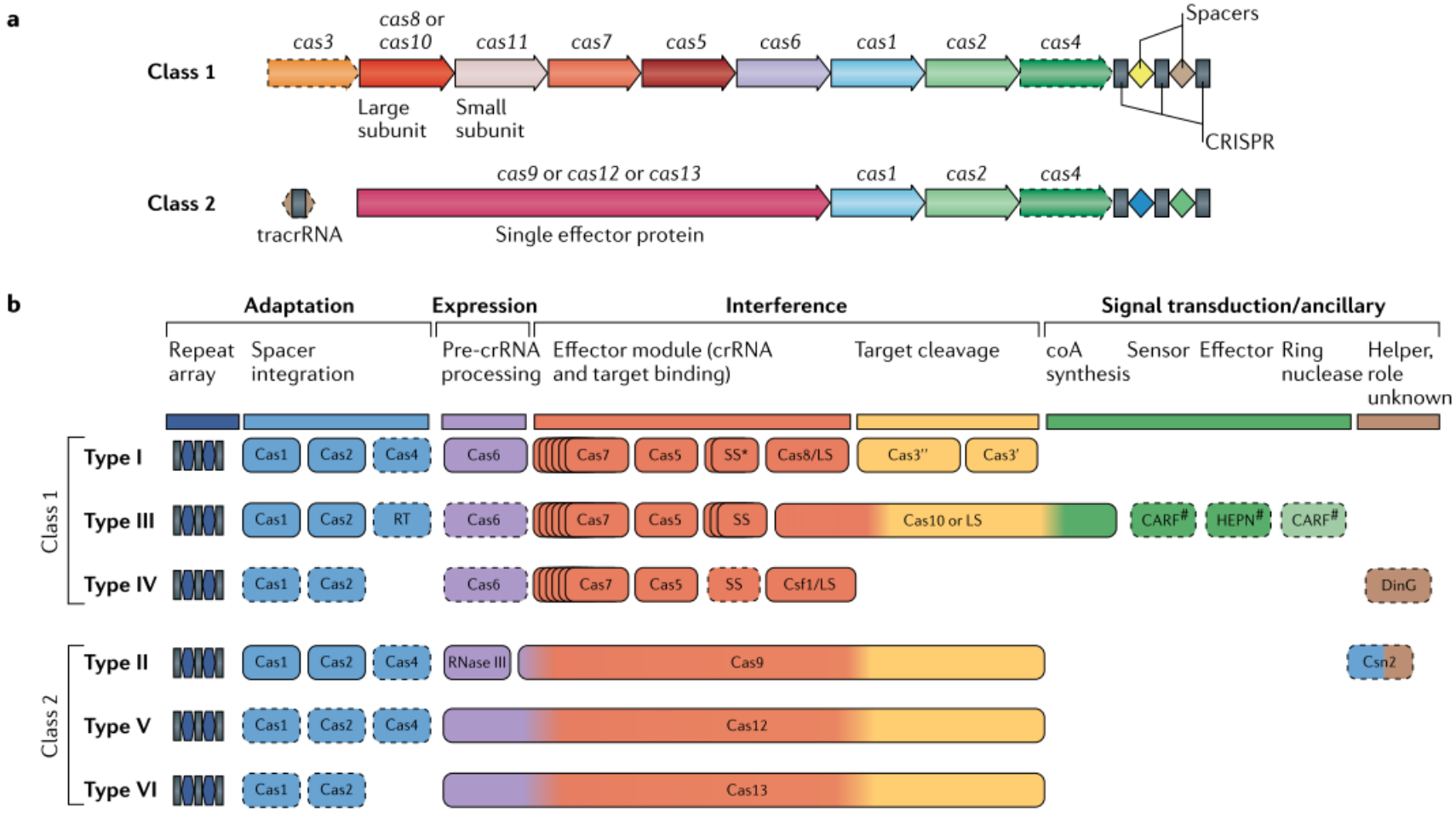
a
Class 1
cas3
cas8 or cas10
cas11
cas7
cas5
cas6
cas1
cas2
cas4
Spacers
CRISPR
Large subunit
Small subunit
Class 2
cas9 or cas12 or cas13
cas1
cas2
cas4
tracrRNA
Single effector protein
b
Adaptation
Expression
Interference
Signal transduction/ancillary
Repeat array
Spacer integration
Pre-crRNA processing
Effector module (crRNA and target binding)
Target cleavage
coA synthesis
Sensor
Effector
Ring nuclease
Helper, role unknown
Class 1
Type I
Cas1
Cas2
Cas4
Cas6
Cas7
Cas5
SS*
Cas8/LS
Cas3''
Cas3'
Type III
Cas1
Cas2
RT
Cas6
Cas7
Cas5
SS
Cas10 or LS
CARF#
HEPN#
CARF#
Type IV
Cas1
Cas2
Cas6
Cas7
Cas5
SS
Csf1/LS
DinG
Class 2
Type II
Cas1
Cas2
Cas4
RNase III
Cas9
Csn2
Type V
Cas1
Cas2
Cas4
Cas12
Type VI
Cas1
Cas2
Cas13

Figure 1.3 Subclassification of type III. Schematic of representative CRISPR–Cas loci of each type III subtype. Dendrogram on the left shows the likely evolutionary relationships between the subtypes. The organism and gene range are shown on the right. Homologous genes are color-coded and identified by a superfamily name. Where both a systematic name and a legacy name are commonly used, the legacy name is given under the systematic name. The small subunit is encoded by *csm2* and *cmr5* denoted cas11. The adaptation module genes *cas1* and *cas2* are dispensable in subtypes III-A and III-E (dashed lines). *cas10* regions colored cream represent the HD nuclease domain. Functionally uncharacterized genes are shown in gray. The teal shading shows genes belonging to the effector complex module. The known nucleic acid substrates are indicated. Most of the subtype III-B, III-C, III-E and III-F loci lack CRISPR arrays and are shown accordingly, although for each of the type III subtypes exceptions have been detected. RT, reverse transcriptase; TPR , tetratricopeptide repeat. Adapted and modified from Makarova et al. 2020 (8).

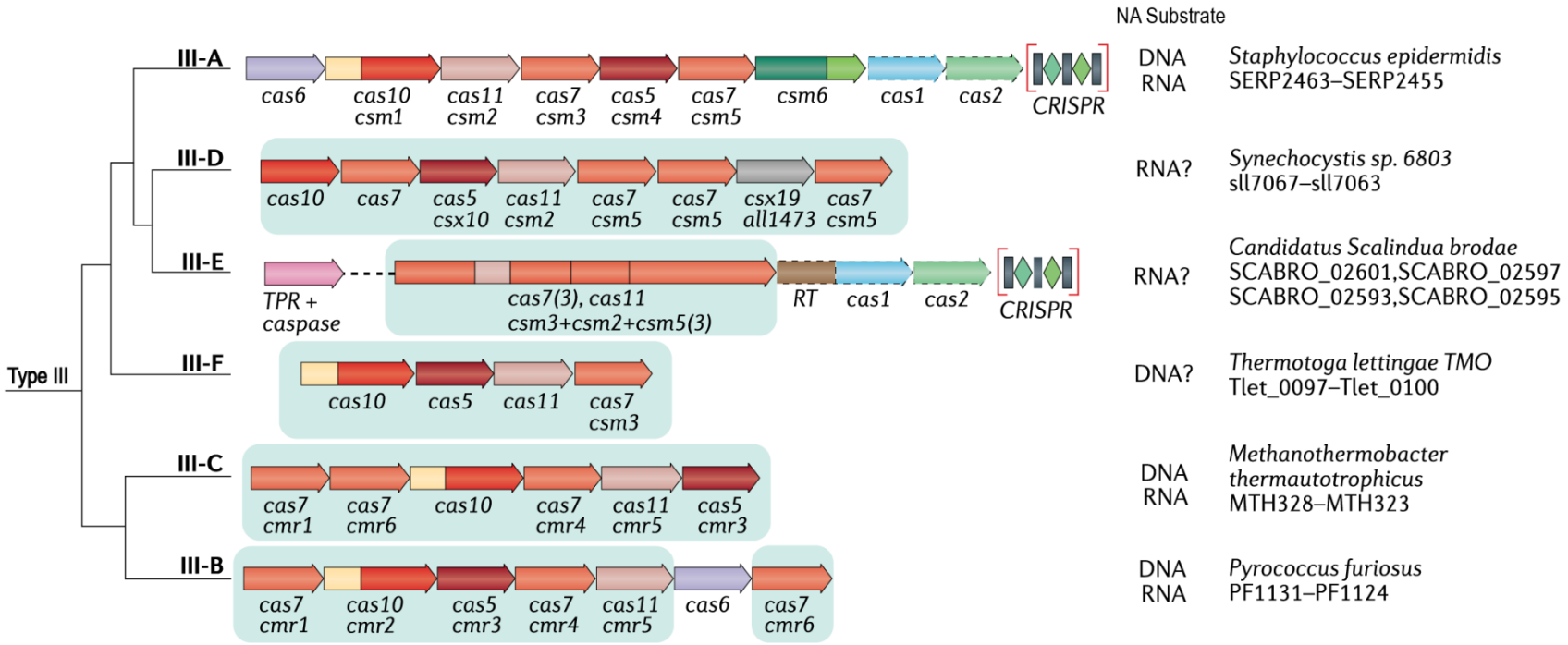
NA Substrate
Type III
III-A
cas6
cas10 csm1
cas11 csm2
cas7 csm3
cas5 csm4
cas7 csm5
csm6
cas1
cas2
CRISPR
DNA RNA
Staphylococcus epidermidis SERP2463–SERP2455
III-D
cas10
cas7
cas5 csx10
cas11 csm2
cas7 csm5
cas7 csm5
csx19 all1473
cas7 csm5
RNA?
Synechocystis sp. 6803 sll7067–sll7063
III-E
TPR + caspase
cas7(3), cas11 csm3+csm2+csm5(3)
RT
cas1
cas2
CRISPR
RNA?
Candidatus Scalindua brodae SCABRO_02601,SCABRO_02597 SCABRO_02593,SCABRO_02595
III-F
cas10
cas5
cas11
cas7 csm3
DNA?
Thermotoga lettingae TMO Tlet_0097–Tlet_0100
III-C
cas7 cmr1
cas7 cmr6
cas10
cas7 cmr4
cas11 cmr5
cas5 cmr3
DNA RNA
Methanothermobacter thermautotrophicus MTH328–MTH323
III-B
cas7 cmr1
cas10 cmr2
cas5 cmr3
cas7 cmr4
cas11 cmr5
cas6
cas7 cmr6
DNA RNA
Pyrococcus furiosus PF1131–PF1124

Figure 1.4 Csm crRNP bound to cognate and non-cognate target RNA. (A) Diagram of crRNP apo-complex and an actively transcribing protospacer. (B) Diagram of a non-cognate target RNA (NTR) -bound crRNP and RNA-RNA complementarity. Complementarity between the crRNA 5' tag and PFS prevents activation of the DNase and cOA production sites (black stars). (C) Diagram of a cognate target RNA (CTR) -bound crRNP and RNA-RNA complementarity. Non-complementarity between the crRNA 5' tag and PFS activates the DNase and cOA production sites (red stars).

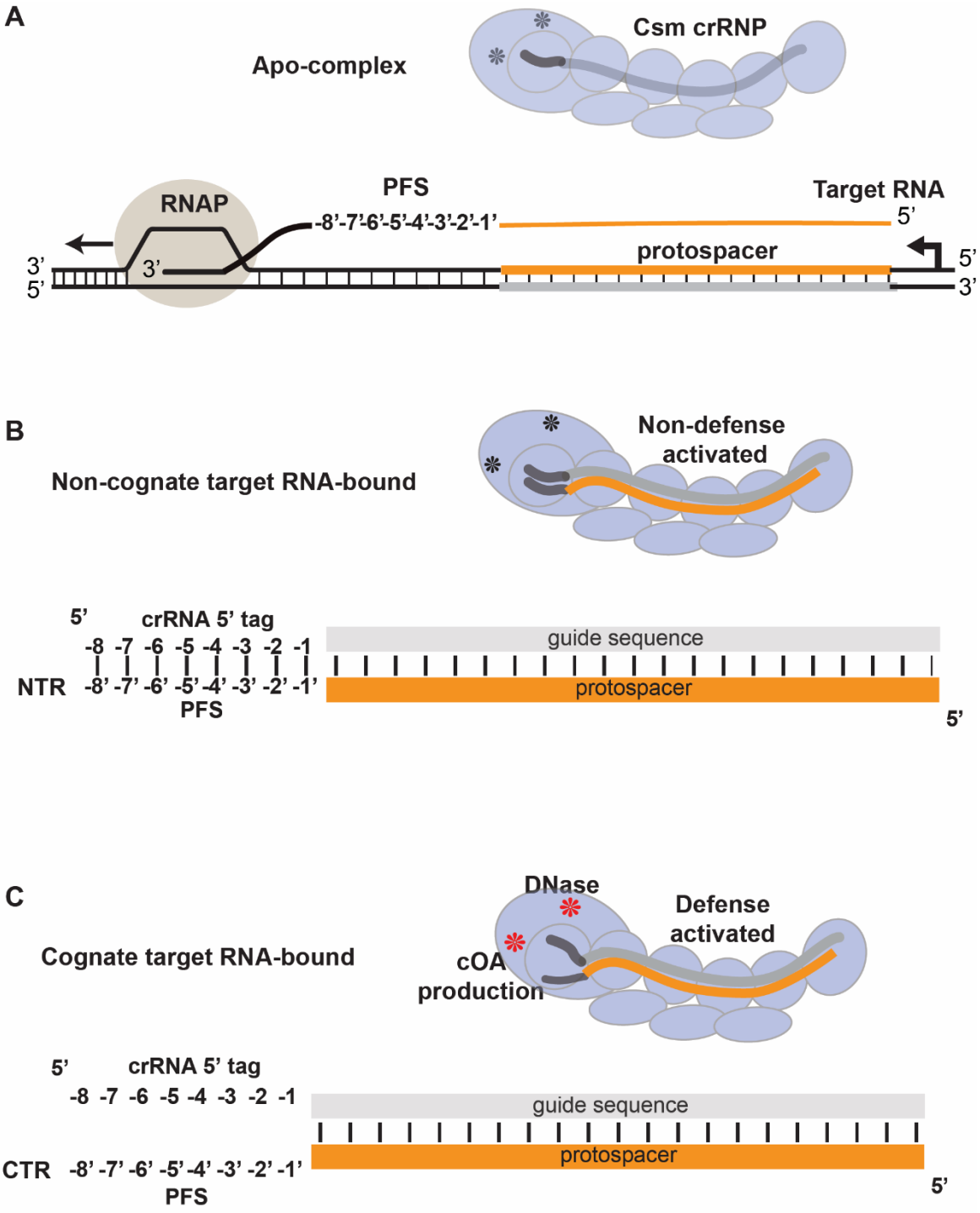
A
Apo-complex
Csm crRNP
RNAP
PFS
-8'-7'-6'-5'-4'-3'-2'-1'
Target RNA
5'
protospacer
3'
5'
3'
5'
3'
B
Non-cognate target RNA-bound
Non-defense
activated
5'
crRNA 5' tag
-8 -7 -6 -5 -4 -3 -2 -1
guide sequence
NTR
-8' -7' -6' -5' -4' -3' -2' -1'
protospacer
PFS
5'
C
Cognate target RNA-bound
DNase
Defense
activated
cOA
production
5'
crRNA 5' tag
-8 -7 -6 -5 -4 -3 -2 -1
guide sequence
CTR
-8' -7' -6' -5' -4' -3' -2' -1'
protospacer
PFS
5'

Chapter 2

TYPE III-A CRISPR SYSTEMS AS A VERSATILE GENE KNOCKDOWN TECHNOLOGY[1]

[1]Walter T. Woodside, Nikita Vantsev, and Michael P. Terns. 2020. Type III-A CRISPR systems as a versatile gene knockdown technology. bioRxiv doi: 10.1101/2020.09.25.310060. Reprinted here with permission of publisher.

ABSTRACT

CRISPR-Cas systems are functionally diverse prokaryotic anti-viral defense systems, which encompass six distinct types (I-VI) that each encode different effector Cas nucleases with distinct nucleic acid cleavage specificities. By harnessing the unique attributes of the various CRISPR-Cas systems, a range of innovative CRISPR-based DNA and RNA targeting tools and technologies have been developed. Here, we exploit the ability of type III-A CRISPR-Cas systems to carry out RNA-guided and sequence-specific target RNA cleavage for establishment of research tools for post-transcriptional control of gene expression. Type III-A systems from three bacterial species (*L. lactis*, *S. epidermidis* and *S. thermophilus*) were each expressed on a single plasmid in *E. coli* and the efficiency and specificity of gene knockdown was assessed by Northern blot analysis. We show that engineered type III-A modules can be programmed using tailored CRISPR RNAs to efficiently knock down gene expression of both coding and non-coding RNAs *in vivo*. Moreover, simultaneous degradation of multiple cellular mRNA transcripts can be directed by utilizing a CRISPR array expressing corresponding gene-targeting crRNAs. Our results demonstrate the utility of distinct type III-A modules to serve as effective gene knockdown platforms in heterologous cells. This transcriptome engineering technology has the potential to be further refined and exploited for key applications including gene discovery and gene pathway analyses in additional prokaryotic and perhaps eukaryotic cells and organisms.

INTRODUCTION

Bacteria and Archaea often harbor CRISPR-Cas systems that provide acquired immunity against viruses and other mobile genetic elements (MGEs) (1, 2). Upon invasion, a portion of prokaryotic cells integrate short (30-40 base pair) sequences from the MGE genomes into host cell CRISPR

(clustered regularly interspaced short palindromic repeat) genomic arrays to provide a heritable record of the captured MGE sequences (3, 4). Immunity requires that the CRISPR arrays are transcribed and the primary CRISPR transcripts processed to generate mature CRISPR (cr)RNAs (5-7). Subsequently, each mature crRNA associates with specific CRISPR-associated (Cas) proteins to form effector crRNPs (crRNA-Cas protein ribonucleoprotein complexes) that mediate crRNA-guided recognition and Cas nuclease-mediated destruction of invasive MGE nucleic acids to prevent further MGE infection (1, 8).

CRISPR-Cas systems are diverse and have been categorized into six distinct types (I-VI) that employ different effector Cas nucleases that target recognition and destruction of either foreign DNA (types I, II, V and possibly IV) (5, 9-11), RNA (type VI) (12) or both DNA and RNA (type III) (13-23). By harnessing the unique attributes of the various CRISPR-Cas systems (such as nucleic acid binding specificity, nuclease activity, etc.), a range of innovative CRISPR-based DNA and RNA targeting tools and technologies have been developed (e.g. for genome editing, control of gene expression, sequence-specific antibiotics, nucleic acid-based viral and pathogen diagnostics) (24-29). Tremendous potential remains to exploit our knowledge of various CRISPR systems and components for establishment of innovative research tools with associated transformative biotechnological and biomedical applications.

In this study, we sought to investigate the potential of type III-A CRISPR systems (also referred to as Csm systems (30)) to be harnessed as a gene knockdown platform in prokaryotes, akin to how RNA interference (RNAi) machinery has been used in eukaryotes for gene expression downregulation and gene discovery applications (31-33). Type III-A effector crRNPs are composed of a single crRNA stably associated with five (Csm 1-5) Cas protein subunits (17, 20, 34-39) (Figure 1A). The mature crRNAs within these complexes are generated through site-

specific cleavage of type III-A CRISPR array primary transcripts (within the repeat regions) by the Cas6 endoribonuclease (6). The processed crRNAs within the effector crRNPs contain eight nucleotides of repeat sequence at the 5' end called the 5' tag (21), followed by a ~30-40 nucleotide guide sequence that base-pairs with the target RNA protospacer. The 3' ends of the crRNAs within the complexes can have variable lengths of repeat-derived sequence (17, 20, 40). While the repeat-derived, 5' tag element is critical for function, crRNA species containing or lacking 3' end repeat sequences are each functional (20, 34, 41).

Type III-A systems can function by both DNA and RNA cleavage mechanisms that are each activated via crRNA-guided recognition of target RNA (17-20, 23, 36, 37, 39, 42-44). Target RNA recognition induces conformational changes within the crRNP (35, 45, 46) leading to activation of intrinsic DNase and RNase activities as well as triggering production of cyclic oligoadenylate (cOA) from ATP precursors (42, 47, 48). In turn, cOA serves as a second messenger that binds to and allosterically activates the RNase activity of a *trans*-acting enzyme called Csm6 (34, 42, 46-48), which has been shown to be capable of acting on both target (crRNA-matching) and non-target (cellular) RNAs (44, 49). Collectively, these multiple activities lead to a dual ability of type III-A systems to cleave DNA and RNA targets for viral or plasmid clearance or growth arrest or death of infected cells.

The structural organization of type III-A crRNPs and functional roles of the individual Csm1-6 protein subunits have been investigated and three of the subunits have been shown to be catalytic (20, 35-38, 43, 50-52). Csm1 (a Cas10 superfamily member (2)) is a large, multiple domain-containing protein that typically contains two highly conserved functional motifs: the HD motif capable of destroying single-stranded DNA (13, 14, 17) and the GGDD motif of one of two Palm domains that can convert ATP into cOA second messenger molecules (42, 47, 48, 53) (Figure

1A). Csm3 is an intrinsic RNA endoribonuclease that cleaves the target RNA in the region defined by crRNA base-pairing at regular six nucleotide intervals (typically 4-5 cuts are made, depending upon the copy number of Cmr3 RNase subunits within the III-A crRNP) (20) (Figure 1A). As noted above, Csm6 is a cOA-activated, trans-acting ribonuclease (44, 47, 49). The DNase (Csm1) and RNase (Csm3 and Csm6) activities of type III-A systems can each contribute to robust immunity against diverse viral and plasmid invaders with notable differences in the dependency on DNase or Csm6-mediated RNase for the various systems investigated (18, 34, 52, 54-56).

Two distinct regions of the target RNA control type III crRNP activities. Extensive complementary binding between the target RNA protospacer region and the crRNA guide region is required to trigger the activities. However, several studies have revealed a key role for the short, 8 nt sequence that flanks the 3' end of the RNA protospacer, termed the protospacer flanking sequence (PFS), in controlling type III activities (Figure 2.1A). If the target RNA PFS exhibits perfect or significant complementarity to the 5' tag element of the crRNA (35, 57); Figure 2.1A), then target RNA-bound crRNP becomes incapable of triggering DNase activities or cOA production (13, 17, 18, 58), but target RNA cleavage is unaffected (20, 41).

We have transplanted functional III-A systems from three bacterial species (*L. lactis*, *S. epidermidis* and *S. thermophilus*) by co-expressing the six Csm proteins, Cas6 (for processing of pre-crRNA transcripts into functional crRNAs), and a CRISPR array on a single, arabinose inducible plasmid in *E. coli*. The expressed III-A modules were previously reported to specifically eliminate invading plasmids and anti-plasmid immunity depends on crRNA homology, transcription of the DNA target sequence, cOA signaling and RNase activity of Csm6, rather than on the DNase activity of Csm1 (34, 39). Here, we have specifically exploited the site-specific (Csm3-mediated) RNA cleavage activity of the three distinct type III-A crRNPs to efficiently

knock down gene expression of both coding and non-coding RNAs *in vivo*. We demonstrate that the III-A modules can be programmed to recognize one or more *E. coli* cellular target RNAs by addition of appropriate crRNA coding sequences to the module. Our findings demonstrate the potential of heterologous type III-A systems as tools for RNA interference and pave the way for expanded utility as functional genomic tools in novel cells and organisms.

RESULTS

Programming *L. lactis* III-A crRNPs for selective cleavage of target mRNAs *in vivo*. To determine if type III-A crRNPs can be harnessed as a gene expression knockdown platform, we introduced a plasmid into *E. coli* cells that results in arabinose-inducible expression of type III-A crRNPs (34, 39) that were programmed with different crRNA sequences rationally designed to recognize specific *E. coli* target mRNAs (Figure 2.1). The *E. coli* host strain (BL21-AI) lacks endogenous CRISPR-Cas systems. Northern blot analyses, using probes against the target mRNAs as well as internal control 5S rRNA, were carried out to assess the efficiency and specificity of directed cleavage of endogenous *E. coli* mRNAs.

One of two distinct approaches were employed in this study to ensure that sequence-dependent target RNA cleavage was specifically mediated by the backbone RNase subunits, Csm3, and not through triggering the non-specific RNase activity of trans-acting Csm6, which requires cOA-signaling by the crRNPs (Figure 2.1A). Initially, this goal was accomplished by searching target RNAs for the presence of 3' PFS sequences with significant homology to the 8 nt 5' crRNA tag. Pairing between the crRNA tag and PFS of the target RNA results in Csm3-directed cleavage of crRNA matching target RNAs but prevents the complex from producing cOA second messenger required for activating non-specific Csm6 RNase activity (17, 35, 57). As a more versatile

strategy, we subsequently employed type III-A crRNPs that have a mutation in the conserved Csm1 Palm motif (GGDD to GGAA) shown to be incapable of producing cOA/Csm6 activation regardless of the sequence nature of the PFS in the desired target RNA (42, 47, 48, 53). Some type III-A systems employ a non-specific DNase activity of the Csm1 HD domain (17, 44, 59), but we previously reported that the systems investigated here do not rely on this activity for immunity against plasmid DNA and therefore we did not employ Csm1 HD mutants (34). Mutation of the Palm or HD motif of Csm1 does not influence the ability of the type III-A crRNPs to cleave target RNA (Figure S2.1).

For the initial test, we assessed the RNA targeting capacity of heterologously expressed, *L. lactis* type III-A crRNPs having a crRNA against the *lpp* mRNA (the *lpp* gene of *E. coli* is non-essential for viability and encodes a major lipoprotein (60)). The *lpp* mRNA target sequence was selected with perfect complementarity to the crRNA guide and to have a 3' PFS with extensive base-pairing potential with the 5' crRNA tag (PFS bases -1 to -5 and -8 were complementary to positions +1-5 and +8 of the 5' crRNA tag) to ensure that only the Csm3-mediated specific target RNA cleavage (and not Csm6 non-specific RNase activity) was triggered. As a specificity control, the same *L. lactis* crRNPs were programmed with a control crRNA (C) that does not contain significant complementarity to any *E. coli* RNA. In the presence of the crRNA against the *lpp* mRNA but not the non-cognate control crRNA (Figure 2.1B, compare lanes 3 and 4), we observed a significant reduction in the steady-state levels of the *lpp* mRNA that was accompanied by the appearance of a *lpp* mRNA breakdown product of the expected size for cleavage in the region recognized by the crRNA (Figure 2.1B, red star in lane 4). Furthermore, crRNA-dependent cleavage of the target *lpp* mRNA was dependent upon arabinose induction of expression of the type III crRNP (Figure 2.1B, compare lanes 2 and 4). As expected, the steady state levels of 5S

rRNA remained constant in the analyzed cells (Figures 2.1C and D). These same samples were also probed to confirm the expression of each engineered crRNA. The size of the main crRNA species matches that expected for the product following Cas6 cleavage of primary transcripts (71 nt) and low levels of presumably 3' trimmed crRNAs was also observed (*lpp* crRNA is shown in Figure 2.1C, lanes 2 and 4 and non-cognate control crRNA is shown in Figure 2.1D, lanes 1 and 3). Mutational analysis of Csm3 (D30A) confirmed that the RNase activity observed by the crRNPs is mediated by the Csm3 backbone subunit cutting within the target RNA protospacer region, as expected (Figure S2.2). The results show that heterologously expressed *L. lactis* type III-A crRNPs can be programmed to efficiently and selectively cleave a desired target mRNA *in vivo*.

***S. thermophilus* and *S. epidermidis* type III-A systems can also be programmed to target mRNA destruction.** To determine if type III-A crRNPs from other bacterial species were also capable of carrying out efficient and specific mRNA knockdown in *E. coli*, we programmed the *S. thermophilus* and *S. epidermidis* type III systems to target the same *lpp* endogenous mRNA transcript (Figure 2.2). Similar to the *L. lactis* system (Figure 2.1), our results revealed that expression of III-A crRNPs from both *S. thermophilus* (Figure 2.2A-C) and *S. epidermidis* (Figure 2.2D) resulted in specific and efficient knockdown of the *lpp* mRNA and the accumulation of mRNA cleavage products of the expected sizes for crRNA-directed cleavage. While *L. lactis* and *S. epidermidis* share the same 5' crRNA tag sequence (5'-ACGAGAAC-3'), the *S. thermophilus* 5' tag differs at positions 4 and 5; 5'-ACGGAAAC-3'). For this reason, we used a Csm1 Palm mutant (GGDD motif mutated to GGAA) for the source of *S. thermophilus* crRNPs to enable testing of the same target RNA region and to ensure that Csm6 non-specific RNase activity was

not triggered due to decreased tag-PFS complementarity. Thus, three distinct bacterial sources of type III-A CRISPR-Cas systems proved to be functional for programmable RNA targeting *in vivo*.

Type III-A crRNPs are capable of acting at different sites along the length of a target mRNA. Next, we investigated whether the position of the target site significantly impacts the efficacy of target mRNA cleavage by testing the ability of the *L. lactis* III-A crRNPs (with Csm1 GGDD motif mutation) to target cleavage at different sites along the *lpp* mRNA transcript. Specifically, we individually tested the effects of five distinct crRNAs that span different regions of the *lpp* mRNA and in each case, Northern analyses was performed with probes specific for either the 5' or 3' terminal regions of the *lpp* mRNA (Figure 2.3A). Each of the tested crRNAs led to a major reduction in the steady state levels of full-length *lpp* transcript relative to the control crRNA, when probing for either the 5' or 3' ends of the mRNA following induction of crRNP formation (Figures 2.3B and C). Moreover, 5' and 3' expected cleavage products were observed with each tested crRNA (Figures 2.3B and C). Following crRNA-guided target RNA cleavage, the 3' mRNA fragments exhibited generally higher steady state levels than 5' mRNA fragments, despite near full cleavage of the full-length transcripts for each of the tested crRNAs. The results indicate that type III crRNPs are capable of targeting mRNA cleavage at multiple sites along the length of transcripts.

Type III-A crRNPs can be programmed to cleave multiple distinct RNA targets simultaneously. We next determined if the *L. lactis* III-A crRNPs could be programmed to target destruction of mRNAs in addition to the *lpp* transcript and addressed if more than one mRNA could be targeted in the cell concurrently. We found that *L. lactis* crRNPs efficiently targeted the

destruction of two additional tested non-essential *E. coli* mRNAs (60) encoding either the cold-shock protein E (*cspE*) or the outer membrane protein F (*ompF*), when individually programmed with single crRNAs against each of these particular transcripts (Figure 2.4B, lane 3 and 2.4C, lane 4; *lpp* mRNA cleavage shown in Figure 2.4A, lane 2). Next, we attempted targeting *lpp*, *cspE*, and *ompF* mRNAs simultaneously upon expressing each of the three distinct crRNAs from a single CRISPR array. A similar reduction in full-length transcript levels and occurrence of expected cleavage products was observed in the strain expressing all three crRNAs compared to individual strains expressing just one crRNA against a single mRNA target (Figure 2.4; compare lanes 2 and 5 in A, lanes 3 and 5 in B, and 4 and 5 in C). These results demonstrate the capacity of type III-A crRNPs to carry out multiplexed and simultaneous knockdown of at least three distinct mRNAs.

Directed cleavage of a non-coding RNA target.

To potentially broaden the application beyond mRNA targeting, we next tested whether *L. lactis* III-A crRNPs (with Csm1 Palm mutation) could effectively cleave a non-coding RNA target. For this purpose, we chose to target destruction of the *rnpB* RNA/ribozyme which is the enzymatic component of RNase P and catalyzes 5' end cleavage of precursor tRNAs (61). In *E. coli*, the *rnpB* RNA is required for the endonucleolytic separation of the *valV-valW* pre-tRNA bicistronic transcript (62, 63). We individually tested a panel of seven different crRNAs that spanned the length of *rnpB* RNA (Figure 2.5 B) for their ability to direct *L. lactis* III-A crRNPs to destroy the RNase P RNA (Figure 2.5C) and lead to decreased processing of the bicistronic pre-tRNA transcript (Figure 2.5E).

Northern analysis revealed that there was a high variability in the ability of the selected crRNAs to significantly lower the steady-state levels of *rnpB* RNA (Figure 2.5C). All seven tested crRNAs exhibited the ability to cleave the *rnpB* RNA as evidenced by the accumulation of

expected size cleavage products, relative to the control crRNA (Figure 2.5C, compare lanes 2-8 with lane 1). However, only one of the seven tested crRNAs resulted in a significant reduction in the steady-state levels of the *rnpB* target RNA (Figure 2.5C, lane 4) and a corresponding accumulation of unprocessed *valV-valW* bicistronic transcript (Figure 2.5E, lane 4). Above background levels of bicistronic pre-tRNA accumulation was also observed for a second tested crRNA (Figure 2.5E, lane 6). The *E. coli* RNase P RNA exhibits a high degree of sequence conservation with the RNase P RNA of *T. maritima*, which has a solved three-dimensional X-ray structure of the folded *rnpB* RNA in complex with tRNA substrate and associated RNase P protein (64) (Figure 2.5A). We note that the two most effective crRNAs (3 and 5) each are predicted to bind to regions of folded *rnpB* ribozyme that are not interacting with pre-tRNA or RNase P protein (Figure 2.5B). These results indicate the feasibility of using type III-A crRNPs for knocking down expression of non-coding RNAs but indicate that the folded structure and/or protein binding of a target RNA may negatively impact the effectiveness of target RNA recognition by type III-A crRNPs.

DISCUSSION

Gene knockdown technologies such as RNA interference (RNAi), play an important role in gene function discovery (especially for essential genes that when knocked out cause lethality) and therapeutic applications (31-33). The RNAi machinery required for small interfering RNA (siRNA) or short hairpin RNA (shRNA) mediated gene knockdown is present in many eukaryotes but absent from prokaryotes. In this study, we sought to harness the type III-A CRISPR system as a post-transcriptional gene knockdown platform that functions in prokaryotic cells. Our proof-of-principle studies demonstrate that type III-A crRNPs from three distinct sources (*L. lactis*, *S.*

epidermidis, and *S. thermophilus*) and conveniently expressed from an 'all-in-one' single plasmid, can be readily programmed with rationally-designed crRNAs to cleave both mRNA and non-coding RNA *in vivo* in a heterologous prokaryotic (*E. coli*) host cell. Moreover, we show that more than one target mRNA can be efficiently cleaved simultaneously when multiple crRNAs are concurrently expressed, paving the way for important applications such as cellular pathway discovery and manipulation. The type III-A gene knockdown technology established here has future potential as an important functional genomics tool for investigating gene function and cellular pathways in a wide range of other prokaryotic and perhaps eukaryotic cells.

Programmable knockdown of diverse RNA transcripts

Our findings show that type III-A systems provide a versatile platform for controlling the levels of endogenous transcripts *in vivo* at a post-transcriptional level. We found that each of the crRNAs that we designed and tested were highly effective at reducing the steady-state levels of all tested mRNAs when assayed individually (Figures 2.1-4) or in a multiplexed fashion (Figure 2.4). Furthermore, crRNAs targeting various locations along the length of a mRNA were comparably effective (Figure 2.3) suggesting no major bias of particular mRNA regions for susceptibility to interaction and cleavage by III-A crRNPs. Because the guide elements of the type III-A crRNAs that we tested are naturally relatively long (35-37 nt), this likely contributes to the observed effectiveness of targeting specific transcripts *in vivo*. When multiple crRNAs were expressed simultaneously, a high degree of sequence-specificity was observed in targeting the efficient destruction of each target RNA (Figure 2.4). However, future transcriptomic experiments are required to more comprehensively determine if any of the tested crRNAs result in any off-target effects on the levels of other cellular transcripts.

In contrast to the efficient targeted destruction of specific mRNAs when several crRNAs were tested, the non-coding RNA component of RNase P (*rnpB*) proved to be more recalcitrant to type III-A crRNP-mediated RNA cleavage (Figure 2.5). Given that each of the panel of seven crRNAs tested did lead to some detectable level of directed cleavage, this indicates that crRNPs were able to recognize and cleave at least a small fraction of the ribozyme. Of note, the two crRNAs found to be most effective at reducing ribozyme levels and blocking pre-tRNA processing function, mapped to regions of the RNA that are predicted to be solvent exposed in the predicted three-dimensional structure and not located in regions known to be engaged in known RNA-protein or RNA-tRNA interactions (Figure 2.5). It remains to be determined if noncoding RNAs will generally be more refractory to III-A-mediated RNA knockdown or if this particularly highly folded and highly interactive RNA target is an exceptional case. A prudent general strategy for targeting either a specific mRNA or non-coding RNA of interest would be to pursue the multiplexing route. Simultaneous expression of multiple crRNAs against different regions of the desired target RNA molecule is expected to increase the probability of efficient cleavage and gene knockdown.

Target RNA cleavage products accumulate *in vivo*

The observation that target RNA cleavage products of the expected sizes relative to the site of crRNA interaction were readily detectable provides strong evidence that the destruction was directed by type III-A crRNPs. However, this phenotype was surprising given *a priori* expectations that cleavage of the phosphodiester bonds within RNA polynucleotide chains normally leads to rapid degradation of the cleavage fragments and given the short half-lives (typically 3-5 mins) of mRNAs in *E. coli* in general (65). It is unclear why RNA fragments located

both 5' and 3' to the site of cleavage persist and are readily observable under steady state conditions. Type III crRNP cleavage results in RNA products having 5' hydroxyl and 2',3'-cyclic phosphate moieties rather than more typical 5' phosphate and 3' hydroxyl ends created by the action of other RNases (21, 66). These particular RNA chemical end groups might impede further RNA turnover by *E. coli* exoribonucleases. Alternatively, the unexpected stability of the 5' and 3' degradation fragments might result from the III-A crRNP sterically protecting these ends from being recognized and destroyed by cellular ribonucleases. However, strong *in vitro* evidence revealed that type III crRNPs normally rapidly dissociate from target RNAs following cleavage making this possibility less likely (14, 48).

Comparison with other RNA targeting CRISPR systems

Most types of CRISPR systems (types I (Cas3), II (Cas9), V (Cas12)) act through crRNA guided Cas nucleases that destroy DNA targets (1, 2). In contrast, type III (Csm3 and Csm4) and type VI (Cas13) CRISPR systems naturally recognize and target sequence-specific cleavage of RNA substrates. Thus, there has been a recent push to develop CRISPR-based systems as much needed, RNA targeting research tools with novel applications (25, 29).

Previous work showed that related type III-B (also known as Cmr (30)) systems could be programmed with engineered crRNAs to guide destruction of target RNAs in hyperthermophilic archaea including *Pyrococcus* and *Sulfolobus* species that naturally contain the type III-B systems (41, 67, 68). In these systems, a CRISPR mini-array plasmid supplies the engineered crRNAs and the endogenous III-B crRNPs are relied upon for the knockdown activity, which requires extreme temperature (optimal growth temperatures of these extremophilic organisms are 70-100 °C). The type III-A systems that we have established potentially have greater utility for use in a broad range

of important prokaryotes given that the entire system (crRNP and crRNAs) has been encoded in one plasmid. Importantly, the activity of the type III-A crRNPs described here work at mesophilic (e.g. 37 °C) temperatures compatible with the optimal growth temperatures of many prokaryotic model organisms currently being investigated.

As a tool for RNA knockdown in prokaryotes, type III-A systems have a distinct advantage over the type IV systems which suffer a significant drawback in that the relevant Cas13 RNase is known to cleave both the target RNA as well as "bystander" RNAs (i.e. cellular RNAs in a sequence-nonspecific fashion, when activated by crRNA-target RNA interaction (69-72)). Interestingly, this "collateral" RNA destruction observed with most Cas13 ribonucleases in bacteria was unexpectedly suppressed when certain Cas13 species were tested in human and plant cells and resulted in efficient and specific knockdown of target mRNAs with fewer off-target effects than is observed with siRNA/shRNA technologies (69, 73, 74). Furthermore, while the type III-affiliated Csm6 (III-A) and Csx1 (type III-B) ribonucleases are also known to induce collateral RNA destruction (28, 49), these proteins work *in trans* and are not required for the sequence-specific RNA cleavage mediated by the type III crRNPs (15, 20, 41). To circumvent collateral RNA cleavage and direct only sequence-specific target RNA destruction, in this work we prevented Csm6 RNase activity through mutating the Csm1 Palm motif essential for cOA generation and Csm6 RNase activation. However, it should also be possible to achieve this same effect by deleting the *csm6* genes from the expression plasmids and we show that deletion of csm6 gene or expression of an RNase-defective Csm6 variant (HEPN mutant) do not impact target RNA cleavage by type III-A crRNPs (Figure S2).

Future promising applications for type III-A systems

Further studies are required to more deeply explore the potential of the type III-A crRNPs as effective posttranscriptional gene knockdown platforms as well as for development of additional applications. Moreover, it will be important to determine if these CRISPR research tools are capable of functioning outside of *E. coli* and in a range of both prokaryotic and eukaryotic cells and organisms. The ability to assemble functional crRNPs through expression of all required components on just a single expression plasmid, makes this a facile system for further refinement and testing these possibilities. Recent success with ectopically expressing similarly complex, type I crRNPs consisting of up to six Cas proteins and a CRISPR RNA in human cells capable of function in genome editing/transcriptional control (75, 76) offers hope that type III-A systems too will be able to be employed in eukaryotic cells for important *in vivo* applications.

The ease by which both type III-A and III-B crRNPs can be expressed and purified as functional complexes (13, 14, 17, 19, 20, 34, 35, 37, 38, 41, 77) offers additional opportunities for delivering programmed, pre-assembled crRNPs directly into cells. Of note, *S. thermophilus* type III-A crRNPs expressed and purified from *E. coli* have recently been shown to efficiently and specifically knockdown maternal mRNAs when microinjected into early zebra fish embryos (78). Moreover, as has been employed with type VI, Cas13-based systems, there is the potential to employ ribonuclease defective type III-A crRNP variants (through inactivating point mutations to create an RNase-defective or dCsm3 subunit (Figure S2.2; (18, 20)) as well as to fuse various effector domains from other proteins to expand the functionalities beyond RNA destruction to potentially influence target RNA splicing, base editing, translation, degradation, and to track the intracellular localization of the transcripts using fluorescent-based microscopy of GFP-fusion systems (25, 29). Purified type III-A crRNPs also offer potential to expand proven CRISPR-based

powerful molecular diagnostic tools (so far employed with Cas13 and Cas12) capable of detecting viral and bacterial pathogens and cancer mutations from patient fluids (28, 71, 79). In summary, the work described here provides an important step in the direction of harnessing the potential of type III-A systems as versatile RNA-targeting CRISPR-based research tools with important future applications.

MATERIALS AND METHODS

Plasmid Construction

pCsm plasmids for expressing *L. lactis*, *S. epidermidis*, or *S. thermophilus* type III-A crRNPs were described previously (34, 39) with the new crRNAs designed to be complementary to a particular target RNA region. For each crRNA guide sequence (Table S2.1), a pair of complementary oligonucleotides, 35 bp for *L. lactis* and *S. epidermidis,* 39 bp for *S. thermophilus,* and 37 bp for the negative control (Table S2.2), was designed with 4 nt 5' overhangs that match 5' overhangs of the pCsm vector left by linearization with *BbsI* (NEB). 10 pmoles of each oligonucleotide set were annealed in 1X CutSmart buffer (NEB) and 0.1 pmole of the annealed products were ligated with 50 ng of the linearized pCsm vector with T4 DNA ligase (NEB). The multispacer array was constructed by amplification of individual spacer arrays with oligonucleotides that were appended with BsaI (NEB) restriction sites such that PCR fragments could be combined in a Golden Gate Assembly (Table S2.2). The ligation and assembly reactions were used to transform chemically competent TOP10 *E. coli* cells (Thermo Fisher). Plasmids were purified (ZymoPURE mini-prep, Zymo Research) and verified by DNA sequencing before transformation of chemically competent BL21-AI *E. coli* cells (Invitrogen). The BL21-AI *E. coli* expression strain has a T7 RNA polymerase under the control of an arabinose inducible promoter.

Splicing overlap extension PCR was used to generate the *L. lactis* Csm1 Palm (D576A, D577A) and HD (and H13A, D14A) motif mutations as well as the *S. thermophilus* Csm1 Palm (D575A, D576A) motif. The gel purified DNA fragments were digested with PspXI and NdeI (*L. lactis*) or BamHI and NdeI (*S. thermophilus*) before ligation into linearized pCsm vector. *L. lactis* Csm3 D30A, ΔCsm6, and Csm6 H360A mutations were transferred from previously generated constructs (34) by digestion and ligation. The oligonucleotide sequences used to generate the mutant constructs are provided in Supplementary Table S2.3 and all mutations were verified by DNA sequencing.

Type III-A crRNP expression

Single *E. coli* colonies were grown at 37°C shaking in Miller's lysogeny broth (Invitrogen) until reaching an OD_{600} of 0.1 when they were induced with a final concentration of 10 mM arabinose to express Csm1-6, Cas6, and crRNA. After 120 minutes of induction, 1-1.5 ml of each culture was centrifuged, the supernatant was aspirated, and the cell pellets were flash frozen in a dry ice and ethanol bath and stored at -80C until RNA extraction.

Northern analysis

Total RNA was prepared using the RNAsnap^{TM} protocol (80). RNA used in Figure 2.5, was further purified by phenol chloroform isoamyl alcohol extraction (pH 4.5) and ethanol precipitation. The RNA samples were quantified using a Qubit fluorimeter 2.0 (Thermo Fisher) and equal amounts of RNA (5 -10 ug) were heat denatured for 5 minutes at 95 °C immediately before electrophoresis on 6-8% polyacrylamide, 8M urea gels in TBE buffer (89 mM Tris base, 89 mM Boric acid, 2mM EDTA, pH 8.0) at 400 volts. 5'-radiolabeled, molecular weight markers were RiboRuler Low

Range RNA Ladder (Thermo Scientific) or 10 bp DNA Ladder (Invitrogen). The RNA was transferred by electro-blotting with a semidry transfer apparatus (Bio-Rad® Trans-Blot SD) to positively charged nylon membrane (Nytran^{TM} SPC, Whatman). ULTRAhyb buffer (Invitrogen) was used for hybridization with oligonucleotides 5'-end labeled with 6,000 Ci/mmol γ-^{32}P ATP (Perkin Elmer) using T4 polynucleotide kinase (NEB). 1 million counts per minute of radiolabeled probe was added for each mL of hybridization buffer. Hybridization was performed at 42°C for 12-16 hours. Membranes were washed of unbound probe with a pre-warmed (42°C) 2X saline-sodium citrate (SSC) buffer and detected by phosphor imaging (Storm^{TM} 840, GE Healthcare).

ACKNOWLEDGEMENTS

We are grateful to Sidney Kushner and Bijoy Mohanty for expert technical advice, helpful discussions, and probe sequence recommendations. We thank members of the Terns laboratory for helpful discussions and Rebecca Terns for her early mentorship role. Ryan Catchpole is gratefully acknowledged for critical reading of the manuscript. This work was supported by the National Institutes of Health [R35GM118160] to M.P.T

REFERENCES

1. Hille, F., H. Richter, S.P. Wong, M. Bratovic, S. Ressel, and E. Charpentier, *The Biology of CRISPR-Cas: Backward and Forward.* Cell, 2018. **172**(6): p. 1239-1259.
2. Makarova, K.S., Y.I. Wolf, J. Iranzo, S.A. Shmakov, O.S. Alkhnbashi, S.J.J. Brouns, E. Charpentier, D. Cheng, D.H. Haft, P. Horvath, S. Moineau, F.J.M. Mojica, D. Scott, S.A. Shah, V. Siksnys, M.P. Terns, C. Venclovas, M.F. White, A.F. Yakunin, W. Yan, F. Zhang, R.A. Garrett, R. Backofen, J. van der Oost, R. Barrangou, and E.V. Koonin, *Evolutionary*

classification of CRISPR-Cas systems: a burst of class 2 and derived variants. Nat Rev Microbiol, 2019.

3. Jackson, S.A., R.E. McKenzie, R.D. Fagerlund, S.N. Kieper, P.C. Fineran, and S.J. Brouns, *CRISPR-Cas: Adapting to change.* Science, 2017. **356**(6333).
4. McGinn, J. and L.A. Marraffini, *Molecular mechanisms of CRISPR-Cas spacer acquisition.* Nat Rev Microbiol, 2019. **17**(1): p. 7-12.
5. Brouns, S.J., M.M. Jore, M. Lundgren, E.R. Westra, R.J. Slijkhuis, A.P. Snijders, M.J. Dickman, K.S. Makarova, E.V. Koonin, and J. van der Oost, *Small CRISPR RNAs guide antiviral defense in prokaryotes.* Science, 2008. **321**(5891): p. 960-4.
6. Carte, J., R.T. Christopher, J.T. Smith, S. Olson, R. Barrangou, S. Moineau, C.V. Glover, 3rd, B.R. Graveley, R.M. Terns, and M.P. Terns, *The three major types of CRISPR-Cas systems function independently in CRISPR RNA biogenesis in Streptococcus thermophilus.* Mol Microbiol, 2014. **93**(1): p. 98-112.
7. Carte, J., R. Wang, H. Li, R.M. Terns, and M.P. Terns, *Cas6 is an endoribonuclease that generates guide RNAs for invader defense in prokaryotes.* Genes Dev, 2008. **22**(24): p. 3489-96.
8. Jackson, R.N., P.B. van Erp, S.H. Sternberg, and B. Wiedenheft, *Conformational regulation of CRISPR-associated nucleases.* Curr Opin Microbiol, 2017. **37**: p. 110-119.
9. Garneau, J.E., M.E. Dupuis, M. Villion, D.A. Romero, R. Barrangou, P. Boyaval, C. Fremaux, P. Horvath, A.H. Magadan, and S. Moineau, *The CRISPR/Cas bacterial immune system cleaves bacteriophage and plasmid DNA.* Nature, 2010. **468**(7320): p. 67-71.
10. Zetsche, B., J.S. Gootenberg, O.O. Abudayyeh, I.M. Slaymaker, K.S. Makarova, P. Essletzbichler, S.E. Volz, J. Joung, J. van der Oost, A. Regev, E.V. Koonin, and F. Zhang,

Cpf1 is a single RNA-guided endonuclease of a class 2 CRISPR-Cas system. Cell, 2015. **163**(3): p. 759-71.

11. Pinilla-Redondo, R., D. Mayo-Munoz, J. Russel, R.A. Garrett, L. Randau, S.J. Sorensen, and S.A. Shah, *Type IV CRISPR-Cas systems are highly diverse and involved in competition between plasmids.* Nucleic Acids Res, 2020. **48**(4): p. 2000-2012.
12. Abudayyeh, O.O., J.S. Gootenberg, S. Konermann, J. Joung, I.M. Slaymaker, D.B. Cox, S. Shmakov, K.S. Makarova, E. Semenova, L. Minakhin, K. Severinov, A. Regev, E.S. Lander, E.V. Koonin, and F. Zhang, *C2c2 is a single-component programmable RNA-guided RNA-targeting CRISPR effector.* Science, 2016. **353**(6299): p. aaf5573.
13. Elmore, J.R., N.F. Sheppard, N. Ramia, T. Deighan, H. Li, R.M. Terns, and M.P. Terns, *Bipartite recognition of target RNAs activates DNA cleavage by the Type III-B CRISPR-Cas system.* Genes Dev, 2016. **30**(4): p. 447-59.
14. Estrella, M.A., F.T. Kuo, and S. Bailey, *RNA-activated DNA cleavage by the Type III-B CRISPR-Cas effector complex.* Genes Dev, 2016. **30**(4): p. 460-70.
15. Hale, C.R., A. Cocozaki, H. Li, R.M. Terns, and M.P. Terns, *Target RNA capture and cleavage by the Cmr type III-B CRISPR-Cas effector complex.* Genes Dev, 2014. **28**(21): p. 2432-43.
16. Han, W., Y. Li, L. Deng, M. Feng, W. Peng, S. Hallstrom, J. Zhang, N. Peng, Y.X. Liang, M.F. White, and Q. She, *A type III-B CRISPR-Cas effector complex mediating massive target DNA destruction.* Nucleic Acids Res, 2017. **45**(4): p. 1983-1993.
17. Kazlauskiene, M., G. Tamulaitis, G. Kostiuk, C. Venclovas, and V. Siksnys, *Spatiotemporal Control of Type III-A CRISPR-Cas Immunity: Coupling DNA Degradation with the Target RNA Recognition.* Mol Cell, 2016. **62**(2): p. 295-306.

18. Samai, P., N. Pyenson, W. Jiang, G.W. Goldberg, A. Hatoum-Aslan, and L.A. Marraffini, *Co-transcriptional DNA and RNA Cleavage during Type III CRISPR-Cas Immunity.* Cell, 2015. **161**(5): p. 1164-1174.

19. Staals, R.H., Y. Agari, S. Maki-Yonekura, Y. Zhu, D.W. Taylor, E. van Duijn, A. Barendregt, M. Vlot, J.J. Koehorst, K. Sakamoto, A. Masuda, N. Dohmae, P.J. Schaap, J.A. Doudna, A.J. Heck, K. Yonekura, J. van der Oost, and A. Shinkai, *Structure and activity of the RNA-targeting Type III-B CRISPR-Cas complex of Thermus thermophilus.* Mol Cell, 2013. **52**(1): p. 135-45.

20. Tamulaitis, G., M. Kazlauskiene, E. Manakova, C. Venclovas, A.O. Nwokeoji, M.J. Dickman, P. Horvath, and V. Siksnys, *Programmable RNA shredding by the type III-A CRISPR-Cas system of Streptococcus thermophilus.* Mol Cell, 2014. **56**(4): p. 506-17.

21. Hale, C.R., P. Zhao, S. Olson, M.O. Duff, B.R. Graveley, L. Wells, R.M. Terns, and M.P. Terns, *RNA-guided RNA cleavage by a CRISPR RNA-Cas protein complex.* Cell, 2009. **139**(5): p. 945-56.

22. Tamulaitis, G., C. Venclovas, and V. Siksnys, *Type III CRISPR-Cas Immunity: Major Differences Brushed Aside.* Trends Microbiol, 2017. **25**(1): p. 49-61.

23. Goldberg, G.W., W. Jiang, D. Bikard, and L.A. Marraffini, *Conditional tolerance of temperate phages via transcription-dependent CRISPR-Cas targeting.* Nature, 2014.

24. Terns, R.M. and M.P. Terns, *CRISPR-based technologies: prokaryotic defense weapons repurposed.* Trends Genet, 2014. **30**(3): p. 111-8.

25. Terns, M.P., *CRISPR-Based Technologies: Impact of RNA-Targeting Systems.* Mol Cell, 2018. **72**(3): p. 404-412.

26. Pickar-Oliver, A. and C.A. Gersbach, *The next generation of CRISPR-Cas technologies and applications.* Nat Rev Mol Cell Biol, 2019. **20**(8): p. 490-507.

27. Bikard, D., C.W. Euler, W. Jiang, P.M. Nussenzweig, G.W. Goldberg, X. Duportet, V.A. Fischetti, and L.A. Marraffini, *Exploiting CRISPR-Cas nucleases to produce sequence-specific antimicrobials.* Nat Biotechnol, 2014. **32**(11): p. 1146-50.

28. Gootenberg, J.S., O.O. Abudayyeh, M.J. Kellner, J. Joung, J.J. Collins, and F. Zhang, *Multiplexed and portable nucleic acid detection platform with Cas13, Cas12a, and Csm6.* Science, 2018. **360**(6387): p. 439-444.

29. Smargon, A.A., Y.J. Shi, and G.W. Yeo, *RNA-targeting CRISPR systems from metagenomic discovery to transcriptomic engineering.* Nat Cell Biol, 2020. **22**(2): p. 143-150.

30. Haft, D.H., J. Selengut, E.F. Mongodin, and K.E. Nelson, *A guild of 45 CRISPR-associated (Cas) protein families and multiple CRISPR/Cas subtypes exist in prokaryotic genomes.* PLoS Comput Biol, 2005. **1**(6): p. e60.

31. Kim, D. and J. Rossi, *RNAi mechanisms and applications.* Biotechniques, 2008. **44**(5): p. 613-6.

32. Setten, R.L., J.J. Rossi, and S.P. Han, *The current state and future directions of RNAi-based therapeutics.* Nat Rev Drug Discov, 2019. **18**(6): p. 421-446.

33. Wilson, R.C. and J.A. Doudna, *Molecular mechanisms of RNA interference.* Annu Rev Biophys, 2013. **42**: p. 217-39.

34. Foster, K., J. Kalter, W. Woodside, R.M. Terns, and M.P. Terns, *The ribonuclease activity of Csm6 is required for anti-plasmid immunity by Type III-A CRISPR-Cas systems.* RNA Biol, 2018: p. 1-12.

35. You, L., J. Ma, J. Wang, D. Artamonova, M. Wang, L. Liu, H. Xiang, K. Severinov, X. Zhang, and Y. Wang, *Structure Studies of the CRISPR-Csm Complex Reveal Mechanism of Co-transcriptional Interference.* Cell, 2019. **176**(1-2): p. 239-253 e16.

36. Liu, T.Y., A.T. Iavarone, and J.A. Doudna, *RNA and DNA Targeting by a Reconstituted Thermus thermophilus Type III-A CRISPR-Cas System.* PLoS One, 2017. **12**(1): p. e0170552.

37. Staals, R.H., Y. Zhu, D.W. Taylor, J.E. Kornfeld, K. Sharma, A. Barendregt, J.J. Koehorst, M. Vlot, N. Neupane, K. Varossieau, K. Sakamoto, T. Suzuki, N. Dohmae, S. Yokoyama, P.J. Schaap, H. Urlaub, A.J. Heck, E. Nogales, J.A. Doudna, A. Shinkai, and J. van der Oost, *RNA targeting by the type III-A CRISPR-Cas Csm complex of Thermus thermophilus.* Mol Cell, 2014. **56**(4): p. 518-30.

38. Dorsey, B.W., L. Huang, and A. Mondragon, *Structural organization of a Type III-A CRISPR effector subcomplex determined by X-ray crystallography and cryo-EM.* Nucleic Acids Res, 2019. **47**(7): p. 3765-3783.

39. Ichikawa, H.T., J.C. Cooper, L. Lo, J. Potter, R.M. Terns, and M.P. Terns, *Programmable type III-A CRISPR-Cas DNA targeting modules.* PLoS One, 2017. **12**(4): p. e0176221.

40. Hatoum-Aslan, A., P. Samai, I. Maniv, W. Jiang, and L.A. Marraffini, *A ruler protein in a complex for antiviral defense determines the length of small interfering CRISPR RNAs.* J Biol Chem, 2013. **288**(39): p. 27888-97.

41. Hale, C.R., S. Majumdar, J. Elmore, N. Pfister, M. Compton, S. Olson, A.M. Resch, C.V. Glover, 3rd, B.R. Graveley, R.M. Terns, and M.P. Terns, *Essential features and rational design of CRISPR RNAs that function with the Cas RAMP module complex to cleave RNAs.* Mol Cell, 2012. **45**(3): p. 292-302.

42. Kazlauskiene, M., G. Kostiuk, C. Venclovas, G. Tamulaitis, and V. Siksnys, *A cyclic oligonucleotide signaling pathway in type III CRISPR-Cas systems.* Science, 2017.

43. Mogila, I., M. Kazlauskiene, S. Valinskyte, G. Tamulaitiene, G. Tamulaitis, and V. Siksnys, *Genetic Dissection of the Type III-A CRISPR-Cas System Csm Complex Reveals Roles of Individual Subunits.* Cell Rep, 2019. **26**(10): p. 2753-2765 e4.

44. Jiang, W., P. Samai, and L.A. Marraffini, *Degradation of Phage Transcripts by CRISPR-Associated RNases Enables Type III CRISPR-Cas Immunity.* Cell, 2016. **164**(4): p. 710-21.

45. Guo, T., F. Zheng, Z. Zeng, Y. Yang, Q. Li, Q. She, and W. Han, *Cmr3 regulates the suppression on cyclic oligoadenylate synthesis by tag complementarity in a Type III-B CRISPR-Cas system.* RNA Biol, 2019. **16**(10): p. 1513-1520.

46. Jia, N., R. Jones, G. Sukenick, and D.J. Patel, *Second Messenger cA4 Formation within the Composite Csm1 Palm Pocket of Type III-A CRISPR-Cas Csm Complex and Its Release Path.* Mol Cell, 2019.

47. Niewoehner, O., C. Garcia-Doval, J.T. Rostol, C. Berk, F. Schwede, L. Bigler, J. Hall, L.A. Marraffini, and M. Jinek, *Type III CRISPR-Cas systems produce cyclic oligoadenylate second messengers.* Nature, 2017. **548**(7669): p. 543-548.

48. Rouillon, C., J.S. Athukoralage, S. Graham, S. Gruschow, and M.F. White, *Control of cyclic oligoadenylate synthesis in a type III CRISPR system.* Elife, 2018. **7**.

49. Rostol, J.T. and L.A. Marraffini, *Non-specific degradation of transcripts promotes plasmid clearance during type III-A CRISPR-Cas immunity.* Nat Microbiol, 2019. **4**(4): p. 656-662.

50. Rouillon, C., M. Zhou, J. Zhang, A. Politis, V. Beilsten-Edmands, G. Cannone, S. Graham, C.V. Robinson, L. Spagnolo, and M.F. White, *Structure of the CRISPR interference complex CSM reveals key similarities with cascade.* Mol Cell, 2013. **52**(1): p. 124-34.

51. Jia, N., C.Y. Mo, C. Wang, E.T. Eng, L.A. Marraffini, and D.J. Patel, *Type III-A CRISPR-Cas Csm Complexes: Assembly, Periodic RNA Cleavage, DNase Activity Regulation, and Autoimmunity.* Mol Cell, 2018.

52. Hatoum-Aslan, A., I. Maniv, P. Samai, and L.A. Marraffini, *Genetic characterization of antiplasmid immunity through a type III-A CRISPR-Cas system.* J Bacteriol, 2014. **196**(2): p. 310-7.

53. Foster, K., S. Grüschow, S. Bailey, M.F. White, and M.P. Terns, *Regulation of the RNA and DNA nuclease activities required for Pyrococcus furiosus Type III-B CRISPR-Cas Immunity.* Nucleic Acids Res, 2020. **48**: p. 4418-4434.

54. Lin, J., M. Feng, H. Zhang, and Q. She, *Characterization of a novel type III CRISPR-Cas effector provides new insights into the allosteric activation and suppression of the Cas10 DNase.* Cell Discov, 2020. **6**: p. 29.

55. Millen, A.M., J.E. Samson, D.M. Tremblay, A.H. Magadan, G.M. Rousseau, S. Moineau, and D.A. Romero, *Lactococcus lactis type III-A CRISPR-Cas system cleaves bacteriophage RNA.* RNA Biol, 2019. **16**(4): p. 461-468.

56. Cao, L., C.H. Gao, J. Zhu, L. Zhao, Q. Wu, M. Li, and B. Sun, *Identification and functional study of type III-A CRISPR-Cas systems in clinical isolates of Staphylococcus aureus.* Int J Med Microbiol, 2016. **306**(8): p. 686-696.

57. Pyenson, N.C., K. Gayvert, A. Varble, O. Elemento, and L.A. Marraffini, *Broad Targeting Specificity during Bacterial Type III CRISPR-Cas Immunity Constrains Viral Escape.* Cell Host Microbe, 2017. **22**(3): p. 343-353 e3.

58. Marraffini, L.A. and E.J. Sontheimer, *Self versus non-self discrimination during CRISPR RNA-directed immunity.* Nature, 2010. **463**(7280): p. 568-71.

59. Park, K.H., Y. An, T.Y. Jung, I.Y. Baek, H. Noh, W.C. Ahn, H. Hebert, J.J. Song, J.H. Kim, B.H. Oh, and E.J. Woo, *RNA activation-independent DNA targeting of the Type III CRISPR-Cas system by a Csm complex.* EMBO Rep, 2017. **18**(5): p. 826-840.

60. Baba, T., T. Ara, M. Hasegawa, Y. Takai, Y. Okumura, M. Baba, K.A. Datsenko, M. Tomita, B.L. Wanner, and H. Mori, *Construction of Escherichia coli K-12 in-frame, single-gene knockout mutants: the Keio collection.* Mol Syst Biol, 2006. **2**: p. 2006 0008.

61. Esakova, O. and A.S. Krasilnikov, *Of proteins and RNA: the RNase P/MRP family.* RNA, 2010. **16**(9): p. 1725-47.

62. Mohanty, B.K. and S.R. Kushner, *Ribonuclease P processes polycistronic tRNA transcripts in Escherichia coli independent of ribonuclease E.* Nucleic Acids Res, 2007. **35**(22): p. 7614-25.

63. Mohanty, B.K., A. Agrawal, and S.R. Kushner, *Generation of pre-tRNAs from polycistronic operons is the essential function of RNase P in Escherichia coli.* Nucleic Acids Res, 2020. **48**(5): p. 2564-2578.

64. Reiter, N.J., A. Osterman, A. Torres-Larios, K.K. Swinger, T. Pan, and A. Mondragon, *Structure of a bacterial ribonuclease P holoenzyme in complex with tRNA.* Nature, 2010. **468**(7325): p. 784-9.

65. Bernstein, J.A., A.B. Khodursky, P.H. Lin, S. Lin-Chao, and S.N. Cohen, *Global analysis of mRNA decay and abundance in Escherichia coli at single-gene resolution using two-color fluorescent DNA microarrays.* Proc Natl Acad Sci U S A, 2002. **99**(15): p. 9697-702.

66. Zhang, J., S. Graham, A. Tello, H. Liu, and M.F. White, *Multiple nucleic acid cleavage modes in divergent type III CRISPR systems.* Nucleic Acids Res, 2016. **44**(4): p. 1789-99.

67. Zebec, Z., A. Manica, J. Zhang, M.F. White, and C. Schleper, *CRISPR-mediated targeted mRNA degradation in the archaeon Sulfolobus solfataricus.* Nucleic Acids Res, 2014. **42**(8): p. 5280-8.

68. Liu, T., S. Pan, Y. Li, N. Peng, and Q. She, *Type III CRISPR-Cas System: Introduction And Its Application for Genetic Manipulations.* Curr Issues Mol Biol, 2018. **26**: p. 1-14.

69. Konermann, S., P. Lotfy, N.J. Brideau, J. Oki, M.N. Shokhirev, and P.D. Hsu, *Transcriptome Engineering with RNA-Targeting Type VI-D CRISPR Effectors.* Cell, 2018. **173**(3): p. 665-676 e14.

70. Smargon, A.A., D.B. Cox, N.K. Pyzocha, K. Zheng, I.M. Slaymaker, J.S. Gootenberg, O.A. Abudayyeh, P. Essletzbichler, S. Shmakov, K.S. Makarova, E.V. Koonin, and F. Zhang, *Cas13b Is a Type VI-B CRISPR-Associated RNA-Guided RNase Differentially Regulated by Accessory Proteins Csx27 and Csx28.* Mol Cell, 2017. **65**(4): p. 618-630 e7.

71. Gootenberg, J.S., O.O. Abudayyeh, J.W. Lee, P. Essletzbichler, A.J. Dy, J. Joung, V. Verdine, N. Donghia, N.M. Daringer, C.A. Freije, C. Myhrvold, R.P. Bhattacharyya, J. Livny, A. Regev, E.V. Koonin, D.T. Hung, P.C. Sabeti, J.J. Collins, and F. Zhang, *Nucleic acid detection with CRISPR-Cas13a/C2c2.* Science, 2017. **356**(6336): p. 438-442.

72. Meeske, A.J., S. Nakandakari-Higa, and L.A. Marraffini, *Cas13-induced cellular dormancy prevents the rise of CRISPR-resistant bacteriophage.* Nature, 2019. **570**(7760): p. 241-245.

73. Abudayyeh, O.O., J.S. Gootenberg, P. Essletzbichler, S. Han, J. Joung, J.J. Belanto, V. Verdine, D.B.T. Cox, M.J. Kellner, A. Regev, E.S. Lander, D.F. Voytas, A.Y. Ting, and F. Zhang, *RNA targeting with CRISPR-Cas13.* Nature, 2017. **550**(7675): p. 280-284.

74. Wessels, H.H., A. Mendez-Mancilla, X. Guo, M. Legut, Z. Daniloski, and N.E. Sanjana, *Massively parallel Cas13 screens reveal principles for guide RNA design.* Nat Biotechnol, 2020. **38**(6): p. 722-727.

75. Pickar-Oliver, A., J.B. Black, M.M. Lewis, K.J. Mutchnick, T.S. Klann, K.A. Gilcrest, M.J. Sitton, C.E. Nelson, A. Barrera, L.C. Bartelt, T.E. Reddy, C.L. Beisel, R. Barrangou, and C.A. Gersbach, *Targeted transcriptional modulation with type I CRISPR-Cas systems in human cells.* Nat Biotechnol, 2019. **37**(12): p. 1493-1501.

76. Cameron, P., M.M. Coons, S.E. Klompe, A.M. Lied, S.C. Smith, B. Vidal, P.D. Donohoue, T. Rotstein, B.W. Kohrs, D.B. Nyer, R. Kennedy, L.M. Banh, C. Williams, M.S. Toh, M.J. Irby, L.S. Edwards, C.-H. Lin, A.L.G. Owen, T. Künne, J. Van Der Oost, S.J.J. Brouns, E.M. Slorach, C.K. Fuller, S. Gradia, S.B. Kanner, A.P. May, and S.H. Sternberg, *Harnessing type I CRISPR–Cas systems for genome engineering in human cells.* Nat Biotechnol, 2019. **37**(12): p. 1471-1477.

77. Osawa, T., H. Inanaga, C. Sato, and T. Numata, *Crystal structure of the CRISPR-Cas RNA silencing Cmr complex bound to a target analog.* Mol Cell, 2015. **58**(3): p. 418-30.

78. Fricke, T., D. Smalakyte, M. Lapinski, A. Pateria, C. Weige, M. Pastor, A. Kolano, C. Winata, V. Siksnys, G. Tamulaitis, and M. Bochtler, *Targeted RNA Knockdown by a Type III CRISPR-Cas Complex in Zebrafish.* CRISPR J, 2020. **3**(4): p. 299-313.

79. Kellner, M.J., J.G. Koob, J.S. Gootenberg, O.O. Abudayyeh, and F. Zhang, *SHERLOCK: nucleic acid detection with CRISPR nucleases.* Nat Protoc, 2019. **14**(10): p. 2986-3012.

80. Stead, M.B., A. Agrawal, K.E. Bowden, R. Nasir, B.K. Mohanty, R.B. Meagher, and S.R. Kushner, *RNAsnap: a rapid, quantitative and inexpensive, method for isolating total RNA from bacteria.* Nucleic Acids Res, 2012. **40**(20): p. e156.

FIGURE 2.1 Programmed mRNA cleavage by *L. lactis* type III-A crRNPs expressed in *E. coli*. (A) Diagram of a representative type III-A effector crRNP containing Csm1-5 subunits and a crRNA, in the process of cleaving a bound target RNA. Each Csm3 RNase subunit cuts the target RNA once (cleavages indicated by arrows) within the region of the target RNA (orange) that base-pairs with the crRNA guide element (blue). The position of the target RNA protospacer flanking sequence (PFS) is indicated as are the HD (DNase) and Palm (cyclic oligoadenylate (cOA) producing) motifs of the Csm1 subunit. (B-D) Expression of *L. lactis* type III-A crRNPs containing either a crRNA against the *lpp* mRNA (*lpp*) or negative control crRNA (C) was induced (+) and Northern analysis was performed using probes against the *lpp* mRNA (B), lpp crRNA (C), control crRNA (D) or constitutively expressed 5S rRNA (C and D). The positions of the RNAs are indicated including those of the full-length *lpp* mRNA (dot) and *lpp* mRNA cleavage products (red star). The dotted line in B indicates that intervening lanes were omitted from the blot. The sizes of the molecular weight markers (M) are indicated in each panel.

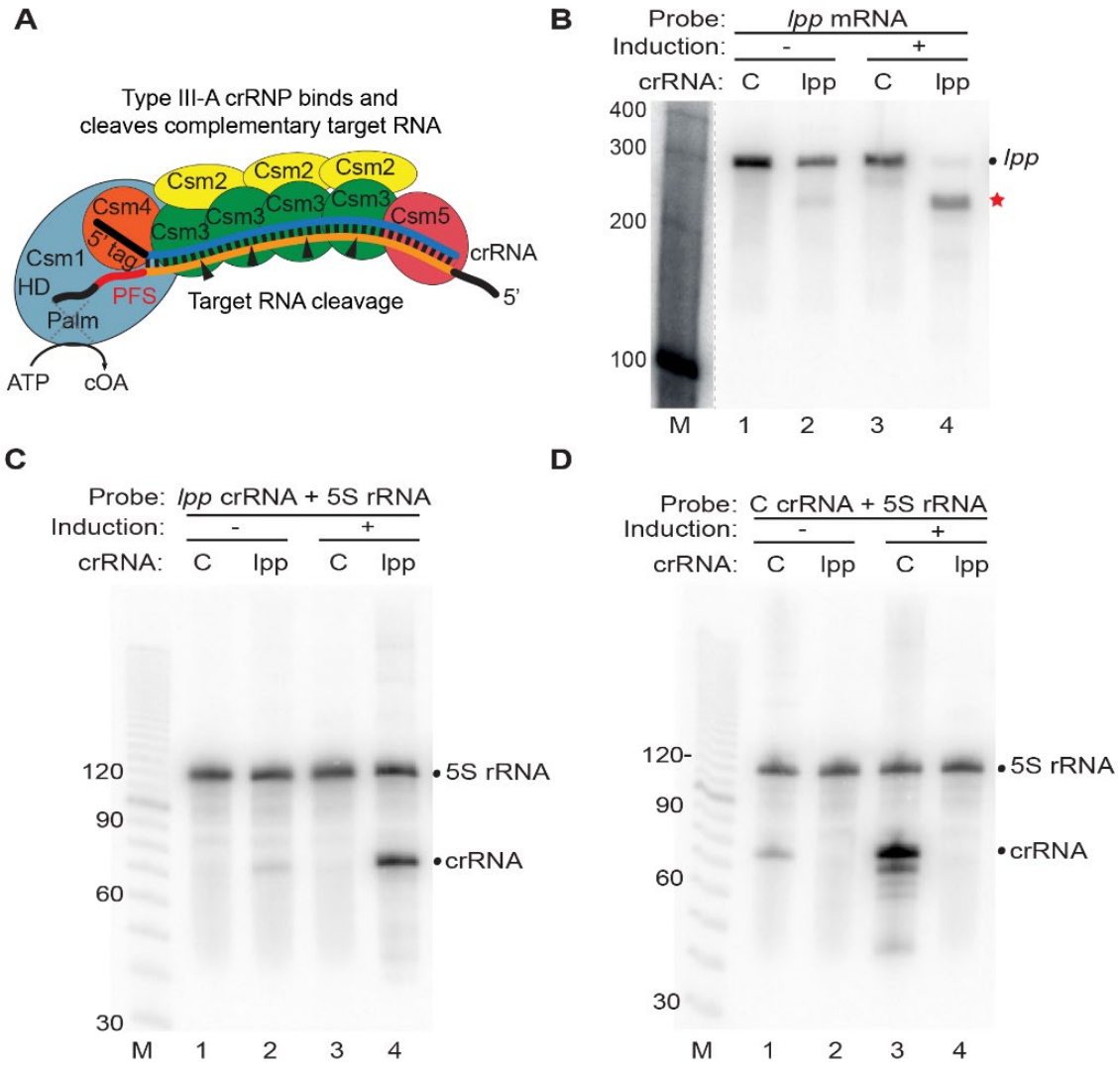
A
Type III-A crRNP binds and
cleaves complementary target RNA
Csm2
Csm2
Csm2
Csm4
Csm3
Csm3
Csm3
Csm5
5' tag
Csm1
HD
PFS
Palm
crRNA
5'
Target RNA cleavage
ATP
cOA
B
Probe: lpp mRNA
Induction: - +
crRNA: C lpp C lpp
400
300
200
100
lpp
M 1 2 3 4
C
Probe: lpp crRNA + 5S rRNA
Induction: - +
crRNA: C lpp C lpp
120
90
60
30
5S rRNA
crRNA
M 1 2 3 4
D
Probe: C crRNA + 5S rRNA
Induction: - +
crRNA: C lpp C lpp
120-
90
60
30
5S rRNA
crRNA
M 1 2 3 4

FIGURE 2.2. Targeted mRNA destruction by *S. thermophilus* and *S. epidermidis* type III-A crRNPs. (A-C) Expression of *S. thermophilus* type III-A crRNPs containing either a crRNA against the *lpp* mRNA (*lpp*) or negative control crRNA (C) was induced (+) and Northern analysis was performed using probes against the *lpp* mRNA (A), lpp crRNA (B), control crRNA (C) or 5S rRNA (B and C). (D) Expression of the *S. epidermidis* (*Sep*) and *L. lactis* (*Lla*) type III-A crRNPs containing either a crRNA against the *lpp* mRNA or control crRNA was induced (+) and Northern analysis was performed using probes against the *lpp* mRNA and 5S rRNA. The positions of the RNAs are indicated including those of the full-length *lpp* mRNA (dot) and *lpp* mRNA cleavage products (red star). (A-C) The dotted lines indicate intervening lanes were omitted from the blot. The sizes of the molecular weight markers (M) are indicated in each panel.

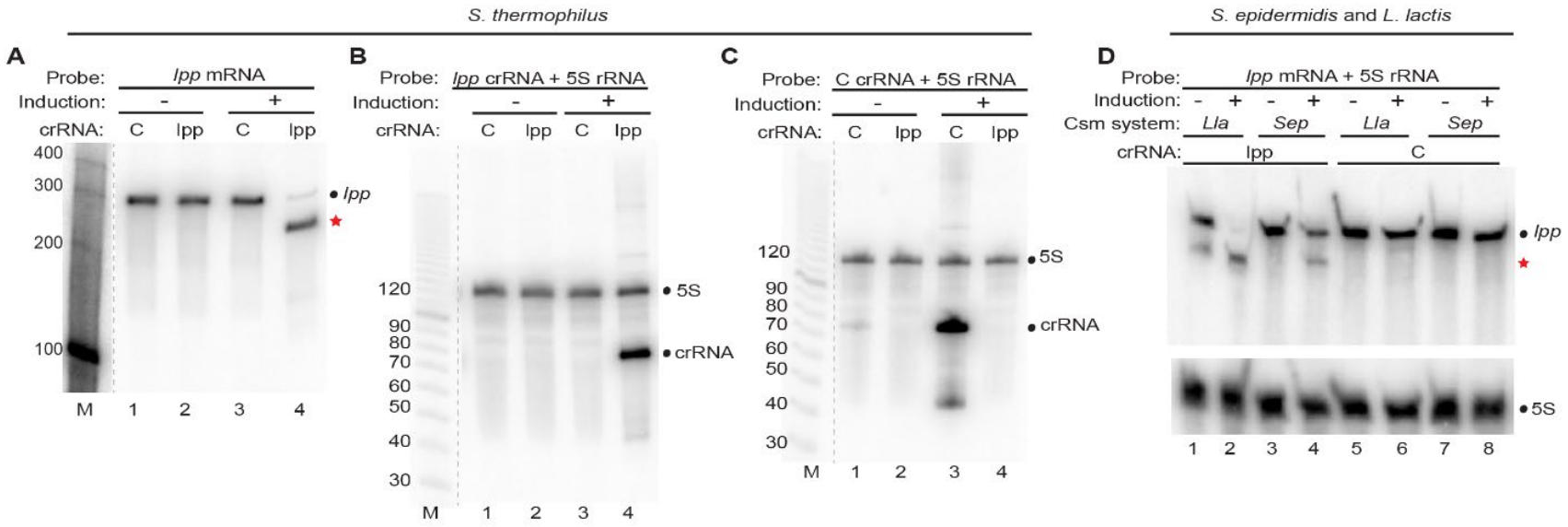
S. thermophilus
S. epidermidis and L. lactis
A
Probe: lpp mRNA
Induction: - +
crRNA: C lpp C lpp
400
300
200
100
lpp
M 1 2 3 4
B
Probe: lpp crRNA + 5S rRNA
Induction: - +
crRNA: C lpp C lpp
120
90
80
70
60
50
40
30
5S
crRNA
M 1 2 3 4
C
Probe: C crRNA + 5S rRNA
Induction: - +
crRNA: C lpp C lpp
120
90
80
70
60
50
40
30
5S
crRNA
M 1 2 3 4
D
Probe: lpp mRNA + 5S rRNA
Induction: - + - + - + - +
Csm system: Lla Sep Lla Sep
crRNA: lpp C
lpp
5S
1 2 3 4 5 6 7 8

FIGURE 2.3. Type III-A crRNPs are effective at targeting cleavage at distinct sites along the length of a mRNA. (A) Diagram of the *lpp* mRNA showing the relative positions of each tested crRNA and Northern probes employed. (B-C) Expression of the *L. lactis* type III-A crRNPs containing different crRNAs (1-5) was induced and Northern analysis was performed using probes against the 5' (B) and 3' (C) termini of the *lpp* mRNA. The positions of the full-length *lpp* mRNA (dot) and cleavage products (red star) are indicated in each panel. The sizes of the molecular weight markers (M) are indicated in each panel.

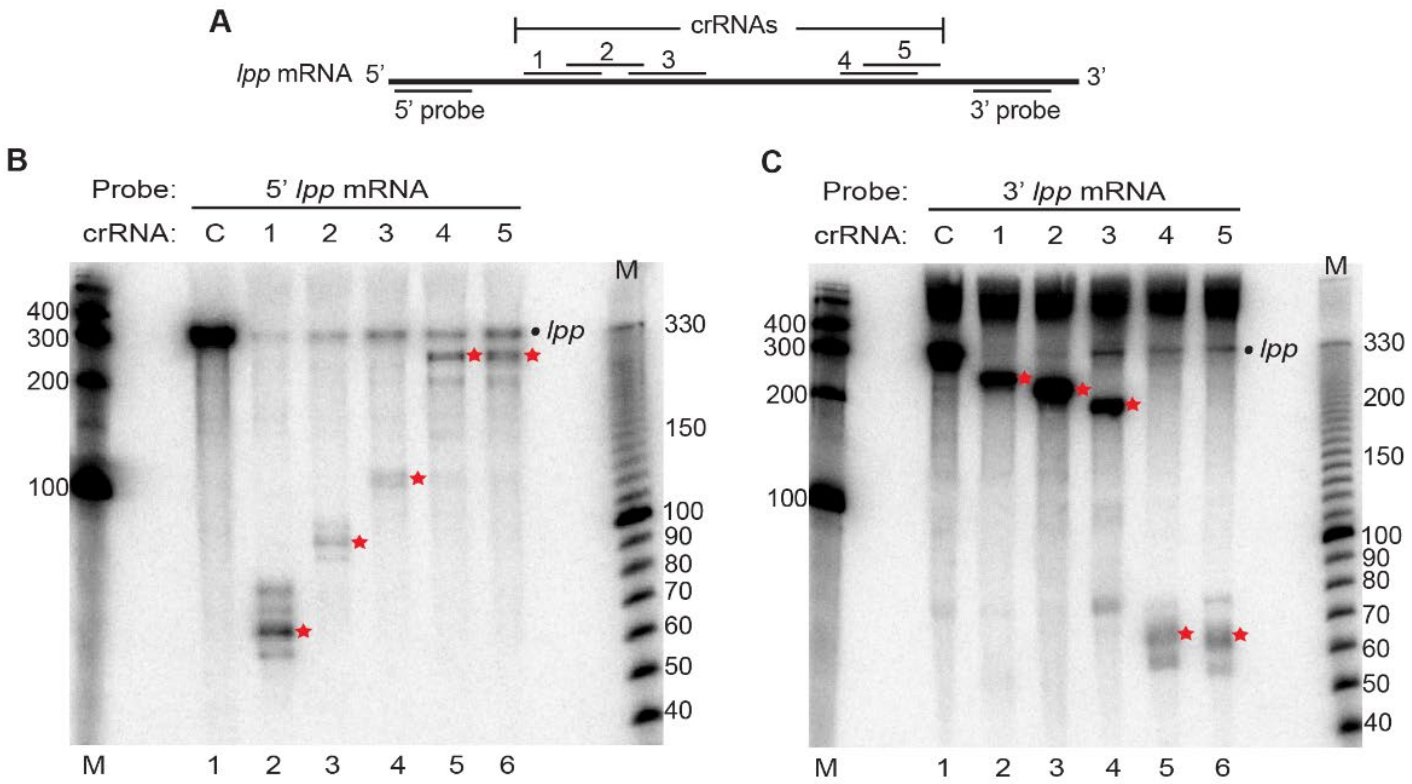
A
crRNAs
1
2
3
4
5
lpp mRNA 5'
3'
5' probe
3' probe
B
Probe:
5' lpp mRNA
crRNA:
C 1 2 3 4 5
M
400
300
200
100
lpp
330
150
100
90
80
70
60
50
40
M 1 2 3 4 5 6
C
Probe:
3' lpp mRNA
crRNA:
C 1 2 3 4 5
M
400
300
200
100
lpp
330
200
150
100
90
80
70
60
50
40
M 1 2 3 4 5 6

FIGURE 2.4. Type III-A crRNPs can effectively target multiple mRNA transcripts simultaneously. (A-C) Expression of the *L. lactis* type III-A crRNPs with single or multiple crRNAs were induced and Northern analysis was performed with probes against *lpp* mRNA (A), *cspE* mRNA (B), *ompF* mRNA (C) or 5S rRNA (A-C). The positions of full-length mRNAs (dot) and expected cleavage products (red star) are indicated in each panel. The sizes of the molecular weight markers (M) are indicated in each panel. The relative positions of the crRNA tested and Northern probe used for each mRNA is shown below each panel.

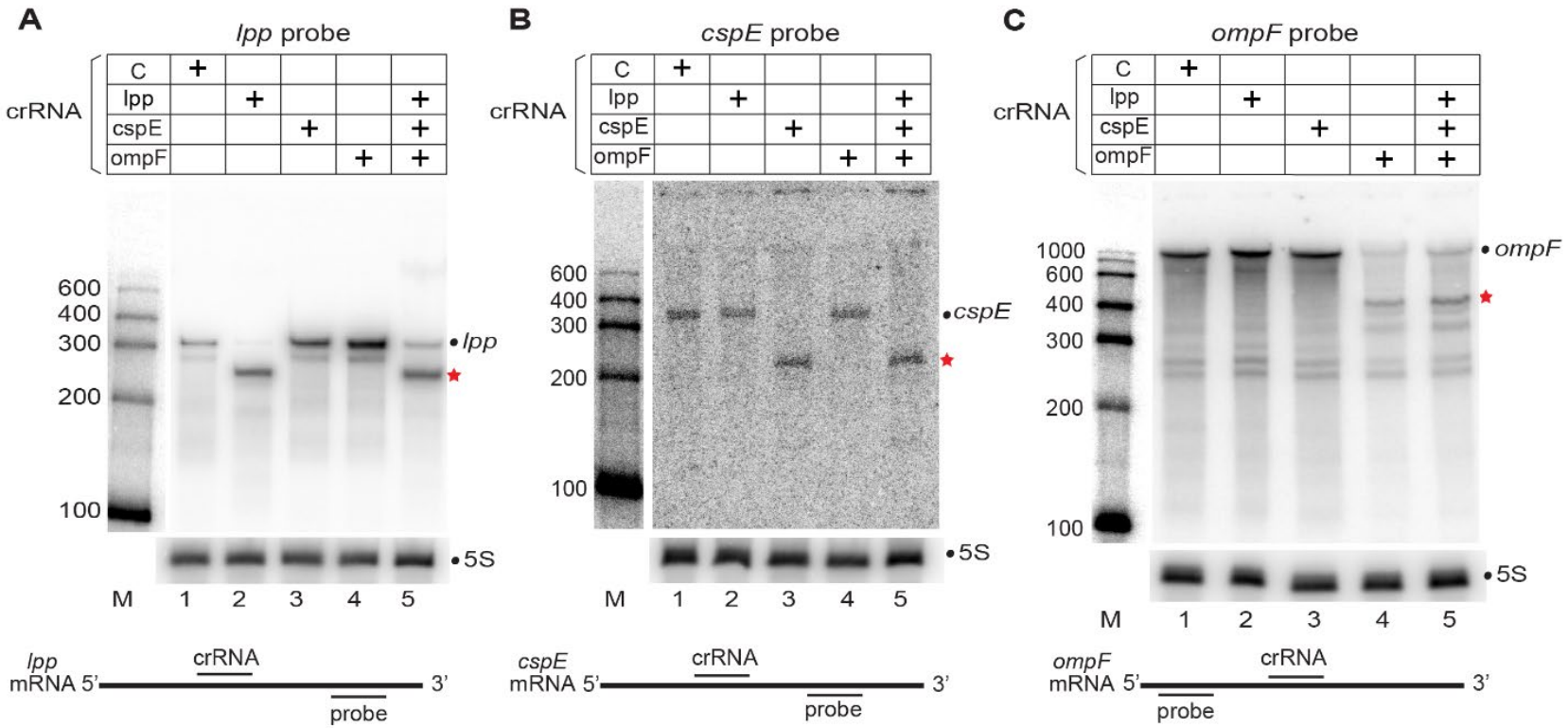
A
lpp probe
crRNA
C
lpp
cspE
ompF
600
400
300
200
100
lpp
5S
M 1 2 3 4 5
lpp mRNA 5'
crRNA
3'
probe
B
cspE probe
cspE
C
ompF probe
1000
ompF

FIGURE 2.5. Targeting the non-coding RNA component of RNase P. (A) Structure of the *T. maritima* RNase P RNA (*rnpB* RNA in cyan) in complex with the RnpA protein (purple) and substrate tRNA (orange) (PDB 3Q1R). (B) The relative positions of each tested crRNA (1-7) is indicated both on the lower diagram as well as superimposed (red) onto the *rnpB* RNA structure (cyan). (C, E) Expression of the *L. lactis* type III-A crRNPs containing a crRNA targeting *rnpB* (1-7) were induced and Northern analysis was performed with probes against the *rnpB* RNA (C), *valV-valW* pre-tRNA (E) or 5S rRNA (C and E). The positions of the *rnpB* RNA full-length (dot) and cleavage products (red stars) and sizes of molecular weight markers (M) are indicated. (D) Schematic of the *valV-valW* pre-tRNA processing by RNase P and binding location of probe used to selectively recognize the uprocessed pre-tRNA transcript (E).

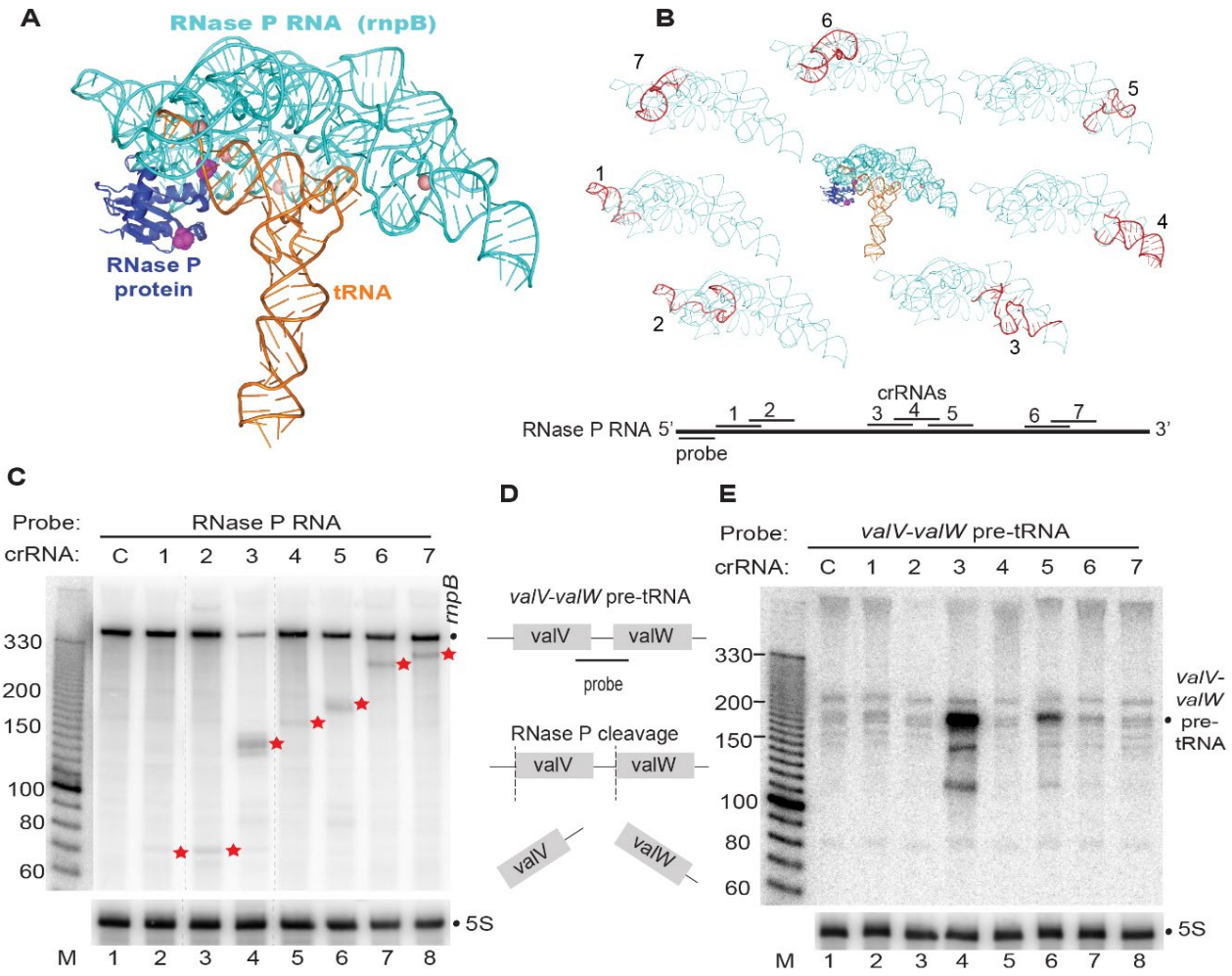
A
RNase P RNA (rnpB)
RNase P protein
tRNA
B
6
7
5
1
4
2
3
crRNAs
RNase P RNA 5'
1 2
3 4 5
6 7
3'
probe
C
Probe:
RNase P RNA
crRNA:
C 1 2 3 4 5 6 7
330
200
150
100
80
60
rnpB
5S
M 1 2 3 4 5 6 7 8
D
valV-valW pre-tRNA
valV
valW
probe
RNase P cleavage
valV
valW
E
Probe:
valV-valW pre-tRNA
crRNA:
C 1 2 3 4 5 6 7
330
200
150
100
80
60
valV-valW pre-tRNA
5S
M 1 2 3 4 5 6 7 8

Supplemental Figure S2.1. Mutagenesis of conserved HD and Palm motifs of Csm1 does not impact target RNA cleavage. Expression of *L. lactis* type III-A crRNPs containing either wildtype (WT) or mutant (HD or Palm mutants as indicated) Csm1 and crRNA targeting *lpp* mRNA was induced with arabinose (+) and Northern analysis was performed with probes against the *lpp* mRNA and 5S rRNA. The positions of both the full-length (dot) and cleavage product (red star) of the *lpp* mRNA are indicated.

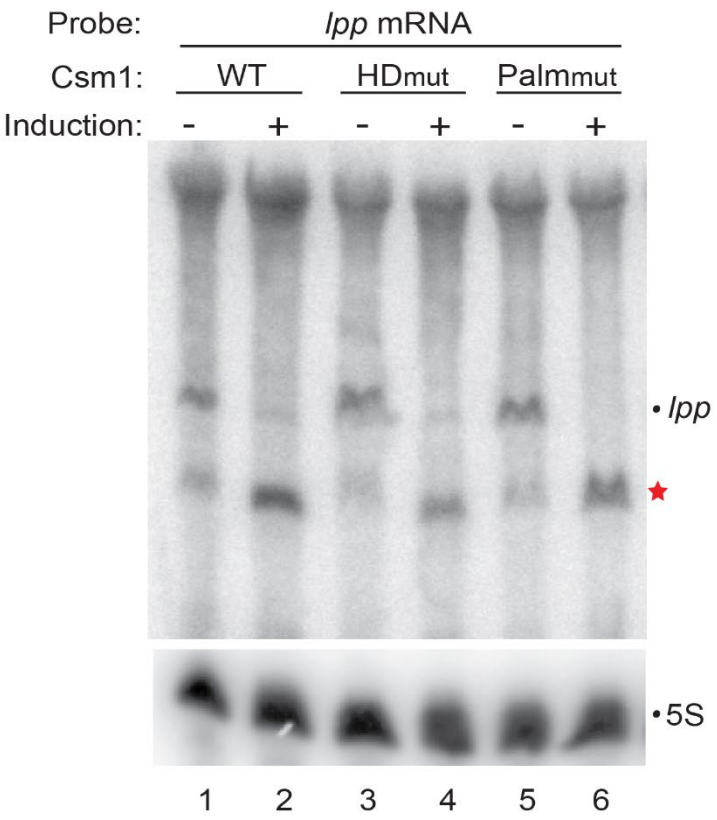
Probe:
lpp mRNA
Csm1:
WT
HDmut
Palmmut
Induction:
- + - + - +
• lpp
★
• 5S
1 2 3 4 5 6

Supplemental Figure S2.2. Mutagenesis of Csm3 (D30A) inhibits target RNA cleavage. The expression of *L. lactis* type III-A crRNPs containing the indicated Csm1, 3 and 6 variants with either the *lpp* crRNA or negative control crRNA (C) was induced with arabinose and Northern analysis was performed with a probe against the *lpp* mRNA. The positions of both the full-length (dot) and cleavage product (red star) of the *lpp* mRNA are indicated. The dotted line indicates the removal of an intervening lane.

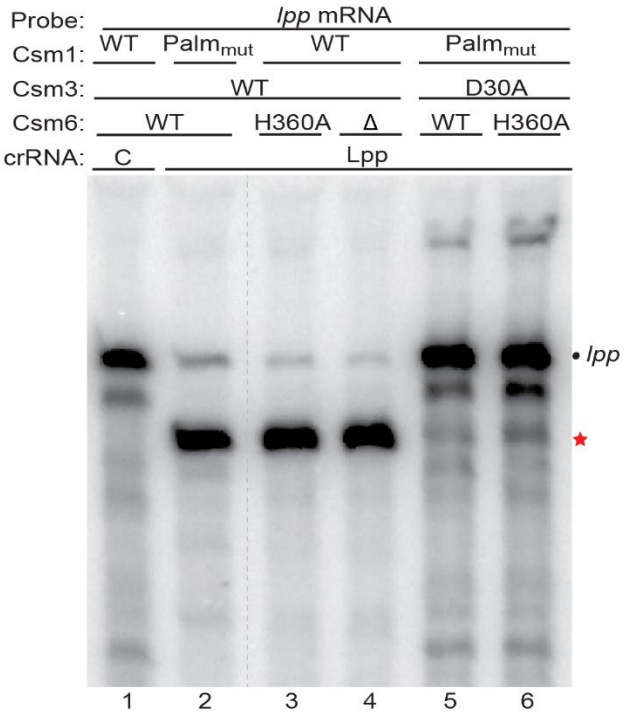
Probe:
lpp mRNA
Csm1:
WT
Palm$_{mut}$
WT
Palm$_{mut}$
Csm3:
WT
D30A
Csm6:
WT
H360A
Δ
WT
H360A
crRNA:
C
Lpp
• lpp
1
2
3
4
5
6

Table S2.1. Guide sequences for each tested target RNA

Target	System	crRNA	Guide sequence 5'-3'
lpp	*L. lactis*	lpp 1	CCAGGAUUACCGCGCCCAGUACCAGUUUAGUAGCU
lpp	*L. lactis*	lpp 2	AGCAACCUGCCAGCAGAGUAGAACCCAGGAUUACC
lpp	*L. lactis*	lpp 3	ACAGCUGAUCGAUUUUAGCGUUGCUGGAGCAACCU
lpp	*L. lactis*	lpp 4	GCGGUAUUUAGUAGCCAUGUUGUCCAGACGCUGGU
lpp	*L. lactis*	lpp 5	CUUGCGGUAUUUAGUAGCCAUGUUGUCCAGACGCU
lpp	*S. epidermidis*	lpp 1	CCAGGAUUACCGCGCCCAGUACCAGUUUAGUAGCU
lpp	*S. thermophilus*	lpp 1	CCAGGAUUACCGCGCCCAGUACCAGUUUAGUAGCUUUCA
cspE	*L. lactis*	cspE 1	GGACUCAUUAAACCACUUAACGUUACCUUUAAUCU
ompF	*L. lactis*	ompF 1	CAACGUCAGCGUAUUUAAGACCCGCGAAUGCCAGA
rnpB	*L. lactis*	rnpB 1	UAUGGAGCCCGGACUUUCCUCCCCUCCGCCCGUCU
rnpB	*L. lactis*	rnpB 2	CCAUCGGCGGUUUGCUCUCUGUUGCACUGGUCGUG
rnpB	*L. lactis*	rnpB 3	CCGGGUUCAGUACGGGCCGUACCUUAUGAACCCCU
rnpB	*L. lactis*	rnpB 4	CCCGUCUCCCCCCGAAGAGGACGACGACGAAGCGGC
rnpB	*L. lactis*	rnpB 5	CCUGAUCCCGCUUGCGCGGGCCAUCGGCGGUUUGC
rnpB	*L. lactis*	rnpB 6	UGCGCUCUUACCGCACCCUUUCACCCUUACCUGAU
rnpB	*L. lactis*	rnpB 7	CUCACUGGCUCAAGCAGCCUACCCGGGUUCAGUAC

Table S2.2. Oligonucleotides used to make crRNA guides

pCsm	crRNA	ID	Oligonucleotide sequence 5'-3'
L. lactis	lpp 1	3025	GAACCCAGGATTACCGCGCCCAGTACCAGTTTAGTAGCT
		3026	ATTTAGCTACTAAACTGGTACTGGGCGCGGTAATCCTGG
S. epidermidis	lpp 1	3025	GAACCCAGGATTACCGCGCCCAGTACCAGTTTAGTAGCT
		3142	CGATAGCTACTAAACTGGTACTGGGCGCGGTAATCCTGG
S. thermophilus	lpp 1	4670	AAACCCAGGATTACCGCGCCCAGTACCAGTTTAGTAGCTTTCA
		4671	TATCTGAAAGCTACTAAACTGGTACTGGGCGCGGTAATCCTGG
L. lactis	C	3205	GAACTTGTAGTATGCGGTCCTTGCGGCTGAGAGCACTTCAG
		3206	ATTTCTGAAGTGCTCTCAGCCGCAAGGACCGCATACTACAA
S. thermophilus	C	4388	AAACTTGTAGTATGCGGTCCTTGCGGCTGAGAGCACTTCAG
		4389	TATCCTGAAGTGCTCTCAGCCGCAAGGACCGCATACTACAA
L. lactis	lpp 2	3146	GAACAGCAACCTGCCAGCAGAGTAGAACCCAGGATTACC
		3147	ATTTGGTAATCCTGGGTTCTACTCTGCTGGCAGGTTGCT
L. lactis	lpp 3	3098	GAACACAGCTGATCGATTTTAGCGTTGCTGGAGCAACCT
		3099	ATTTAGGTTGCTCCAGCAACGCTAAAATCGATCAGCTGT
L. lactis	lpp 4	4686	GAACGCGGTATTTAGTAGCCATGTTGTCCAGACGCTGGT
		4687	ATTTACCAGCGTCTGGACAACATGGCTACTAAATACCGC
L. lactis	lpp 5	4684	GAACCTTGCGGTATTTAGTAGCCATGTTGTCCAGACGCT
		4685	ATTTAGCGTCTGGACAACATGGCTACTAAATACCGCAAG
L. lactis	cspE 1	3649	GAACGGACTCATTAAACCACTTAACGTTACCTTTAATCT
		3650	ATTTAGATTAAAGGTAACGTTAAGTGGTTTAATGAGTCC
L. lactis	ompF 1	3152	GAACCAACGTCAGCGTATTTAAGACCCGCGAATGCCAGA
		3153	ATTTTCTGGCATTCGCGGGTCTTAAATACGCTGACGTTG
L. lactis	rnpB 1	4009	GAACTATGGAGCCCGGACTTTCCTCCCCTCCGCCCGTCT
		4010	ATTTAGACGGGCGGAGGGGAGGAAAGTCCGGGCTCCATA
L. lactis	rnpB 2	4011	GAACCCATCGGCGGTTTGCTCTCTGTTGCACTGGTCGTG
		4012	ATTTCACGACCAGTGCAACAGAGAGCAAACCGCCGATGG
L. lactis	rnpB 3	4013	GAACCCGGGTTCAGTACGGGCCGTACCTTATGAACCCCT
		4014	ATTTAGGGGTTCATAAGGTACGGCCCGTACTGAACCCGG
L. lactis	rnpB 4	5212	GAACCCCGTCTCCCCCGAAGAGGACGACGACGAAGCGGC
		5213	ATTTGCCGCTTCGTCGTCGTCCTCTTCGGGGGAGACGGG
L. lactis	rnpB 5	5214	GAACCCTGATCCCGCTTGCGCGGGCCATCGGCGGTTTGC
		5215	ATTTGCAAACCGCCGATGGCCCGCGCAAGCGGGATCAGG
L. lactis	rnpB 6	5216	GAACTGCGCTCTTACCGCACCCTTTCACCCTTACCTGAT
		5217	ATTTATCAGGTAAGGGTGAAAGGGTGCGGTAAGAGCGCA
L. lactis	rnpB 7	5218	GAACCTCACTGGCTCAAGCAGCCTACCCGGGTTCAGTAC
		5219	ATTTGTACTGAACCCGGGTAGGCTGCTTGAGCCAGTGAG

Paired oligonucleotides were annealed and ligated into linearized pCsm to program guide RNAs

Multispacer array	lpp 1	3721	CAGCAAGGTCTCAGAACCCAGGATTACCGC
		3722	GATGCTGGTCTCAGGAGCGGTTGTATTTAGCTAC
	cspE 1	3723	CAGCAAGGTCTCGCTCCTCGATAAAAGGGGACGAGAACGGAC
		3724	GATGCTGGTCTCCCCTTTTATCGAGGAGCGGTTGTATTTAGAT
	ompF 1	3725	CAGCAAGGTCTCAAAGGGGACGAGAACCAAC
		3726	GATGCTGGTCTCGCGGTTGTATTTTCTGGCATT

Paired oligonucleotides were used to amplify fragments from single spacer array plasmids, which were then combined in a Golden Gate Assembly into pCsm.

Table S2.3. Oligonucleotides used to make mutations

Mutation	ID	Oligonucleotide sequence 5'-3'
L. lactis Csm1 H13A D14A D576A D577A	3197	AAGCAACCTCGAGGCTGTGGTCTA
	3186	GTGCCACGATAGATAATTTTGCCAATAGCAGCCAGCAGGCTACCACAAACC
	3187	ATTGGCAAAATTATCTATCGTGGCAC
	3188	CGCCACCGGCATAAATAAC
	3189	GTTATTTATGCCGGTGGCGCCGCCCTGTTTATGATTGGTGCATGGC
	3198	AAAAGCCATATGTTAGCGTTCACG
S. thermophilus Csm1 D575A D576A	3892	GGGAGAGGATCCATAAAGGAGG
	3895	ACCACCGGCATAGATAATGGA
	3896	TCCATTATCTATGCCGGTGGTGCAGCAGTTTTTGCAATTGGTAGCTGGC
	3897	CGCAGCCATATGTTAATCTTTACG

Table S2.4. Northern analysis oligonucleotide probes

Probe	ID	Oligonucleotide sequence 5'-3'
5S rRNA	4636	TTCTGAATTCGGCATGGGGTCAGGTGG
C crRNA	3206	ATTTCTGAAGTGCTCTCAGCCGCAAGGACCGCATACTACAA
lpp 3' (Fig 2.1-2)	3233	GAACGTCGGAACGCATTGCGTTCACGTCGTTGCTCAGCT
lpp crRNA	3026	ATTTAGCTACTAAACTGGTACTGGGCGCGGTAATCCTGG
lpp 3' (Fig S2.1)	3098	ACAGCTGATCGATTTTAGCGTTGCTGGAGCAACCT
lpp 5'	4673	ATACCCTCTAGATTGAGTTAATCTCCATGTAGCG
lpp 3' (Fig 2.3)	4750	TGCGCCATTTTTCACTTCACAGGTACTATTACTT
cspE 3'	4681	GACGTATCTTACAGAGCGAT
ompF 5'	3203	CTGCCAGAATATTGCGCTTCATCATTATTTATTAC
rnpB 5'	5236	CGGCGACTGTCTGGTCAGCTTC
valV-valW	3190	CGGACGCAGGATGGTGCGTT

CHAPTER 3

SELF VERSUS NON-SELF ACTIVATION OF TYPE III-A CRISPR-CAS SYSTEMS

[1]Walter T. Woodside, Sandra Garrett, and Michael P. Terns. Self versus non-self activation of type III-A CRISPR-Cas systems. To be submitted to RNA Biology.

Abstract

All CRISPR-Cas systems must manage their host cell defensive function against foreign nucleic acids without targeting destruction of their own genomes causing potentially lethal autoimmunity. Since crRNA guides can bind to the host genome within the CRISPR array or to antisense CRISPR RNAs, the complexes need a mechanism to be activated only by invading DNA or RNA and not host DNA or RNA. Type III systems are unique in that they lack a specific PAM found in DNA-targeting CRISPR systems. These systems bind and specifically cleave crRNA guide complementary RNA within the duplex regardless of flanking sequence identity (1, 2). Two additional activities (DNase activation and cyclic oligoadenylate production) that support invader interference only occur when the complex binds target RNAs containing certain activating protospacer flanking sequences (PFSs), heretofore assumed to be those that lack significant complementarity to the 8-nucleotide crRNA 5' tag sequence (3). Here we tested plasmid interference with three heterologously expressed type III-A systems (*Streptococcus thermophilus*, *Staphylococcus epidermidis*, and *Lactococcus lactis*) using target libraries containing thousands of PFS variants. We demonstrate that PFSs with 5' tag complementarity at positions (-2)'-(-5)' inactivate interference, while most non-complementary PFSs led to varying levels of plasmid interference. We further show that this range of type III-A mediated interference variance occurs in the native *S. thermophilus* host. Additionally, we demonstrate that plasmid interference in *S. thermophilus* is dependent on non-specific RNase activity of Csm6, and not the DNase activity of Csm1 or RNase activity of Csm3.

Introduction

CRISPR-Cas systems are an expansive family of microbial heritable adaptive immune systems that provide protection against viruses and mobile genetic elements (MGE). The clustered

regularly interspaced short palindromic repeats (CRISPR) and their associated proteins (Cas) add fragments of invader DNA to an ever-extending historic DNA tapestry, as the host encounters new foes. To form defensive complexes, the CRISPR array is first transcribed into a pre-CRISPR RNA (crRNA) which is processed into mature crRNAs each containing a single, historical invader-derived fragment. A Cas protein complex composed of a single protein or multiple protein subunits binds to the crRNA. The crRNA then guides the complex to find, bind, and destroy complementary nucleic acids (protospacers) of future invaders using integral or recruited Cas nucleases.

Research into the activation of effector complexes of CRISPR-Cas systems has determined that the protospacer adjacent sequence, whether on the DNA or RNA target, is often key to activation by a bona fide target. In types I, II, and V a short-conserved sequence (1-5 base pair) adjacent to a crRNA-complementary DNA protospacer is also required for defense activation (4-7). The short-conserved sequences, called protospacer adjacent motifs (PAMs), vary between species and systems. In all cases however, the PAM sequence is not found in the repeat sequence of the CRISPR array. Spacers in some type IV arrays share the conserved protospacer adjacent sequences of the type I systems from which they borrow an adaptation module from, but whether they target DNA or RNA is unknown. Type III systems are unique because they reportedly lack a specific activating PAM.

Type III CRISPR-Cas systems have intricate crRNA ribonucleoprotein (crRNP) effector complexes composed of multiple Cas subunits and are capable of multiple defense mechanisms (8-15). The type III-A and -B crRNPs (Csm and Cmr, respectively) are RNA guided, RNA binding, endoribonucleases that cleave target RNAs (via Csm3/Cmr4) within the RNA-RNA duplex at regular six-nucleotide intervals (16). Upon target RNA binding, a DNase in the large subunit, Cas10 (Csm1/Cmr2), can be activated to cleave single-stranded DNA (ssDNA) in a non-sequence

specific manner (2, 8, 17, 18). Target RNA binding can also activate a Palm domain within Cas10 to produce cyclic oligoadenylates (cOA) (8, 19, 20). An associated Cas protein, Csm6/Csx1, that is found as a dimer independent of the crRNP, binds to the cOA, activating an RNase catalytic site and non-specific RNA degradation (21-25) (Figure 3.1A). DNase activation and cOA production both depend on the presence of an activating protospacer flanking sequence (PFS), not found in the CRISPR array, in addition to crRNA- target RNA binding (20, 26-29). Cleavage and dissociation of the protospacer target RNA from the crRNP inactivates both the DNase activity and cOA production of Cas10 (30, 31). While contribution of the DNase or Csm6 RNase activities to defense against phages and mobile genetic elements varies among the studied systems, the combined effect of these mechanisms can halt the growth of cells with actively transcribed protospacers (27, 32-35).

Recognition of a cognate target RNA (CTR), containing a crRNA guide-complementary sequence flanked by a 5' tag- non-complementary PFS has been reported to be required for DNase and cOA production by Cas10 (2, 36-38). A strain of *Staphylococcus epidermidis* with a type III-A CRISPR system could be transformed with a conjugative plasmid containing a transcribed target sequence only when the PFS contained complementarity with the 5' tag sequence at positions (-2)-(-5) (3). Recently reported structures of Csm effector complexes have helped elucidate the intricacies of the interaction between the PFS and 5' tag of the crRNA and explain why these four positions are critical. CryoEM structures of *S. thermophilus* and *Thermococcus onnurineus* Csm complexes showed that positions (-2)-(-5) of the 5' tag are uniquely solvent exposed in the apo complex (39, 40). When the Csm complex is bound to a non-cognate target RNA (NTR), complementary to the entire crRNA, positions (-2)-(-5) of the 5' tag form base pairs with the PFS at positions (-2)'-(-5)'. When the Csm complex is bound to a CTR, instead of forming a duplex

with the 5' tag, positions (-2)'-(-5)' of the PFS interact with a loop and linker region of Csm1, stabilizing both (39). This interaction results in a conformation change in Csm1 that likely allosterically activates the HD nuclease and Palm domain cOA synthetase.

We have previously demonstrated that type III-A CRISPR-Cas systems from *Staphylococcus epidermidis*, *Lactococcus lactis*, and *S. thermophilus*, heterologously expressed in *Escherichia coli*, can mediate plasmid interference (41). The plasmid interference required transcription of a CTR, was abrogated if either the cOA generating Csm1 Palm domain or Csm6 HEPN nuclease domain were mutated, and the Csm1 ssDNase domain was dispensable (33). Here we examined the role of PFSs on type III-A CRISPR-Cas mediated plasmid interference using a heterologous expression system and a plasmid library of degenerate PFSs. As expected, we found that a lack of significant complementarity between the 5' tag and PFS results in plasmid interference. Additionally, we found even among completely non-complementary PFSs, there exists a range of interference activation levels. We confirmed this finding by testing a subset of non-complementary PFS variants in the native *S. thermophilus* host. Then, we examined the contributions of each Csm RNase and DNase towards plasmid interference and found that Csm6 RNase mediated activity is the main defensive force.

Results

The majority of PFSs activate plasmid interference and the complementarity of PFS and 5' tag protect against plasmid interference.

To determine which PFSs activate type III-A CRISPR-Cas effector complex mediated plasmid interference, we programmed plasmid-based Csm expression systems from *S. epidermidis* (SepCsm), *L. lactis* (LlpCsm), and *S. thermophilus* (StpCsm) with a spacer designed to generate a

crRNA guide sequence complementary to a protospacer (cognate crRNA or CCR) flanking a fully degenerate 8-nucleotide PFS on a pUC19 vector (pDegenPFS) (42). *E. coli* cells carrying these expression systems were transformed with pDegenPFS and transformants harboring both the expression and target plasmids were collected (Figure 3.1B). Plasmid DNA was extracted from these cells and the degenerate region of pDegenPFS was amplified and sequenced. We compared the relative abundance of each 8-nucleotide sequence (raw count/ total number of accepted reads) between pCsm carrying the CCR or a non-cognate crRNA (NCR) that lacks complementarity with the host genome and target plasmid. If all PFSs activate interference equally, we would expect that the log2 ratio would be zero for each 8-mer. Instead, we found that the majority (>60%) of PFS variants were depleted by Csm carrying a CCR (Figure 3.2A-C). We expected that PFS sequences complementary to the 5' tag of the crRNA between positions (-2)-(-5) would not activate interference and would be the most relatively-enriched sequences. We found that PFSs with 5' tag-complementary nucleotides in this region were enriched in LlpCsm (Figure 3.2A), StpCsm (Figure 3.2C), and to a lesser extent, SepCsm (Figure 3.2B). The sequences that did not activate StpCsm interference and were, therefore, highly enriched, generated a high bit score sequence logo (Figure 3.2C WebLogo) that could form a duplex with the 5' tag of the crRNA at positions (-2)-(-5).

Non-complementary PFSs do not equally activate interference

To determine if PFSs lacking complementarity at positions (-2')-(-5') equally activate interference, we created a degenerate PFS library that only contains non-complementary nucleotides, including G-U wobble bases, at the four positions for the crRNA 5' tag of StpCsm (Figure 3.3A). We hypothesized that this complete set of 13824 target plasmid variants would lead to plasmid interference. When we compared the ratio of relative abundances of PFSs recovered from *E. coli,*

carrying StpCsm with CCR or NCR, transformed with the reduced degenerate PFS library, we found that 97% of all PFS variants decreased relative abundance while the remaining 3% increased relative abundance (CCR/NCR) (Figure 3.3B, S3.1). The sequence logos for the most enriched and most depleted PFSs seem to reflect the constricted degenerate PFS library rather than indicate either activating or protective sequences. To further test whether PFSs completely lacking 5' tag-complementary nucleotides, are equally defense activating, we examined interference with single target plasmid transformations in the native *S. thermophilus*. While *S. thermophilus* transformed with a plasmid that generates an NTR quickly begins exponential growth, each non-complementary PFS variant is slower to grow. The range of growth inhibition within the 16 PFS variants tested is large. Since none of these PFSs are capable of base pairing with the 5' tag and instead are free to engage with the Csm1 linker and loop region, this clearly indicates that those protein-RNA interactions are likely sequence dependent to some degree (39).

Csm6 RNase activity is responsible for growth inhibition.

To determine which interference mechanisms, activated by the PFS, are contributing to *in vivo* plasmid interference, we generated a set of catalytic site mutations and subunit deletions in *S. thermophilus* to compare plasmid interference (Figure 3.4). Interestingly, the type III-A CRISPR-Cas locus of *S. thermophilus* JIM8232 contains an interference module with two Csm6 annotated genes, so we tested mutations and deletions with both variants. We designed CTR and NTR plasmids for this experiment to constitutively express three protospacers corresponding to the first three spacers of the CRISPR array and each of the protospacers was designed with a highly activating PFS based on the pDegenPFS assay (Figure 3.2). We found that mutation of the Csm1 ssDNase domain alone did not abrogate plasmid interference. Mutation of the Csm3 RNase

domain in addition to the Csm1 ssDNase did not change the level of interference. Only when the non-specific RNase activity mediated by both Csm6 variants was halted by mutation or deletion, or by mutation of the cyclic oligoadenylate-generating Csm1 Palm domain, was any decrease in interference activity observed. Total abrogation of plasmid interference only occurred in the absence of Csm6 RNase and Csm1 ssDNase activities.

Discussion

Previous studies demonstrated that type III-A complexes are capable of three different enzymatic activities, all dependent on a crRNA-RNA binding event, and leading to the destruction of MGE. Two of the enzymatic activities, ssDNA cleavage and cOA synthesis, only take place if there is a certain target RNA flanking sequence lacking extensive complementarity with the crRNA 5' tag. Our interference assays and deep sequencing analyses revealed that complementarity between 5' tag and 3' target flanking regions at nucleotides (-2)'-(-5)' prevents activation of the ssDNA cleavage and cOA synthesis. Interestingly, we also found that a complementary nucleotide (C) in position (-6)' had higher representation in non-activating PFSs for LlpCsm and StpCsm, even though cryoEM structures have shown this position is unable to form a duplex with the 5' tag (39). We also show that while all non-complementary 3' PFSs activate type III-A interference, they vary in activation levels, as evidenced by plasmid transformation and growth inhibition comparisons. Further structural studies of the Csm complex bound to a larger set of activating CTR may add to our understanding of the interaction of the PFS with Csm1 and Csm4 residues.

The enzymatic activities required for type III-mediated invader defense have been shown to vary between species, systems, protospacer context, and invader type (27, 32-35). Here we show that in the model organism, *S. thermophilus,* Csm6 RNase and Csm1 ssDNase activities contribute

to type III-A mediated plasmid interference. We discovered that both annotated Csm6 proteins (35.2% pairwise residue identity) are individually active and sufficient for mediating *in vivo* plasmid interference activity. It is still unclear whether Csm6 has a preference for degrading invader RNA or if the non-specific RNase activity acts as an abortive infection system that prevents host replication and growth inducing dormancy or cellular death (43). Further studies to decipher the activities of both *S. thermophilus* Csm6 variants may determine that each have different cOA binding and RNase substrate affinities. From the continued interference activity seen in the single Csm6 knockout strains, we assume that each Csm6 variant can form an RNase-functional homoduplex. It is unknown if the Csm6 variants preferentially form hetero- or homoduplexes or if the heteroduplex is functional. It is possible that formation of a non-functional heteroduplex may be an additional regulatory mechanism.

Materials and Methods

Degenerate PFS library construction

The 8-nucleotide degenerate PFS library used for Figure 3.1 was a pUC19 based plasmid generously shared by Dr. Feng Zhang (6). The reduced degenerate PFS library used in Figure 3.3 was constructed by first synthesizing an oligo with hand-mixed degenerate bases (Eurofins Genomics) designed to completely preclude RNA duplex formation with positions (-2)-(-5) of the 5' tag. This oligo was made double-stranded by using the Klenow fragment (NEB) for second strand synthesis. The dsDNA fragment was purified by agarose gel electrophoresis, recovered, and cloned into linearized pUC19 with Gibson Assembly (NEB). This assembly mixture was purified by silica column DNA recovery (Zymo Research) and then transformed into electrocompetent TOP10 *E. coli* (Thermo Fisher), recovered in SOC medium, and spread onto selective LB agar.

More than 2 x 10^6 transformants were harvested from which the degenerate plasmid library was extracted.

Degenerate PFS library transformation assays

In quintuplicate, 50 µL electrocompetent BL21-AI *E. coli* cells carrying LlpCsm, SepCsm, or StpCsm, each programmed with a cognate or non-cognate spacer were transformed with 100 ng of degenerate PFS target library (33, 42). Transformations were recovered in 950 µL SOC for 1 hour at 37ºC and duplicate transformations were combined and evenly spread with glass beads onto 3, 25 cm x 25 cm LB agar plates containing 34 ug/mL chloramphenicol and 100 ug/mL ampicillin and incubated overnight at 37ºC. The StpCsm transformants were additionally induced with 10 mM arabinose. Serial dilutions were spot plated in parallel to estimate total CFUs. All colonies were scraped off of the 25 cm x 25 cm agar plates with a clean utility blade. Plasmid DNA was extracted from the cell mass (ZymoPURE Plasmid Midiprep Kit, Zymo Research).

High throughput screening of PFS region

A region containing the degenerate PFS was amplified in a PCR with Phusion polymerase (NEB) using GC rich optimization buffer. The primers were appended with MiSeq barcode adapters. The product of this PCR was purified by agarose gel electrophoresis followed by DNA recovery (Zymo Research). This purified product was then used as template for a barcoding PCR. Final gel-purified amplicon libraries were normalized according to concentration and pooled before carrying out sequencing on an illumina MiSeq. After sequencing, the samples were de-multiplexed by index and the sequence corresponding to the PFS was extracted from each read.

Natural transformation and mutagenesis of JIM 8232 Streptococcus thermophilus

Streptococcus thermophilus JIM8232 was grown overnight in LM17 (Difco). 1 mL of overnight culture was centrifuged at 2,600 x g for 9 minutes and the cell pellet was resuspended and washed twice in a chemically defined medium (CDM) devoid of peptides (44). After a final resuspension in 1 mL CDM, the culture was diluted to an OD_{600} of 0.05 and incubated for 90 minutes at 37ºC and used immediately or stored at -20ºC. To 100 µL thawed cells, 1 µM of competence inducing peptide ComS was added (44, 45). Splicing by overlap extension PCR was used to generate DNA fragments with 700 bp homology arms. 300-700 ng of this DNA fragment was added to the naturally competent cells. The transformation mixtures were incubated at 37ºC for 3 hours and then diluted 1: 1000 and spread onto non-selective LM17 agar to isolate individual colonies. Colonies were directly screened with OneTaq (NEB) polymerase. Point mutations were screened for using primers with 3' ends specific for the mutagenized nucleotides. Sanger sequencing was used to verify all mutations. All cloning related oligos and mutant sequences are available upon request.

***S. thermophilus* plasmid interference assays**

Cells were made naturally competent, as described above, and transformed with 100 ng pWAR plasmid DNA. CTR plasmids contain a constitutively transcribed RNA containing three protospacer sequences each flanked by a PFS previously found to activate interference. The NTR plasmids are identical except the PFSs are complementary to the 5' tag. Transformation mixtures were incubated at 37ºC for 3 hours before spreading onto selective LM17 + 5 µM chloramphenicol agar. Plates were incubated at 37ºC and colonies were counted after 48 hours.

Growth curves

Naturally competent *S. thermophilus* strains were transformed with 100 ng of a CTR or NTR plasmid and incubated for 3 hours at 37ºC. Transformations were then subcultured 1:20 into fresh selective LM17 broth and transferred to a 96 well plate. Growth was monitored on a BioTek Epoch 2 plate reader with OD_{600} measurements taken every 10 minutes.

References

1. Maniv, I., W. Jiang, D. Bikard, and L.A. Marraffini, *Impact of Different Target Sequences on Type III CRISPR-Cas Immunity.* J Bacteriol, 2016. **198**(6): p. 941-50.
2. Elmore, J.R., N.F. Sheppard, N. Ramia, T. Deighan, H. Li, R.M. Terns, and M.P. Terns, *Bipartite recognition of target RNAs activates DNA cleavage by the Type III-B CRISPR-Cas system.* Genes Dev, 2016. **30**(4): p. 447-59.
3. Marraffini, L.A. and E.J. Sontheimer, *Self versus non-self discrimination during CRISPR RNA-directed immunity.* Nature, 2010. **463**(7280): p. 568-71.
4. Plagens, A., V. Tripp, M. Daume, K. Sharma, A. Klingl, A. Hrle, E. Conti, H. Urlaub, and L. Randau, *In vitro assembly and activity of an archaeal CRISPR-Cas type I-A Cascade interference complex.* Nucleic Acids Res, 2014. **42**(8): p. 5125-38.
5. Chylinski, K., K.S. Makarova, E. Charpentier, and E.V. Koonin, *Classification and evolution of type II CRISPR-Cas systems.* Nucleic Acids Res, 2014. **42**(10): p. 6091-105.
6. Zetsche, B., J.S. Gootenberg, O.O. Abudayyeh, I.M. Slaymaker, K.S. Makarova, P. Essletzbichler, S.E. Volz, J. Joung, J. van der Oost, A. Regev, E.V. Koonin, and F. Zhang, *Cpf1 is a single RNA-guided endonuclease of a class 2 CRISPR-Cas system.* Cell, 2015. **163**(3): p. 759-71.

7. Chen, J.S., E. Ma, L.B. Harrington, M. Da Costa, X. Tian, J.M. Palefsky, and J.A. Doudna, *CRISPR-Cas12a target binding unleashes indiscriminate single-stranded DNase activity.* Science, 2018. **360**(6387): p. 436-439.

8. Foster, K., S. Gruschow, S. Bailey, M.F. White, and M.P. Terns, *Regulation of the RNA and DNA nuclease activities required for Pyrococcus furiosus Type III-B CRISPR-Cas immunity.* Nucleic Acids Res, 2020. **48**(8): p. 4418-4434.

9. Zhang, J., S. Graham, A. Tello, H. Liu, and M.F. White, *Multiple nucleic acid cleavage modes in divergent type III CRISPR systems.* Nucleic Acids Res, 2016. **44**(4): p. 1789-99.

10. Goldberg, G.W., W. Jiang, D. Bikard, and L.A. Marraffini, *Conditional tolerance of temperate phages via transcription-dependent CRISPR-Cas targeting.* Nature, 2014. **514**(7524): p. 633-7.

11. Spilman, M., A. Cocozaki, C. Hale, Y. Shao, N. Ramia, R. Terns, M. Terns, H. Li, and S. Stagg, *Structure of an RNA silencing complex of the CRISPR-Cas immune system.* Mol Cell, 2013. **52**(1): p. 146-52.

12. Park, J.H., J. Sun, S.Y. Park, H.J. Hwang, M.Y. Park, M. Shin, and J.S. Kim, *Crystal structure of Cmr5 from Pyrococcus furiosus and its functional implications.* FEBS Lett, 2013. **587**(6): p. 562-8.

13. Osawa, T., H. Inanaga, and T. Numata, *Crystal structure of the Cmr2-Cmr3 subcomplex in the CRISPR-Cas RNA silencing effector complex.* J Mol Biol, 2013. **425**(20): p. 3811-23.

14. Makarova, K.S., D.H. Haft, R. Barrangou, S.J. Brouns, E. Charpentier, P. Horvath, S. Moineau, F.J. Mojica, Y.I. Wolf, A.F. Yakunin, J. van der Oost, and E.V. Koonin,

Evolution and classification of the CRISPR-Cas systems. Nat Rev Microbiol, 2011. **9**(6): p. 467-77.

15. Hale, C.R., P. Zhao, S. Olson, M.O. Duff, B.R. Graveley, L. Wells, R.M. Terns, and M.P. Terns, *RNA-guided RNA cleavage by a CRISPR RNA-Cas protein complex.* Cell, 2009. **139**(5): p. 945-56.

16. Benda, C., J. Ebert, R.A. Scheltema, H.B. Schiller, M. Baumgartner, F. Bonneau, M. Mann, and E. Conti, *Structural model of a CRISPR RNA-silencing complex reveals the RNA-target cleavage activity in Cmr4.* Mol Cell, 2014. **56**(1): p. 43-54.

17. Johnson, K., B.A. Learn, M.A. Estrella, and S. Bailey, *Target sequence requirements of a type III-B CRISPR-Cas immune system.* J Biol Chem, 2019. **294**(26): p. 10290-10299.

18. Wang, L., C.Y. Mo, M.R. Wasserman, J.T. Rostol, L.A. Marraffini, and S. Liu, *Dynamics of Cas10 Govern Discrimination between Self and Non-self in Type III CRISPR-Cas Immunity.* Mol Cell, 2019. **73**(2): p. 278-290 e4.

19. Niewoehner, O., C. Garcia-Doval, J.T. Rostol, C. Berk, F. Schwede, L. Bigler, J. Hall, L.A. Marraffini, and M. Jinek, *Type III CRISPR-Cas systems produce cyclic oligoadenylate second messengers.* Nature, 2017. **548**(7669): p. 543-548.

20. Kazlauskiene, M., G. Kostiuk, C. Venclovas, G. Tamulaitis, and V. Siksnys, *A cyclic oligonucleotide signaling pathway in type III CRISPR-Cas systems.* Science, 2017. **357**(6351): p. 605-609.

21. Sheppard, N.F., C.V. Glover, 3rd, R.M. Terns, and M.P. Terns, *The CRISPR-associated Csx1 protein of Pyrococcus furiosus is an adenosine-specific endoribonuclease.* RNA, 2016. **22**(2): p. 216-24.

22. Gruschow, S., J.S. Athukoralage, S. Graham, T. Hoogeboom, and M.F. White, *Cyclic oligoadenylate signalling mediates Mycobacterium tuberculosis CRISPR defence.* Nucleic Acids Res, 2019. **47**(17): p. 9259-9270.

23. Han, W., S. Stella, Y. Zhang, T. Guo, K. Sulek, L. Peng-Lundgren, G. Montoya, and Q. She, *A Type III-B Cmr effector complex catalyzes the synthesis of cyclic oligoadenylate second messengers by cooperative substrate binding.* Nucleic Acids Res, 2018. **46**(19): p. 10319-10330.

24. Garcia-Doval, C., F. Schwede, C. Berk, J.T. Rostol, O. Niewoehner, O. Tejero, J. Hall, L.A. Marraffini, and M. Jinek, *Activation and self-inactivation mechanisms of the cyclic oligoadenylate-dependent CRISPR ribonuclease Csm6.* Nat Commun, 2020. **11**(1): p. 1596.

25. Smalakyte, D., M. Kazlauskiene, F.H. J, A. Ruksenaite, A. Rimaite, G. Tamulaitiene, N.J. Faergeman, G. Tamulaitis, and V. Siksnys, *Type III-A CRISPR-associated protein Csm6 degrades cyclic hexa-adenylate activator using both CARF and HEPN domains.* Nucleic Acids Res, 2020. **48**(16): p. 9204-9217.

26. Hale, C.R., S. Majumdar, J. Elmore, N. Pfister, M. Compton, S. Olson, A.M. Resch, C.V. Glover, 3rd, B.R. Graveley, R.M. Terns, and M.P. Terns, *Essential features and rational design of CRISPR RNAs that function with the Cas RAMP module complex to cleave RNAs.* Mol Cell, 2012. **45**(3): p. 292-302.

27. Samai, P., N. Pyenson, W. Jiang, G.W. Goldberg, A. Hatoum-Aslan, and L.A. Marraffini, *Co-transcriptional DNA and RNA Cleavage during Type III CRISPR-Cas Immunity.* Cell, 2015. **161**(5): p. 1164-1174.

28. Staals, R.H., Y. Zhu, D.W. Taylor, J.E. Kornfeld, K. Sharma, A. Barendregt, J.J. Koehorst, M. Vlot, N. Neupane, K. Varossieau, K. Sakamoto, T. Suzuki, N. Dohmae, S. Yokoyama, P.J. Schaap, H. Urlaub, A.J. Heck, E. Nogales, J.A. Doudna, A. Shinkai, and J. van der Oost, *RNA targeting by the type III-A CRISPR-Cas Csm complex of Thermus thermophilus.* Mol Cell, 2014. **56**(4): p. 518-30.

29. Tamulaitis, G., M. Kazlauskiene, E. Manakova, C. Venclovas, A.O. Nwokeoji, M.J. Dickman, P. Horvath, and V. Siksnys, *Programmable RNA shredding by the type III-A CRISPR-Cas system of Streptococcus thermophilus.* Mol Cell, 2014. **56**(4): p. 506-17.

30. Nasef, M., M.C. Muffly, A.B. Beckman, S.J. Rowe, F.C. Walker, A. Hatoum-Aslan, and J.A. Dunkle, *Regulation of cyclic oligoadenylate synthesis by the Staphylococcus epidermidis Cas10-Csm complex.* RNA, 2019. **25**(8): p. 948-962.

31. Rouillon, C., J.S. Athukoralage, S. Graham, S. Gruschow, and M.F. White, *Control of cyclic oligoadenylate synthesis in a type III CRISPR system.* Elife, 2018. **7**.

32. Hatoum-Aslan, A., I. Maniv, P. Samai, and L.A. Marraffini, *Genetic characterization of antiplasmid immunity through a type III-A CRISPR-Cas system.* J Bacteriol, 2014. **196**(2): p. 310-7.

33. Foster, K., J. Kalter, W. Woodside, R.M. Terns, and M.P. Terns, *The ribonuclease activity of Csm6 is required for anti-plasmid immunity by Type III-A CRISPR-Cas systems.* RNA Biol, 2019. **16**(4): p. 449-460.

34. Millen, A.M., J.E. Samson, D.M. Tremblay, A.H. Magadan, G.M. Rousseau, S. Moineau, and D.A. Romero, *Lactococcus lactis type III-A CRISPR-Cas system cleaves bacteriophage RNA.* RNA Biol, 2019. **16**(4): p. 461-468.

35. Deng, L., R.A. Garrett, S.A. Shah, X. Peng, and Q. She, *A novel interference mechanism by a type IIIB CRISPR-Cmr module in Sulfolobus.* Mol Microbiol, 2013. **87**(5): p. 1088-99.

36. Kazlauskiene, M., G. Tamulaitis, G. Kostiuk, C. Venclovas, and V. Siksnys, *Spatiotemporal Control of Type III-A CRISPR-Cas Immunity: Coupling DNA Degradation with the Target RNA Recognition.* Mol Cell, 2016. **62**(2): p. 295-306.

37. Estrella, M.A., F.T. Kuo, and S. Bailey, *RNA-activated DNA cleavage by the Type III-B CRISPR-Cas effector complex.* Genes Dev, 2016. **30**(4): p. 460-70.

38. Pyenson, N.C., K. Gayvert, A. Varble, O. Elemento, and L.A. Marraffini, *Broad Targeting Specificity during Bacterial Type III CRISPR-Cas Immunity Constrains Viral Escape.* Cell Host Microbe, 2017. **22**(3): p. 343-353 e3.

39. You, L., J. Ma, J. Wang, D. Artamonova, M. Wang, L. Liu, H. Xiang, K. Severinov, X. Zhang, and Y. Wang, *Structure Studies of the CRISPR-Csm Complex Reveal Mechanism of Co-transcriptional Interference.* Cell, 2019. **176**(1-2): p. 239-253 e16.

40. Jia, N., C.Y. Mo, C. Wang, E.T. Eng, L.A. Marraffini, and D.J. Patel, *Type III-A CRISPR-Cas Csm Complexes: Assembly, Periodic RNA Cleavage, DNase Activity Regulation, and Autoimmunity.* Mol Cell, 2019. **73**(2): p. 264-277 e5.

41. Ichikawa, H.T., J.C. Cooper, L. Lo, J. Potter, R.M. Terns, and M.P. Terns, *Programmable type III-A CRISPR-Cas DNA targeting modules.* PLoS One, 2017. **12**(4): p. e0176221.

42. Abudayyeh, O.O., J.S. Gootenberg, S. Konermann, J. Joung, I.M. Slaymaker, D.B. Cox, S. Shmakov, K.S. Makarova, E. Semenova, L. Minakhin, K. Severinov, A. Regev, E.S. Lander, E.V. Koonin, and F. Zhang, *C2c2 is a single-component programmable RNA-guided RNA-targeting CRISPR effector.* Science, 2016. **353**(6299): p. aaf5573.

43. Lopatina, A., N. Tal, and R. Sorek, *Abortive Infection: Bacterial Suicide as an Antiviral Immune Strategy.* Annu Rev Virol, 2020. **7**(1): p. 371-384.

44. Fontaine, L., C. Boutry, M.H. de Frahan, B. Delplace, C. Fremaux, P. Horvath, P. Boyaval, and P. Hols, *A novel pheromone quorum-sensing system controls the development of natural competence in Streptococcus thermophilus and Streptococcus salivarius.* J Bacteriol, 2010. **192**(5): p. 1444-54.

45. Gardan, R., C. Besset, C. Gitton, A. Guillot, L. Fontaine, P. Hols, and V. Monnet, *Extracellular life cycle of ComS, the competence-stimulating peptide of Streptococcus thermophilus.* J Bacteriol, 2013. **195**(8): p. 1845-55.

Figure 3.1 Model for immunity by the type III-A crRNP and plasmid interference assay. (A) Model for transcription-dependent immunity by the type III-A crRNP. Transcription across a protospacer target generates a nascent transcript that is complementary to the guide sequence of a crRNP. Binding to the target RNA activates RNA cleavage by Csm3 subunits. A protospacer flanking sequence on the bound RNA activates cyclic oligoadenylate (cOA) synthesis and DNase activity by the Csm1 subunit. The cOA molecules bind to and activates the Csm6 RNase. (B) Schematic of the degenerate PFS library transformation assay.

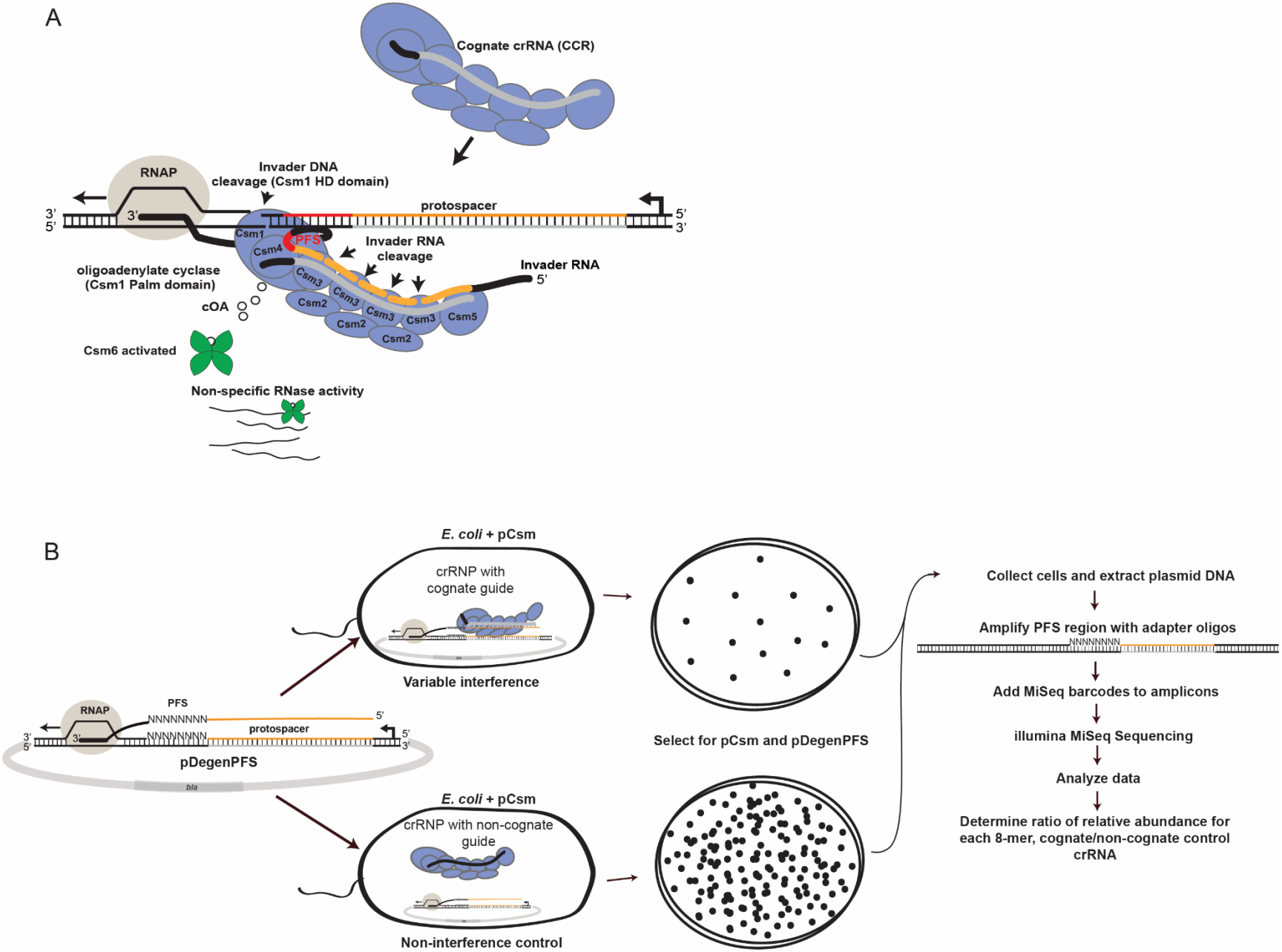
A
Cognate crRNA (CCR)
RNAP
Invader DNA cleavage (Csm1 HD domain)
protospacer
3'
5'
Csm1
Csm4
PFS
Invader RNA cleavage
Invader RNA
oligoadenylate cyclase (Csm1 Palm domain)
cOA
Csm3
Csm2
Csm5
Csm6 activated
Non-specific RNase activity
B
E. coli + pCsm
crRNP with cognate guide
Variable interference
PFS
NNNNNNNN
protospacer
pDegenPFS
bla
Select for pCsm and pDegenPFS
Collect cells and extract plasmid DNA
Amplify PFS region with adapter oligos
Add MiSeq barcodes to amplicons
illumina MiSeq Sequencing
Analyze data
Determine ratio of relative abundance for each 8-mer, cognate/non-cognate control crRNA
E. coli + pCsm
crRNP with non-cognate guide
Non-interference control

Figure 3.2 Degenerate PFS plasmid library transformation assay deep sequencing analysis. Relative abundance of each 8-nucleotide PFS after interference assay with (A) *L. lactis*, (B) *S. epidermidis*, and (C) *S. thermophilus*, are shown in a line graph. A log2 value greater than zero indicates a relative enrichment, and below zero a relative depletion, of a given 8-mer. The percentage of 8-mers that increased or decreased in abundance is shown below the line graph. Sequence logo for the 100 most enriched and 100 most depleted 8-mers are shown on the right. The 5' tag sequence of the crRNA is aligned above the logo. CCR is cognate crRNA and NCR is noncognate crRNA.

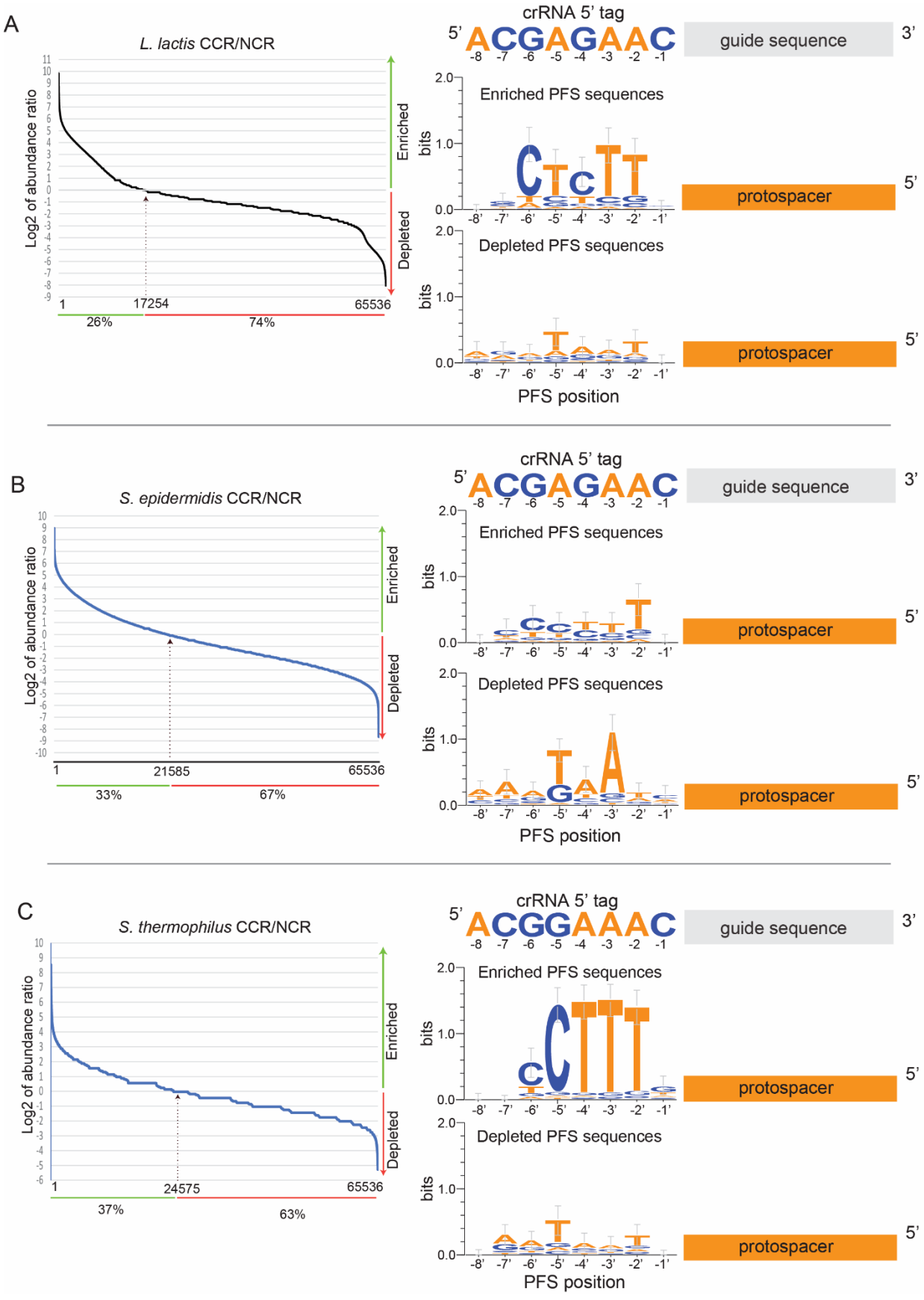
A
L. lactis CCR/NCR
Log2 of abundance ratio
Enriched
Depleted
1
17254
65536
26%
74%
crRNA 5' tag
5' ACGAGAAC 3'
guide sequence
Enriched PFS sequences
bits
protospacer
5'
Depleted PFS sequences
PFS position
B
S. epidermidis CCR/NCR
1
21585
65536
33%
67%
5' ACGAGAAC 3'
C
S. thermophilus CCR/NCR
1
24575
65536
37%
63%
5' ACGGAAAC 3'

Figure 3.3 Non-complementary PFSs variably activate interference. (A) Diagram of degenerate PFS library designed to lack crRNA 5' tag complementary nucleotides at positions (-2)'-(-5)'. (B) Plasmid interference assay and deep sequencing was carried out as in Fig. 3.2 and sequence logos generated from the 100 most enriched and 100 most depleted PFSs. (C) Plasmids carrying a protospacer matching spacer 1 in the native type III-A CRISPR array and a PFS that completely lacks complementarity to the 5' tag were used to transform naturally competent *S. thermophilus*. After three hours of incubation at 37 ºC, transformation mixtures were subcultured 1:20 into selective LM17 broth, loaded onto a 96 well plate, and incubated at 37ºC in a BioTek Epoch2 plate reader and optical density was monitored. Untransformed cells, an empty vector control, and a perfect 5' tag complementary PFS target plasmid transformation are indicated. PFS sequences and abundance ratios calculated for each PFS in (B) are shown above growth curves.

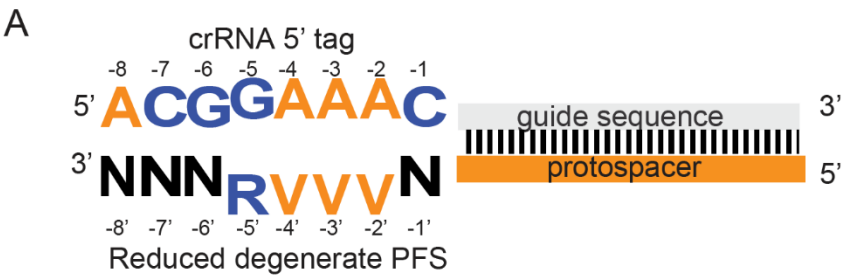
A
crRNA 5' tag
-8 -7 -6 -5 -4 -3 -2 -1
5' ACGGAAAC
guide sequence
3'
protospacer
5'
3' NNNRVVVN
-8' -7' -6' -5' -4' -3' -2' -1'
Reduced degenerate PFS

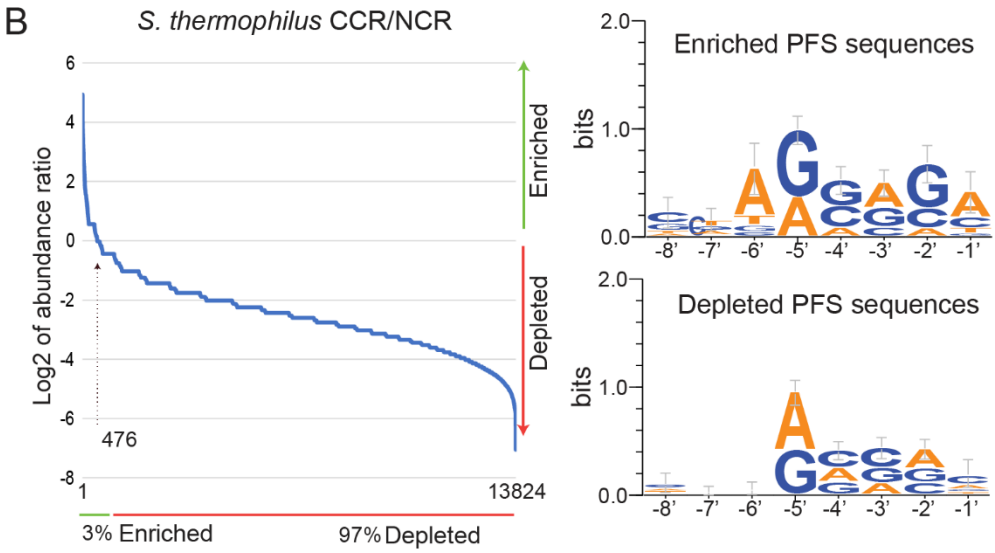
B
S. thermophilus CCR/NCR
Log2 of abundance ratio
6
4
2
0
-2
-4
-6
-8
476
1
13824
Enriched
Depleted
3% Enriched
97% Depleted
Enriched PFS sequences
bits
2.0
1.0
0.0
-8' -7' -6' -5' -4' -3' -2' -1'
Depleted PFS sequences
bits
2.0
1.0
0.0
-8' -7' -6' -5' -4' -3' -2' -1'

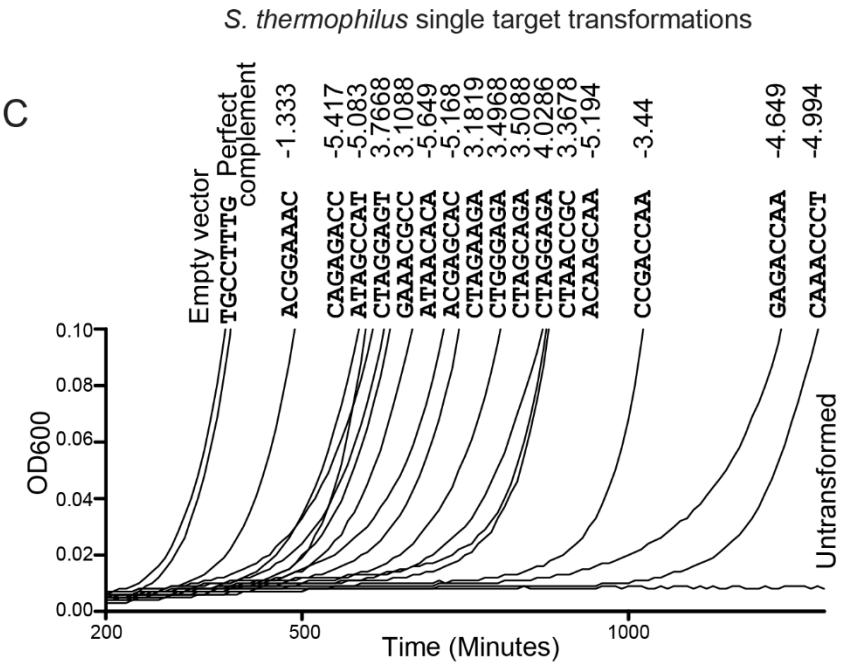
S. thermophilus single target transformations
C
Empty vector
Perfect complement TGCCTTTG
ACGGAAAC -1.333
CAGAGACC -5.417
ATAGCCAT -5.083
CTAGGAGT 3.7668
GAAACGCC 3.1088
ATAACACA -5.649
ACGAGCAC -5.168
CTAGAAGA 3.1819
CTGGGAGA 3.4968
CTAGCAGA 3.5088
CTAGGAGA 4.0286
CTAACCGC 3.3678
ACAAGCAA -5.194
CCGACCAA -3.44
GAGACCAA -4.649
CAAACCCT -4.994
Untransformed
OD600
0.10
0.08
0.06
0.04
0.02
0.00
200
500
1000
Time (Minutes)

Figure 3.4 Csm6 RNase activity is required for total plasmid interference. *S. thermophilus* strains with the indicated mutations were transformed with a CTR or NTR plasmids. Colonies were counted after 48 hours and the ratio of transformation efficiency (CTR/NTR) is shown in a bar graph. A relative transformation efficiency of 1 indicates no interference while zero indicates total plasmid interference.

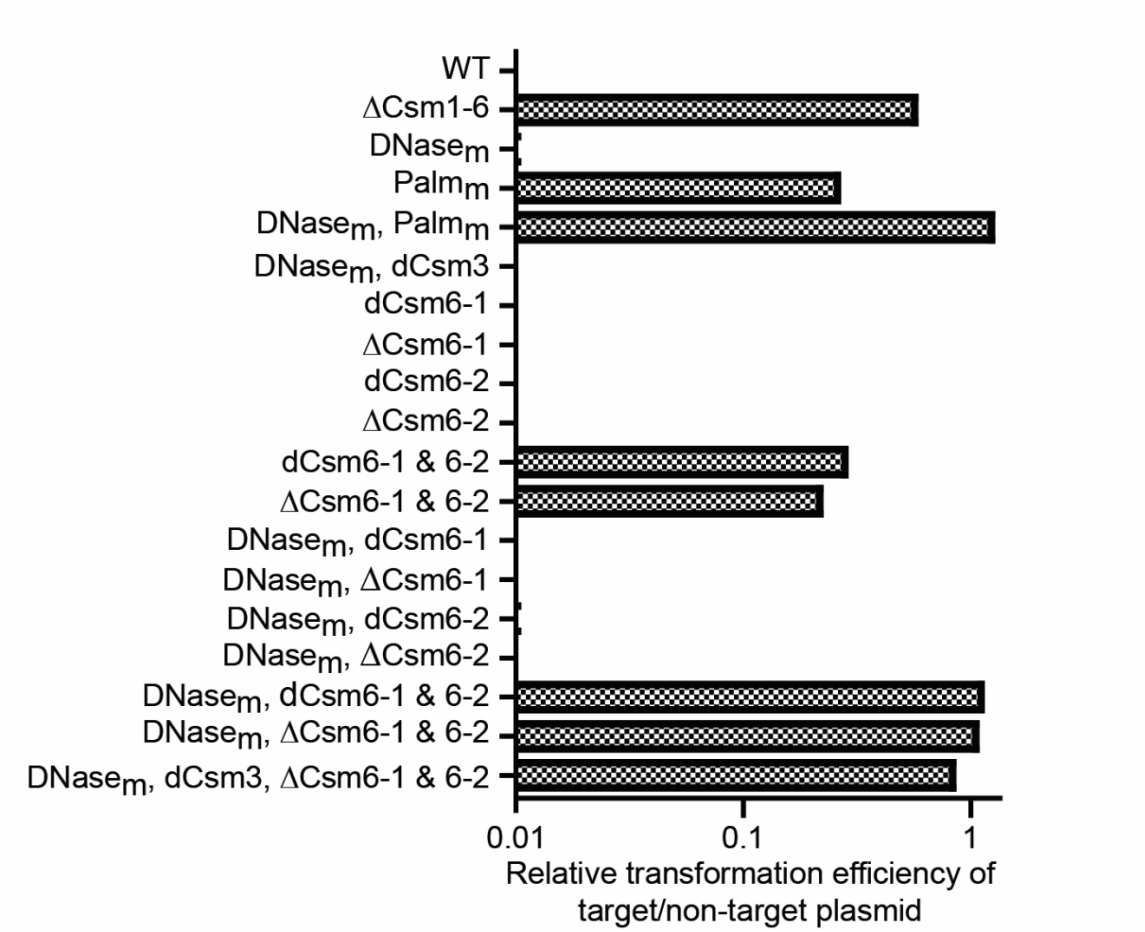
WT
ΔCsm1-6
DNase$_m$
Palm$_m$
DNase$_m$, Palm$_m$
DNase$_m$, dCsm3
dCsm6-1
ΔCsm6-1
dCsm6-2
ΔCsm6-2
dCsm6-1 & 6-2
ΔCsm6-1 & 6-2
DNase$_m$, dCsm6-1
DNase$_m$, ΔCsm6-1
DNase$_m$, dCsm6-2
DNase$_m$, ΔCsm6-2
DNase$_m$, dCsm6-1 & 6-2
DNase$_m$, ΔCsm6-1 & 6-2
DNase$_m$, dCsm3, ΔCsm6-1 & 6-2
0.01
0.1
1
Relative transformation efficiency of target/non-target plasmid

Figure S3.1 Reduced degenerate PFS library transformation assay serial dilutions. Serial 10-fold dilutions of transformations from Figure 3.3B were spot plated onto LB agar containing 34 ug/mL chloramphenicol, 100 ug/mL ampicillin, and 10 mM arabinose. CCR is cognate crRNA and NCR is noncognate crRNA. Empty pACYC does not contain CRISPR system genes or an array.

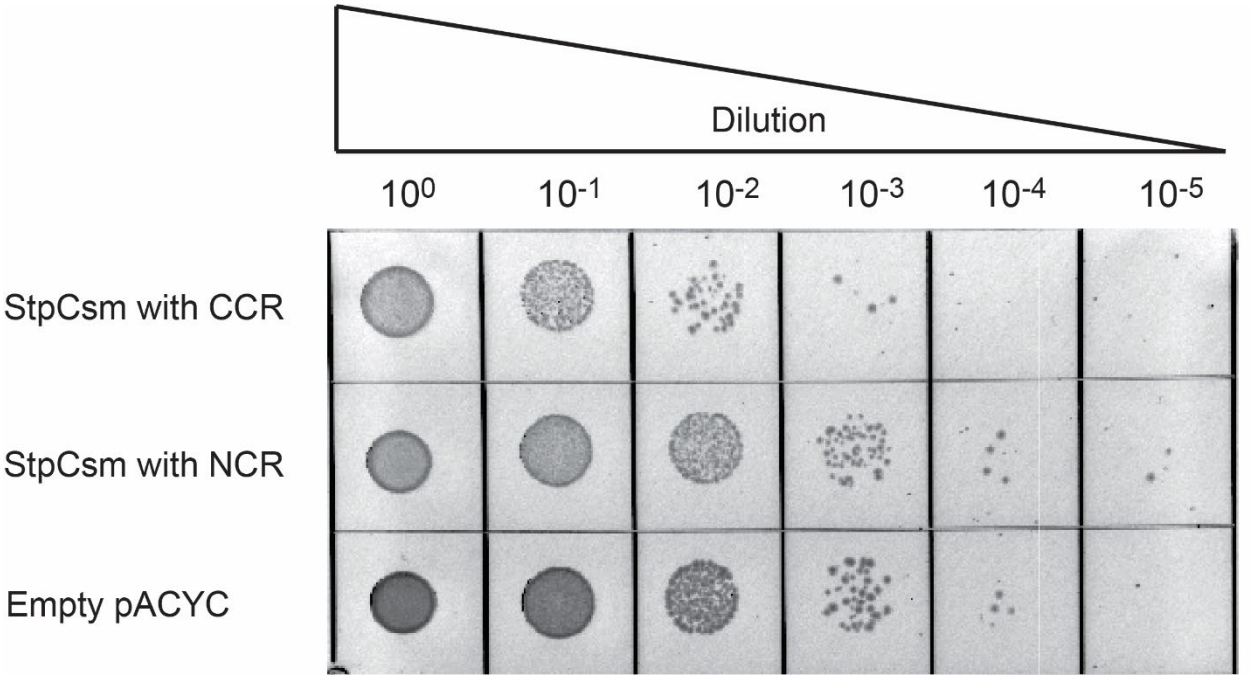
Dilution
10^0
10^-1
10^-2
10^-3
10^-4
10^-5
StpCsm with CCR
StpCsm with NCR
Empty pACYC

CHAPTER 4

DISCUSSION

CRISPR-Cas mediated RNA interference in prokaryotes

Microbes lack the RNA interference systems routinely used in eukaryote research to determine the function of genes. Recently discovered RNA targeting CRISPR-Cas systems from types II, III and VI may have the potential to fill this role for prokaryotic research. Stepping back and looking at the broad picture of CRISPR based RNA targeting systems can help us see how our new data fits into the expanding body of knowledge.

Bacteria derived CRISPR-Cas systems capable of targeted DNA cleavage, such as Cas9, have been harnessed for genome modification in bacteria, and eukarya. Some Cas9 complexes have also been found to bind and cleave CRISPR (cr)RNA complementary single-stranded RNA *in vitro* when supplemented with an oligonucleotide that contains a protospacer adjacent motif (PAM) and partial guide complementarity (1). *Campylobacter jejuni* Cas9 was shown to cleave endogenous mRNA complementary to the crRNA, *in vivo,* in a PAM independent manner (2). Catalytic site inactivated Cas9 (dCas9) variants have also been used to repress gene expression by binding to and remaining tightly bound to the target RNA, thus obstructing the ribosome (3, 4). Further studies of Cas9 variants will undoubtedly result in the discovery of more RNA targeting Cas9 systems capable of exploitable RNA interference.

Type VI Cas13 systems specifically cleave crRNA complementary target RNA. When expressed in *E. coli,* and upon target binding, they also activate non-specific trans-RNA cleavage

at their dual HEPN domain RNase sites like in Csm6 and Csx1 (5). Mutagenesis of either one of the HEPN domains in Cas13 abrogates both the cis and trans RNase activities (6). Interestingly, Cas13 does not seem to have this collateral RNase activity when expressed heterologously in plants, insects, and mammals (7-9). While this non-specific trans-RNA cleavage activity has made these systems particularly useful for transcript detection tools like SHERLOCK, it doesn't make them viable options for directed RNA destruction in prokaryotes (10). However, like Cas9, a catalytically dead (d)Cas13 can still specifically bind target RNA and impede translation (11). Additionally, there is still a possibility that Cas13 variants discovered and described in the future will exhibit only the desired specific cis-RNA cleavage activity in microbes.

A native type III-B system of *Sulfolobus solfataricus* with a plasmid borne CRISPR array programmed to target the endogenous β-galactosidase mRNA showed a ~50% reduction of mRNA and protein activity (12). We sought to expand on the implications of this finding and determine the potential for other type III systems to be exploited to carry out RNA-guided sequence-specific RNA cleavage for post-transcriptional control of gene expression. Type III-A defense systems from *Lactococcus lactis*, *Staphylococcus epidermidis* and *Streptococcus thermophilus* were each expressed from single plasmids in *E. coli.* We designed crRNAs to target endogenous gene transcripts and assessed the efficiency and specificity of gene knockdown by Northern blot analysis. These expression systems successfully targeted single and multiple gene transcripts simultaneously and both coding and non-coding RNAs. Our results demonstrate the ability of type III-A modules to serve as effective RNA interference platforms in heterologous microbes, adding to the shared toolbox of CRISPR-based technologies.

We did not determine rules for choosing spacer sequences to confer optimal target mRNA cleavage, and as seen in the follow-up *S. solfataricus* study, we found large variations in percentage

of cleaved target transcript (13). This variation was especially pronounced when we targeted the highly structured RNase P ribozyme. The variation in cleavage activity we observed was likely due to the secondary and tertiary RNA structures which were similarly seen to impact the ability of the other RNA targeting effector complexes to bind their targets.

The Csm1 subunits of each plasmid based Csm expression system still contain an HD domain DNase. While we did not observe any interference effect due to this nuclease here or in our previous plasmid interference assays, it would still be prudent to mutate the HD domain (14). We prevented plasmid loss and growth inhibition with these constructs by mutation of the cOA producing Csm1 Palm domain. Alternatively, mutation or deletion of Csm6 would have the same effect. Additionally, deletion of Csm6 would reduce the plasmid size and waste less of the cell's resources. We did not examine or compare the specific RNA cleavage mediated gene knockdown with dCsm3 crRNP mediated translation inhibition, however it is possible that this configuration could improve the overall effect on gene repression.

We did not examine the effects of programming multiple spacer guides for simultaneous targeting of different regions of the same RNA, however, in *S. solfataricus,* such programming increased the total RNA interference and gene repression by Cmr (13). I suspect that our expression systems would similarly increase gene repression by increasing the number of spacers against a target RNA.

When trying to compare the utility of type II, III, and VI CRISPR-Cas systems for microbial RNA interference, we recognize the limited data sets that we have. Each system, from each species, may behave differently depending on unknown factors and empirical testing may be the only way to know what works in each. While the type III-A heterologous expression systems that we have developed work well in *E. coli* they may not function in another host. Therefore,

those that desire to utilize CRISPR based RNA interference would be prudent to try multiple methods including coopting endogenous CRISPR-Cas systems.

Self versus non-self activation of type III-A CRISPR-Cas systems

All CRISPR-Cas systems must manage their defensive function against foreign nucleic acids without targeting destruction of their own genomes causing potentially lethal autoimmunity. Since crRNA guides can bind to the host genome within the CRISPR array or to antisense crRNAs, the complexes need a mechanism to be activated only by invading DNA or RNA and not the host DNA or RNA.

In DNA targeting CRISPR systems, a PAM sequence, found adjacent to the protospacer DNA sequence but not in the repeat sequence of the CRISPR array, is key to interference activation (15). The PAM sequence and length varies between systems and species. Type III-A systems are unique in that they lack a specific PAM. These systems bind and specifically cleave crRNA guide-complementary RNA within the duplex regardless of flanking sequence identity (16, 17). Two additional activities (DNase activation and cyclic oligoadenylate production) that support invader interference only occur when the complex binds target RNAs containing certain activating protospacer flanking sequences (PFSs), heretofore assumed to be those that lack significant complementarity to the 8-nucleotide crRNA 5' tag sequence (18). In contrast, the type III-B Cmr systems from *Thermotoga maritima* and *Pyrococcus furiosus* are activated or inactivated by the first 3 positions of the RNA PFS denoted as (-1)'-(-3)' (17, 19, 20). The *T. maritima* Cmr complex DNase activity is only completely inhibited by a three nucleotide sequence that is perfectly complementary to the 5' tag (19). *P. furiosus* Cmr plasmid interference is inactivated by a perfectly complementary three nucleotide sequence as well as an additional 27 out of the 64 possible three

nucleotide sequences (17). The difference between the activation rules for these Cmr systems is emblematic of the diversity of CRISPR system functions even within a subtype.

To clarify the activating PFSs in type III-A systems, here we tested plasmid interference with three heterologously expressed type III-A systems (*S. thermophilus*, *S. epidermidis*, and *L. lactis)* using target libraries containing thousands of PFS variants. We demonstrate that PFSs with 5' tag complementarity at positions (-2)'-(-5)' inactivate interference, while most non-complementary PFSs led to varying levels of plasmid interference. We further show that this range of type III-A mediated interference variance occurs in the native *S. thermophilus* host. These results align with, support, and expand on the conclusions from published Csm system plasmid interference assays (18, 21-23). The results we present here (Figure 3.3) beg the question: How do different 5' tag non-complementary PFSs lead to different interference activation levels? The answer may await in cryoEM structures of crRNP bound to a greater variety of target RNAs and in *in vitro* DNase and cOA production assays with a greater variety of target RNAs.

Required catalytic activities for *S. thermophilus* type III-A CRISPR-Cas mediated interference

Many variables lead to different interference levels and observed defense outcomes with type III-A systems. We know that activation of all four Csm catalytic activities (sequence dependent RNase of Csm3, sequence independent Csm1 DNase, Csm1 oligoadenylate cyclase, and sequence independent Csm6 RNase) can contribute to a robust defense, but not all of them are always needed for a robust defense. With our *L. lactis*, *S. epidermidis*, and *S. thermophilus* heterologous expression systems, we previously determined that target transcription, the Csm1 cOA synthetase, and Csm6 RNase are all required for plasmid interference while the DNase is disposable (14, 24).

In contrast, a DNA phage infection model in *S. aureus,* carrying a Csm expression system from *S. epidermidis,* demonstrated that DNase defense activity is sufficient to clear a phage infection without the aid of the sequence specific Csm3 RNase or sequence independent Csm6 RNase when there is an early-expressed phage gene protospacer (25). In the same model, Csm6 RNase activity is required to clear the infection when there is a late-expressed phage gene protospacer. In both experiments, the ratio of phage particles to bacteria, the multiplicity of infection (M.O.I.) is 5. I hypothesize that increasing or decreasing the M.O.I., would result in different outcomes and would call for a more complex conclusion about the requirements for each defensive catalytic activity. Likely, increasing or decreasing plasmid copy number, target transcript promoter strength, Csm protein expression levels, etc, could very well change the conclusions we arrive at in any interference assay.

The *S. thermophilus* type III-A system has two adjacent *csm6* variants. Here we demonstrate that type III-A mediated plasmid interference is dependent on non-specific RNase activity of either Csm6 variant, and not the DNase activity of Csm1 or RNase activity of Csm3. In the absence Csm6 RNase activity, a relatively smaller level of plasmid interference was observed and attributed to the DNase (Figure 3.4). The contribution of the DNase towards plasmid interference was not previously detectable (data not shown) when the target plasmid had fewer protospacers and weaker PFSs. This suggests again that the context of the target matters for determining required catalytic activities in type III defense.

References

1. O'Connell, M.R., B.L. Oakes, S.H. Sternberg, A. East-Seletsky, M. Kaplan, and J.A. Doudna, *Programmable RNA recognition and cleavage by CRISPR/Cas9.* Nature, 2014. **516**(7530): p. 263-6.
2. Dugar, G., R.T. Leenay, S.K. Eisenbart, T. Bischler, B.U. Aul, C.L. Beisel, and C.M. Sharma, *CRISPR RNA-Dependent Binding and Cleavage of Endogenous RNAs by the Campylobacter jejuni Cas9.* Mol Cell, 2018. **69**(5): p. 893-905 e7.
3. Strutt, S.C., R.M. Torrez, E. Kaya, O.A. Negrete, and J.A. Doudna, *RNA-dependent RNA targeting by CRISPR-Cas9.* Elife, 2018. **7**.
4. Liu, Y., Z. Chen, A. He, Y. Zhan, J. Li, L. Liu, H. Wu, C. Zhuang, J. Lin, Q. Zhang, and W. Huang, *Targeting cellular mRNAs translation by CRISPR-Cas9.* Sci Rep, 2016. **6**: p. 29652.
5. Abudayyeh, O.O., J.S. Gootenberg, S. Konermann, J. Joung, I.M. Slaymaker, D.B. Cox, S. Shmakov, K.S. Makarova, E. Semenova, L. Minakhin, K. Severinov, A. Regev, E.S. Lander, E.V. Koonin, and F. Zhang, *C2c2 is a single-component programmable RNA-guided RNA-targeting CRISPR effector.* Science, 2016. **353**(6299): p. aaf5573.
6. O'Connell, M.R., *Molecular Mechanisms of RNA Targeting by Cas13-containing Type VI CRISPR-Cas Systems.* J Mol Biol, 2019. **431**(1): p. 66-87.
7. Abudayyeh, O.O., J.S. Gootenberg, P. Essletzbichler, S. Han, J. Joung, J.J. Belanto, V. Verdine, D.B.T. Cox, M.J. Kellner, A. Regev, E.S. Lander, D.F. Voytas, A.Y. Ting, and F. Zhang, *RNA targeting with CRISPR-Cas13.* Nature, 2017. **550**(7675): p. 280-284.
8. Huynh, N., N. Depner, R. Larson, and K. King-Jones, *A versatile toolkit for CRISPR-Cas13-based RNA manipulation in Drosophila.* Genome Biol, 2020. **21**(1): p. 279.

9. Aman, R., Z. Ali, H. Butt, A. Mahas, F. Aljedaani, M.Z. Khan, S. Ding, and M. Mahfouz, *RNA virus interference via CRISPR/Cas13a system in plants.* Genome Biol, 2018. **19**(1): p. 1.

10. Kellner, M.J., J.G. Koob, J.S. Gootenberg, O.O. Abudayyeh, and F. Zhang, *SHERLOCK: nucleic acid detection with CRISPR nucleases.* Nat Protoc, 2019. **14**(10): p. 2986-3012.

11. Wilson, C., P.J. Chen, Z. Miao, and D.R. Liu, *Programmable m(6)A modification of cellular RNAs with a Cas13-directed methyltransferase.* Nat Biotechnol, 2020.

12. Zebec, Z., A. Manica, J. Zhang, M.F. White, and C. Schleper, *CRISPR-mediated targeted mRNA degradation in the archaeon Sulfolobus solfataricus.* Nucleic Acids Res, 2014. **42**(8): p. 5280-8.

13. Zebec, Z., I.A. Zink, M. Kerou, and C. Schleper, *Efficient CRISPR-Mediated Post-Transcriptional Gene Silencing in a Hyperthermophilic Archaeon Using Multiplexed crRNA Expression.* G3 (Bethesda), 2016. **6**(10): p. 3161-3168.

14. Foster, K., J. Kalter, W. Woodside, R.M. Terns, and M.P. Terns, *The ribonuclease activity of Csm6 is required for anti-plasmid immunity by Type III-A CRISPR-Cas systems.* RNA Biol, 2019. **16**(4): p. 449-460.

15. Shmakov, S., O.O. Abudayyeh, K.S. Makarova, Y.I. Wolf, J.S. Gootenberg, E. Semenova, L. Minakhin, J. Joung, S. Konermann, K. Severinov, F. Zhang, and E.V. Koonin, *Discovery and Functional Characterization of Diverse Class 2 CRISPR-Cas Systems.* Mol Cell, 2015. **60**(3): p. 385-97.

16. Maniv, I., W. Jiang, D. Bikard, and L.A. Marraffini, *Impact of Different Target Sequences on Type III CRISPR-Cas Immunity.* J Bacteriol, 2016. **198**(6): p. 941-50.

17. Elmore, J.R., N.F. Sheppard, N. Ramia, T. Deighan, H. Li, R.M. Terns, and M.P. Terns, *Bipartite recognition of target RNAs activates DNA cleavage by the Type III-B CRISPR-Cas system.* Genes Dev, 2016. **30**(4): p. 447-59.

18. Marraffini, L.A. and E.J. Sontheimer, *Self versus non-self discrimination during CRISPR RNA-directed immunity.* Nature, 2010. **463**(7280): p. 568-71.

19. Johnson, K., B.A. Learn, M.A. Estrella, and S. Bailey, *Target sequence requirements of a type III-B CRISPR-Cas immune system.* J Biol Chem, 2019. **294**(26): p. 10290-10299.

20. Foster, K., S. Gruschow, S. Bailey, M.F. White, and M.P. Terns, *Regulation of the RNA and DNA nuclease activities required for Pyrococcus furiosus Type III-B CRISPR-Cas immunity.* Nucleic Acids Res, 2020. **48**(8): p. 4418-4434.

21. Goldberg, G.W., W. Jiang, D. Bikard, and L.A. Marraffini, *Conditional tolerance of temperate phages via transcription-dependent CRISPR-Cas targeting.* Nature, 2014. **514**(7524): p. 633-7.

22. Pyenson, N.C., K. Gayvert, A. Varble, O. Elemento, and L.A. Marraffini, *Broad Targeting Specificity during Bacterial Type III CRISPR-Cas Immunity Constrains Viral Escape.* Cell Host Microbe, 2017. **22**(3): p. 343-353 e3.

23. Kazlauskiene, M., G. Tamulaitis, G. Kostiuk, C. Venclovas, and V. Siksnys, *Spatiotemporal Control of Type III-A CRISPR-Cas Immunity: Coupling DNA Degradation with the Target RNA Recognition.* Mol Cell, 2016. **62**(2): p. 295-306.

24. Ichikawa, H.T., J.C. Cooper, L. Lo, J. Potter, R.M. Terns, and M.P. Terns, *Programmable type III-A CRISPR-Cas DNA targeting modules.* PLoS One, 2017. **12**(4): p. e0176221.

25. Jiang, W., P. Samai, and L.A. Marraffini, *Degradation of Phage Transcripts by CRISPR-Associated RNases Enables Type III CRISPR-Cas Immunity.* Cell, 2016. **164**(4): p. 710-21.